

AD-A088 853

SCIENCE APPLICATIONS INC TUCSON AZ  
ABLE IMAGE CHAIN ANALYSIS. REVISION.(U)  
AUG 80 J ZELENKA

F/6 17/9

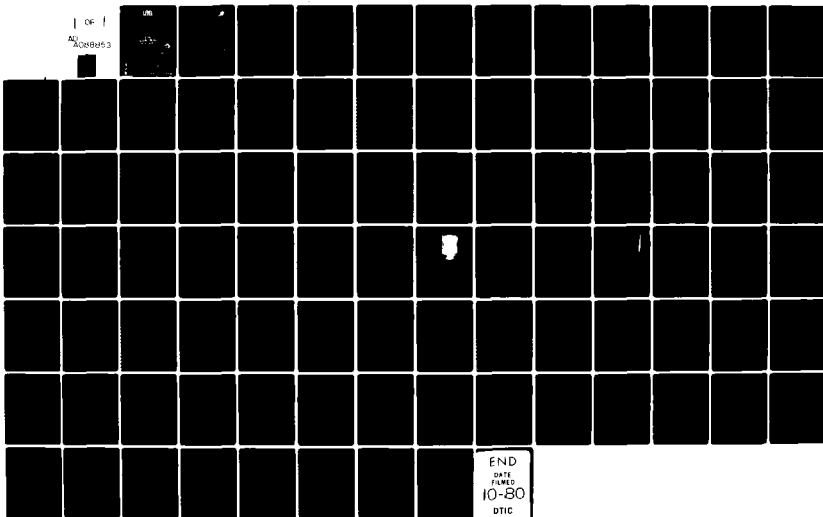
F33657-79-C-0178

UNCLASSIFIED

SAI-TR-04-165-1-REV

NL

1 OF 1  
AL  
A088853

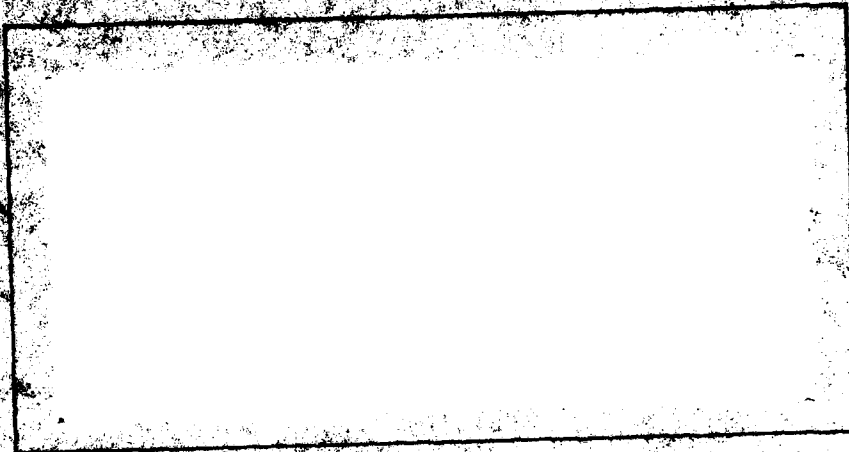


AD A088853

LEVEL

(12)

SC



SCIENCE  
APPLICATIONS  
INCORPORATED

See 1473 DTIC



64 9 2 088

12



ABLE IMAGE CHAIN ANALYSIS

TR 04-165-1

Prepared for  
USAF SYSTEMS COMMAND  
Aeronautical System Division  
UPD-X Program Office

Prepared by  
Jerry Zelenka  
and  
Tucson Technical Staff

Contract F33657-79-C-0178  
CDRL 1008  
Project 1-125-04-165

July 25, 1979  
REVISED  
August 27, 1980

DTIC  
SEP 4 1980  
C

This document has been approved  
for public release and sale; its  
distribution is unlimited.

# TABLE OF CONTENTS

	<u>PAGE</u>
1.0 INTRODUCTION AND SCOPE	1
2.0 SYSTEM DESCRIPTION AND IMAGE QUALITY CRITERIA (TOP LEVEL)	2
2.1 OVERVIEW	2
2.2 ABLE SUBSYSTEM DISCUSSIONS (TOP LEVEL)	7
2.2.1 Radar Image Quality Considerations and Verifications	7
2.2.2 Radar System Considerations (APD-10/APD-11)	10
2.2.3 SAPPHIRE Subsystem	10
2.2.4 ACD Subsystem	13
2.2.5 Exploitation Subsystem (ES)	14
3.0 SUBSYSTEM ANALYSIS/DESCRIPTION	15
3.1 UPD-4 RADAR SYSTEM	15
3.1.1 General Comments	15
3.1.2 Interface Requirements	22
3.1.3 Test Requirements	24
3.1.4 Sampling, Quantization and Compression	26
3.2 SAPPHIRE PROCESSOR	27
3.2.1 General Comments	27
3.2.2 Image Quality	27
3.3 AUTOMATIC CHANGE DETECTOR (ACD)	35
3.4 EXPLOITATION SUBSYSTEM (ES)	39
3.4.1 General Description	39
3.4.2 Interface Requirements	39
3.4.3 Compression	48
3.4.4 Sampling	64
3.4.5 Testing	77
4.0 CONCLUSIONS AND RECOMMENDATIONS	83

Accession For	
NTIS GRA&I	<input checked="" type="checkbox"/>
DDC TAB	<input type="checkbox"/>
Unannounced	<input type="checkbox"/>
Justification	
By _____	
Distribution/ _____	
Availability Codes	
Dist	Avail and/or special
<i>A</i>	

## LIST OF TABLES

	<u>PAGE</u>
2-1 SAR SYSTEM DEGRADATION FACTORS AND THEIR DEFINITION	11
2-2 SYSTEM DEGRADATION FACTORS AND THEIR RELATIONSHIP TO THE SAR SUBSYSTEM	12
3-1 ABLE DPCM CODE	54

## LIST OF FIGURES

	<u>PAGE</u>
2-1 ABLE Image Chain Elements	3
3-1 Signal to Noise and Clutter to Noise Characteristics	21
3-2 UPD-4 Radar System Image Chain	23
3-3 Analog-to-Digital Conversion Loss as a Function of Quantization Bits	25
3-4 Simulated Output Zero Phase Shift	30
3-5 Simulated SAPPHIRE Output 25% Phase Shift	31
3-6 Simulated SAPPHIRE Output 50% Phase Shift	32
3-7 Simulated SAPPHIRE Output Two Targets Separated by Two IPR's	33
3-8 Simulated SAPPHIRE Outputs Two Targets Separated by Three IPR's	34
3-9 ACDS Mission Image Path (10 Foot)	36
3-10 ACDS Mission Image Path (20 Foot)	37
3-11 Exploitation Subsystem	40
3-12 11 Bit to 8 Bit Log Encoding	42
3-13 Percent Error for 11 Bit to 8 Bit Log Encoding	43
3-14 11 Bit to 5 Bit Log Encoding	44
3-15 Percent Error for 11 Bit to 5 Bit Log Encoding	45
3-16 11 Bit to 8 Bit Power-Law Encoding	46
3-17 11 Bit to 5 Bit Power-Law Encouding	47
3-18 Example of Irregularities in Digital CRT Display's Gamma Function (Real Data) (From Briggs - Ref. 1)	49

# LIST OF FIGURES - continued

	<u>PAGE</u>
3-19 Four Point Targets Quantized to 11 Bits	51
3-20 Comparison of Power-Law & Logarithmic Compression Schemes	52
3-21 Log Encoded/Power-Law Compressed to 8 Bits	55
3-22 Direct Power-Law Compression to 8 Bits	56
3-23 Log Encoded/Power-Law Compressed to 5 Bits	57
3-24 Direct Power-Law Compression to 5 Bits	58
3-25	59
3-26	60
3-27	61
3-28	62
3-29 Gaussian Spot $\sigma$ 20% of Sample Distance	65
3-30 Gaussian Spot $\sigma$ 40% of Sample Distance	66
3-31 Gaussian Spot $\sigma$ 60% of Sample Distance	67
3-32 Gaussian Spot $\sigma$ 80% of Sample Distance	68
3-33 Gaussian Spot $\sigma$ 100% of Sample Distance	69
3-34 Sampling Rate 1 x Nyquist	71
3-35 Sampling Rate 1.25 x Nyquist	72
3-36 Sampling Rate 1.5 x Nyquist	73
3-37 Sampling Rate 1.75 x Nyquist	74
3-38 Sampling Rate 2 x Nyquist	75
3-39	76
3-40 Effects of Sampling (1 x Nyquist) on Two Point Targets	78
3-41 Effects of Sampling (1.25 x Nyquist) on Two Point Targets	79
3-42 Effects of Sampling (1.5 x Nyquist) on Two Point Targets	80
3-43 Effects of Sampling (2 x Nyquist) on Two Point Targets	81
3-44 Modulation Depth vs. Sampling Frequency	82

## 1.0 INTRODUCTION AND SCOPE

Presented in this report are a brief discussion and analysis of key ABLE image chain elements. The need for a common framework of reference from which to assess key technical issues which influence the ABLE subsystem interfaces and, subsequently, the radar image usefulness has become critical. It is the motivation behind this effort. It is hoped that this report will become the basis from which to evaluate and investigate a more detailed series of subsystem image chain element simulations and analysis results. These results could then be used to guide in setting interface requirements, testing, operational image quality checks and maintenance procedures.

This report seeks to help in establishing ABLE system image chain elements, the ABLE data flow, and ABLE interface and test requirements. The document also reviews critical ABLE image chain problem areas, including image sampling requirements, radar image quantization, radar image compression techniques (DPCM, MAPS, etc.), and radar image data display requirements for both hard and soft copy devices. Once formulated, this document should become a management and engineering resource tool, defining ABLE system/subsystem image quality requirements, interface requirements, and test and verification methodologies and procedures.

The intended forum for the review and analysis of these issues is the Interface Control Working Group (ICWG), supplemented by detailed associate contractor analysis and presentations at IDR, FDR, and follow-up meetings. Outputs from this effort are intended to support image quality maintenance.

## 2.0 SYSTEM DESCRIPTION AND IMAGE QUALITY CRITERIA (TOP LEVEL)

### 2.1 OVERVIEW

The ABLE image chain consists of the following segments:

1. UPD - 4/6 radars
2. SAPPHIRE subsystem
3. ACD subsystem
4. Exploitation subsystem

Figure 2-1 diagrammatically shows the complete ABLE image chain including the interfaces to the command control and communication (C<sup>3</sup>) segment, the Tactical Reconnaissance Squadron (TRS) operations (TUOC) segment, and, indirectly, the user community. It is a complex system where the utility of the output product--image quality and verification of the image--are the unique factors of success. From each of the areas shown in Fig. 2-1, factors which affect the final output are considered and listed here in brief form. These factors must be taken into account when evaluating and estimating image quality; they are:

#### Target Environment

Topology  
Vegetation (masking effects)  
Weather

#### Atmosphere

Phase errors  
Attenuation  
Backscatter (rain)



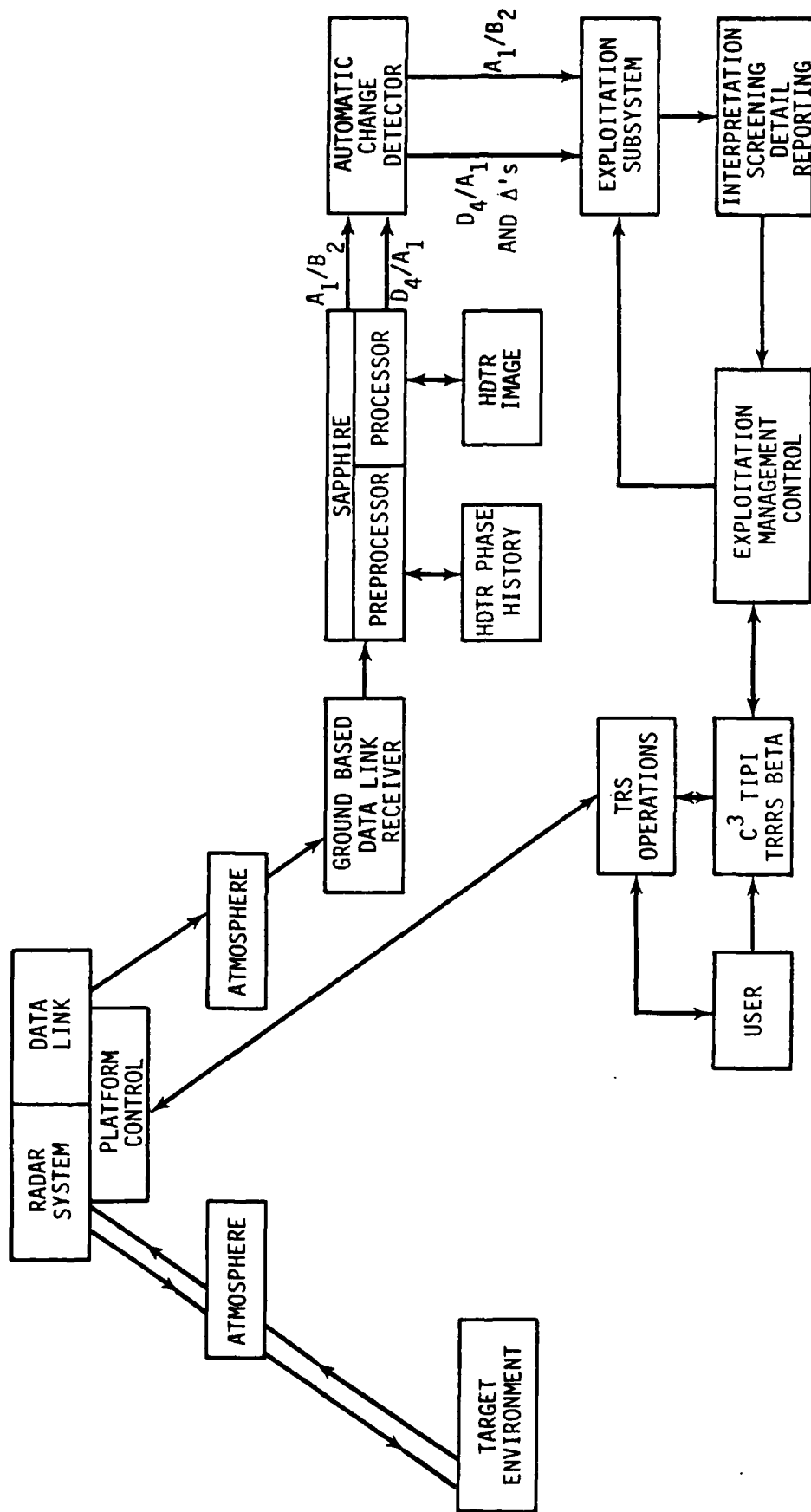


Figure 2-1. ABLE Image Chain Elements

### Radar System

Transmitter (power, bandwidth, phase errors, etc.)

Receiver (phase errors, noise, bandwidth, limiting, etc.)

Antenna (gain, beam width, sidelobes, pointing accuracy,  
phase errors, etc.)

### Vehicle Control

Navigation

Motion compensation (phase errors)

Operational modes

### Data Link

Bandwidth

Signal-to-noise

Range

### Atmosphere

Attenuation

### Ground Data Link

Bandwidth

Signal-to-noise

### SAPPHIRE Processor

#### Preprocessor

A/D convertor (quantization, I/Q balance)

Sampling rate

PRF buffering

Data rate

Quantization

#### Processor

Data rate

Weighting (range and azimuth)

Range and azimuth (MOCOMP)

### SAPPHIRE Processor (cont.)

Mode control (APD-10/APD-11)

Arithmetic Noise

Noncoherent integration

Adjacent cell averaging

Output (sampling, quantization, compression

$A_1B_2$  vs.  $D_4A_1$  dual port)

Motion compensation

### HDTR (Phase History)

Data rate

Quantization

BER (bit error rate)

Data volume

Shortage/retrieval

### Automatic Change Detector

Data rate

Data storage

Data retrieval/control signals

Data compression (MAPS)

BER

Registration/change detection/FOP

Reference update (mission/reference)

### Exploitation Subsystem

- Data rate
- Data storage (buffer)
- Data retrieval (timelines, accuracy)
- Collateral data integration (cue insertion)
- Coordinate matching (reference) for target location
- Data compression
- Data display
  - Data sampling
  - Data quantization
  - Spot size
  - Data correction (gamma correction)
  - Data interlace (CRT display)
  - Interactive considerations (special function features)

### Interpretation

- Timelines (report generation, etc.)
- Efficiency
- Performance (detection, classification, identification)
- Collateral data (cues, situations update data)

### Exploitation Management Control Subsystem

- Control monitoring functions
- Cue data base
- Situation data base
- Report data base
- Systems interactions (other subsystems/segments)
- Mission requirements interfaces
  - TRS operations (coverage, timelines)
  - User community (EEI's)
  - C<sup>3</sup> (ABLE/USER)

### Quality Control

Operational QC procedures

Test signals (interface verification & subsystem elements verification)

Test arrays (European)

Image quality control

One can see from this list the complexity and interdependence of the system, and appreciate the necessity for checking and analysis of the effective functioning of each segment of the ABLE system. We feel that testing for the image quality and its verification will require the utilization of contractor/program resources, such as system simulation, systems analysis, supplementary data collection (FTB effort), data analysis modeling, testability analysis, and image evaluation (utility) analysis. The identification, structuring, and scheduling of the necessary resources will draw strongly on previously developed UPD-X results and Program Office and contractor capabilities.

## 2.2 ABLE SUBSYSTEM DISCUSSIONS (TOP LEVEL)

### 2.2.1 Radar Image Quality Considerations and Verification

Methods of image quality verification shall include analysis, inspections, subsystem tests, and demonstrations. It is anticipated that the UPD-4/UPD-6 current capabilities, as represented by previous optical imagery measurements shall represent the baseline for comparison for the ABLE subsystems and integrated system performance characteristics. In this effort, the UPD-4 and the UPD-6 radar systems, platform control, data link, and ground-based data link receiver are GFE, and, as such, we anticipate current levels of performance and capabilities to remain constant.

The primary radar image quality parameters are presented and discussed in Section 3.0 (p. 15). Then they are specifically defined for the UPD-4 radar system, giving values based on previous system measurements; they include the conventional operational processor effects.

In the ABLE system the primary radar data display will be softcopy display devices. Thus, our primary verification procedure for the image chain considerations should concentrate on softcopy data verification procedures. It is suggested that direct measurements from the CRT screens be made. Direct measures require many scenes to be scanned with a photometer to establish display values. Indirect measures shall be considered using the following criteria:

- A. The CRT spot size and shape shall be measured as a function of intensity and screen position for both scan and cross scan directions.
- B. The digital signal at its appropriately weighted and sampled frequency (i.e., the same sampling and weighting to be used for display inputs) shall be digitally measured prior to D/A at the CRT.
- C. The digital input signal shall be convolved with the CRT spot as a function of brightness and position and thus plotted on a display.
- D. Measurements will be made at the appropriate points on the plotted curves (i.e., the points that relate to the linear intensity values at the SAPPHIRE output).
- E. The results of these tests will be compared to the particular image quality parameter value as specified.

This test will satisfy all image quality parameters except geometric distortion and image intensity uniformity which can be measured directly from the CRT face and the digital data stream.

Oversampling, data compression, and other applicable data display procedures should be subjected to the same direct and indirect measurement criteria described above, since these techniques will be performed on the radar data prior to detailed exploitation.

Key parameters relating to image quality factors include:

- Image intensity
- Displayed contrast ratio
- Displayed spurious response
- Displayed peak sidelobe levels
- Displayed geometric distortion
- Displayed dynamic range
- Displayed image intensity uniformity
- Displayed bit errors
- Display human visual response comparison

Actual performance requirements for these parameters should be determined prior to IDR for all ABLE subsystems and should be consistent with the ABLE specification. All measurement techniques and procedures should include considerations of sampling compression techniques, data remapping and specific device transfer curve characteristics. Specific subsystem/system test verification procedures remain to be determined.

### 2.2.2 Radar System Considerations (APD-10/APD-11)

It is instructive to examine how various SAR system errors affect resulting SAR image quality characteristics. These initial observations and their relationship to specific SAR system degradation factors will provide a reference for the discussion in later sections and also provide valuable insight as to the importance of certain system specifications. Some typical SAR system error sources and their impact on SAR data image quality characteristics are presented in Table 2-1. Table 2-2 relates these various degradation factors to the specific SAR subsystem components. Section 3.3 discusses some of these factors in more detail.

### 2.2.3 SAPPHIRE Subsystem

The SAPPHIRE subsystem provides the primary digital radar image stream to the other ABLE subsystems. Principal areas of concern include:

- Azimuth focus errors,
- Arithmetic noise,
- Range and azimuth weighting characteristics,
- I & Q amplitude and phase errors,
- Bit errors and dropouts,
- 11 bit to N bit compression techniques,
- Noncoherent integration and adjacent cell averaging,
- Spectral noise components, and
- Saturation effects (A/D convertor).

These represent the major image chain degradation factors.

The SAPPHIRE subsystem is the first stage in the image chain where direct measurement of the image quality parameters can be made. Consequently,



TABLE 2-1

## SAR SYSTEM DEGRADATION FACTORS AND THEIR DEFINITION

<u>Specific Parameters</u>	<u>Definition</u>
1) System Focus Error	Focus is a generic term which can be used to indicate an imaging system's capability to separate closely spaced objects (targets). In radar, typically, quantitative statements about focus (resolution capability) are made in terms of the system impulse response mainlobe width (3 dB width). For SAR systems, focus errors (resolution degradation) can affect either range or azimuth focus independently or jointly depending on the error source. In general, any SAR subsystem component which introduces phase errors can impact the system focus (resolution) capability.
2) Peak Sidelobe Levels	Peak sidelobes are defined as the secondary maxima in the system impulse response characteristic. High peak sidelobe levels introduce spurious, displaced returns for strong targets and contribute to the overall image background noise (contrast reduction).
3) High Integrated Sidelobe Levels	Integrated sidelobes are defined as the ratio of the total sidelobe energy to the total mainlobe energy. High integrated sidelobe levels degrade the image contrast ratio and reduce target detectability.
4) Spectrum Foldover (Ambiguity Noise)	These are spurious noise responses in both range and/or azimuth which typically result in an increase in the background noise in the image field. This effect can be caused by sampling errors (azimuth), lack of appropriate offset (range and/or azimuth) and simultaneous signal returns from multiple ranges.
5) Small Signal Suppression	This artifact introduces loss of weak radar returns in the area of strong radar returns because of system nonlinearities caused by insufficient dynamic range.
6) Intermodulation Noise	This noise artifact in the SAR system is associated with nonlinear operation at various stages in the radar system. This noise results in the addition of either focussed or unfocussed energy to the final SAR image. Intermodulation is caused by the interaction of at least one strong target with other targets in close proximity (within one beamwidth or pulse length).
7) Harmonic Noise	Harmonic noise is similar to intermodulation noise and results whenever the signal drives the system into saturation. Harmonic noise is principally a problem at video where the harmonic energy cannot be readily filtered from the desired image.

Table 2-2  
SYSTEM DEGRADATION FACTORS AND THEIR RELATIONSHIP TO THE SAR SUBSYSTEM

<u>Degradation Factor</u>	<u>SAR Subsystem</u>				
	<u>Antenna</u>	<u>Transmitter</u>	<u>MOCOMP</u>	<u>Receiver</u>	<u>Recorder</u> <u>Processor</u>
1) System Focus Error		✓	✓	✓	✓
2) High Peak Sidelobes	✓	✓	✓	✓	✓
3) High Integrated Sidelobes	✓	✓	✓	✓	✓
4) Spectrum Foldover	✓	✓	✓		✓
5) Small Signal Suppression				✓	✓
6) Intermodulation Noise				✓	✓
7) Harmonic Noise				✓	✓

it is historically the location where the total system is specified and quantified for performance. For the ABLE system, the tangible output product is the interpreter's report which utilizes and formalizes the image quality and image verification effectiveness. Therefore, in the image chain we will consider SAPPHIRE as just one subsystem.

#### 2.2.4 ACD Subsystem

SAPPHIRE will provide a dual port output to the ACD subsystem, consisting of 8 bit, log compressed  $2 \times 2$  pixel adjacent cell averaged 10-foot sampled radar imagery ( $A_1B_2$ ) and 11 bit,  $4 \times 4$  noncoherently integrated (16 look) 20-foot sampled radar imagery ( $D_4A_1$ ). The  $A_1B_2$  data will be buffer stored for subsequent transmission to the ES. Potential ACD degradation factors include:

- Bit errors,
- Pixel dropouts, and
- Transmission added noise.

The  $D_4A_1$  data will be used for automatic change detection and subsequent screening analysis in the ES. Prior to ACD operation the data will be MAPS compressed (N bits), registered with previous mission data (ES input control) and change detected MAPS decompressed (M bits) and transmitted to the ES.

Primary image quality questions arise concerning the MAPS compression techniques, bit errors, pixel dropouts, and transmission noise, all of which have potential impact on image quality and resulting image utility to the screening and detailed analysis functions.

### 2.2.5 Exploitation Subsystem (ES)

The ES accepts both the high resolution data ( $A_1/B_2$ ) and the  $D_4/A_1$  screening data ( $D_4A_1$ ) including the change data for subsequent data exploitation. The ES buffers, initiates control signals, and performs radar data screening and detail analysis functions on the above described radar digital image stream. Internal to the ES additional image compression, resampling, remapping and gamma correction are performed on the data stream prior to data display. All of these functions have the potential for introducing radar image degradations and reducing image utility.

The primary areas of concern include:

- Image compression techniques,
- Image resampling techniques,
- Bit errors,
- Pixel dropouts,
- Gamma corrections,
- Digital image intensity/human visual response characteristics,
- CRT screen display characteristics and human factors considerations for interpreter viewing conditions.

The EMC generated situation data display characteristics and collateral data base information also may impact data utility, and, as such, need consideration during the ABLE image chain analysis task.

This section has tried to present a general view of the ABLE image chain elements along with some parameters for image quality criteria (direct and indirect measurement from CRT screens, pp. 8-9). Section 3 covers in detail the technical ramifications of these generalized comments, and it includes detailed current UPD-4 radar quality standards. A series of recommendations for action items is presented in Section 4.

### 3.0 SUBSYSTEM ANALYSIS/DESCRIPTION

In this section we will look in more detail at the various subsystems unique to the ABLE image chain. The four primary subsystems are:

- the UPD-4 (APD-10) radar system,
- the SAPPHIRE digital processor,
- the automatic change detector, and
- the exploitation system

For each subsystem we will describe its functions and pay specific attention to the those functions that effect the image chain and consequently the image quality.

#### 3.1 UPD-4 RADAR SYSTEM

##### 3.1.1 General Comments

The AN/UPD-4 Synthetic Aperture Radar (SAR) system as currently configured represents the baseline of operational SAR performance capability in the Air-Force inventory.

In general, this SAR system is a very complex system in which subtle subsystem errors can introduce serious degradations in the image chain and to the overall data (image) utility. In particular, most of the important SAR system errors which introduce large degradations in the SAR data utility are characterized by the parameters discussed in Section 2.2.1., and we re-list them on the following page for convenience.

Key parameters relating to image quality factors include:

- Image intensity (mapping from 11 bits to N bits)
- Displayed impulse response width (resolution)
- Displayed contrast ratio
- Displayed spurious response
- Displayed peak sidelobe levels
- Displayed geometric distortion
- Displayed dynamic range
- Displayed image intensity uniformity
- Displayed bit errors
- Display human visual response comparison

The UPD-4 radar system output quality parameters and hence the image utility can be characterized by the following parameters, even though in many cases they are not directly measurable at the radar output (i.e., the literal radar image is formed at the SAPPHIRE output):

- impulse response -3dB widths (resolution)
- contrast ratio (i.e., the relationship of clutter levels to no return noise levels over a given dynamic range)
- peak sidelobe levels
- spurious responses (i.e., nonlinear distortions such as harmonic and intermodulation or ambiguous signals)
- intensity fidelity (i.e., the relationship of target intensity or density to the relative input target size)
- dynamic range (i.e., the system response to the variation of real target size or cross section and the radar output characterization of these targets)
- geometric distortion (i.e., those errors in the mapping process that distort the radar map with respect to the real world)
- image intensity uniformity (i.e., the intensity variations which are caused by antenna fall off or its equivalent).

The following items summarize the performance characteristics of the UPD-4 radar system including the conventional optical processor effects. These parameter values are based on previous system measurements.

- Impulse Response - 3dB width

The system has demonstrated an overall impulse response width of 1.5 to 3.0 meters (5 to 10 feet) over the desired ground range interval (4.9 km to 55.6 km).

- Peak Sidelobes

The system peak sidelobe levels can be maintained below -12dB through the use of both azimuth and range bandwidth limiting, while still maintaining the specified system impulse response width.

- Image Focus

It is often necessary to manually adjust the processor focus to achieve optimum system focus. Focus is usually maintained over a synthetic aperture length for the above IPR's.

- System Noise

There is insufficient data available to unambiguously define the magnitude and exact source of the system noise (integrated sidelobe levels, ambiguities, nonlinearities, etc.), but there is strong evidence that the UPD-4 is working at less than optimum performance. Based on selected data evaluations it appears that the system detection performance is limited by the system noise sources.

- Motion Compensation

The current UPD-4 motion compensation system appears inadequate in that processor azimuth refocus is required to optimize the image data for long strips. The motion compensation is adequate for single focus over short (a few miles) azimuth lengths.

- Navigation

The current (RF-4C) navigation system appears adequate for the current system usage. However, it does impact on image location accuracy.



- Processor (optical not intended for the ABLE program)

To obtain optimum optical processor performance it is necessary that a dedicated, knowledgeable operator operate and maintain the current four-channel optical processor (ES-83A). Severe image degradation can result if this requirement is not met.

- Dynamic Range

The output dynamic range of the UPD-4 radar system is linear and extends up to a range of about 50dB.

The other image quality factors such as contrast ratio and geometric distortion have not been directly measured, but the outputs can be estimated at least for contrast ratio. The upper end of the contrast ratio curve is established by the ISLR (integrated sidelobe ratio) and is given by

$$CR = 1 + \frac{1}{ISLR}.$$

Since the ISLR budget is made up from all the high frequency phase error sources plus the inherent budget from the sidelobe structure of the unweighted theoretical impulse response function, we can estimate the contrast ratio of the output image by considering the processor architecture for both the optical and digital processors. For the optical system we do not weight the processing aperture and hence for a rectangular aperture we have:

$$ISLR = -6.5dB$$

and the contrast ratio for the best case (i.e., no phase errors)

$$CR = 1 + \frac{1}{-6.5} = 7.4dB$$

Based on qualitative observations, the digitally processed data from SAPPHIRE appears similar to the optically processed data. Thus, we would estimate a contrast ratio of no better than 5dB to 7dB, since we have not assumed any losses for phase errors. The digital processor (SAPPHIRE) utilizes -30dB Taylor weighting, but, due to phase errors, we do not seem to realize the theoretical improvement.

The contrast ratio on the low end of the clutter spectrum is equal to

$$CR = 1 + CNR$$

for a slant range of 20 n. miles (37km); the clutter-to-noise ratio is about 9dB for arid desert terrain, and this yields a contrast ratio of

$$CR = 1 + 9dB = 9.5dB$$

with respect to a noise (shadow) background. For an arid desert terrain, a radar cross section density,  $\sigma_0$ , of -25 dB has been assumed.

The clutter-to-noise and signal-to-noise ratios for the UPD-4 radar are shown in Figure 3-1. UPD-4 optically correlated imagery was examined to determine the operational signal-to-noise ratio. Imagery from Luke Aux-3 area taken in mode 5 channel B at 27.8 km was used for this estimate. The theoretical signal-to-noise ratio for a one meter square reflector should be 27.5dB above system noise. From the Luke Aux-3 imagery, an array of reflectors was recorded that ranged in size from  $50 \text{ m}^2$  to  $0.1 \text{ m}^2$ . These reflectors were placed on the asphalt runway which was assumed to be 3dB above the system noise level. The  $0.3 \text{ m}^2$  target could not be detected but the  $0.5 \text{ m}^2$  target was observable. From this it was

UPD-4

C/N, C/N (DB)

$P_{AVE} = 50 \text{ W}$   
 $G = 30 \text{ DB}$   
 $NF\&L = 9.3 \text{ DB}$   
 $\sigma = 1 \text{ M}^2$   
 $\sigma_0 = -25 \text{ DB}$   
 $\rho = 3.0 \text{ M}$   
 $H = 1.8 \text{ KM}$   
 $6.1 \text{ KM}$   
 $10.7 \text{ KM}$   
 $1, 2, 3 \text{ MODE}$   
 $4 \text{ MODE}$   
 $5, 6 \text{ MODE}$   
 $V = 213 \text{ M/SEC}$

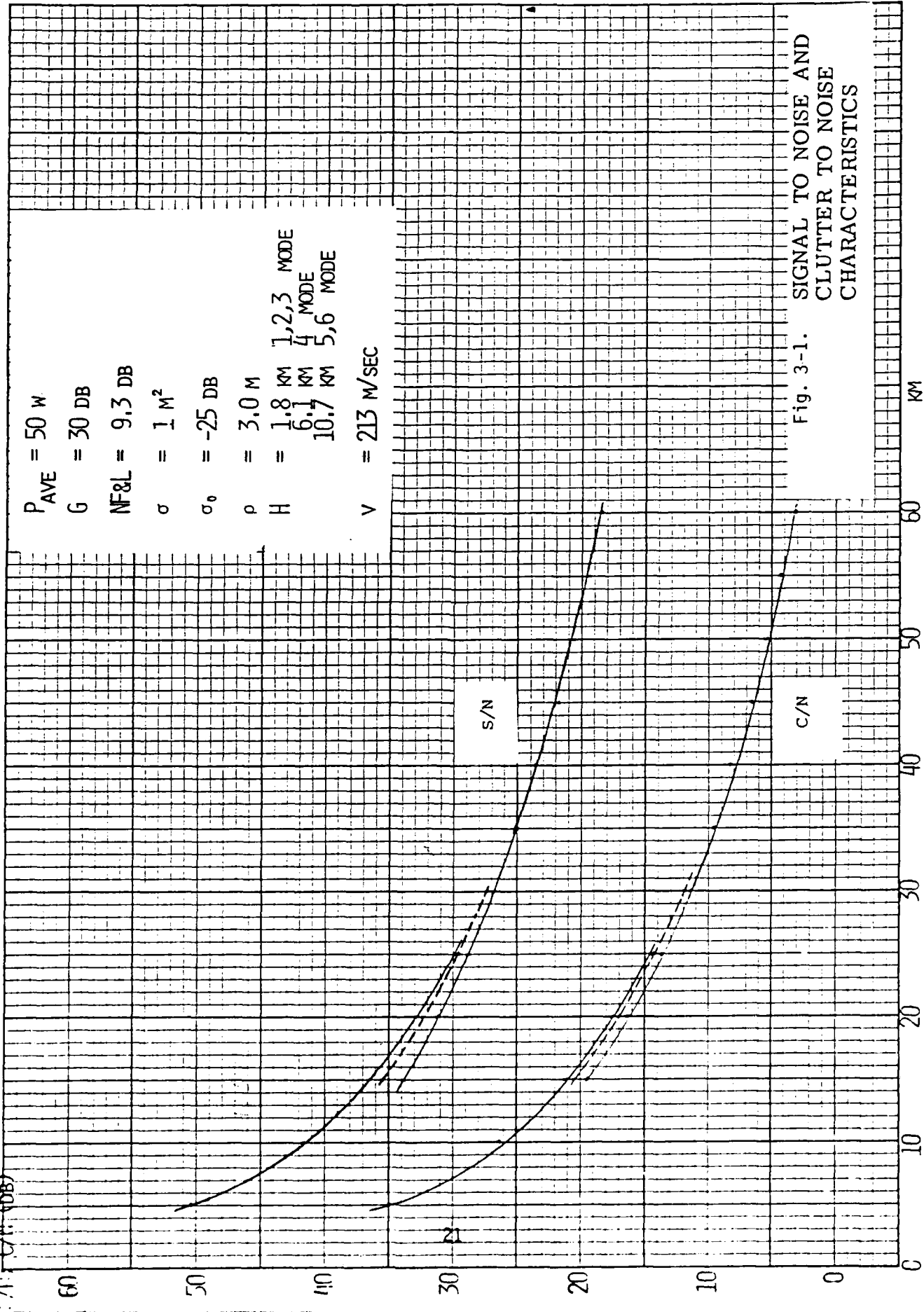


Fig. 3-1. SIGNAL TO NOISE AND CLUTTER TO NOISE CHARACTERISTICS

GROUND RANGE

KM

estimated that the  $0.3 \text{ m}^2$  target was 5dB above the rms total noise level. From the asphalt clutter estimate and the  $0.3 \text{ m}^2$  response, it was concluded that this target was about 8dB (3dB from asphalt clutter plus 5dB above asphalt rms clutter) above system noise. If we extrapolate to a  $1 \text{ m}^2$  target, we note that the signal level is about 14dB lower than would be estimated, if receiver noise and its losses were the dominant noise source.

### 3.1.2 Interface Requirements

The UPD-4 radar system must interface with the target environment, the SAPPHIRE processor, and high density tape recorder (see Figure 3-2). The image chain for this sequence includes the atmosphere, the radar components (transmitter, receiver, waveform generator, antenna, etc.) data link, and ground components (receiver, preprocessor and A/D convertor, ground data reformatter, and phase history tape recorder). Each of these components can, and do, introduce errors in the radar image chain which can reduce the image utility by the reduction in image quality characteristics. For the transmit function which includes the waveform, antenna and atmosphere, we have low and high frequency phase errors as well as amplitude errors. The effect of these errors is that each image quality parameter can be modified by the perturbation to the image chain. For example, atmospheric disturbance can affect the ISLR and consequently, the contrast ratio. Antenna motion can cause either or both low and high frequency errors which can cause a loss of ISLR or a reduction of IPR (resolution). It is also possible to generate sinusoidal phase errors which appear

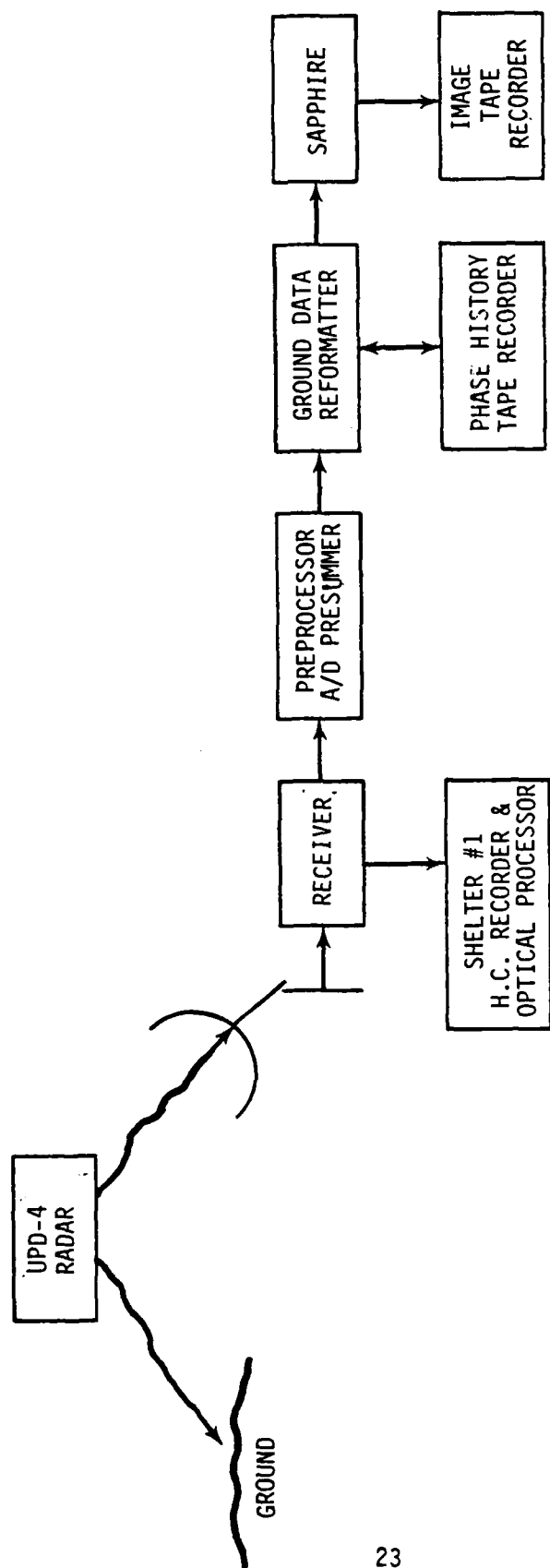


Figure 3-2. UPD-4 Radar System Image Chain

as a spurious response in the image and can be identified as false targets. The receiver is also affected by phase errors, causing the same image quality problems mentioned above. Here we can also have nonlinear effects, thus generating false (spurious) responses which might be identified as false targets.

In the ground equipment there are two primary problem areas. The A/D convertor can add significant quantization and saturation noise, and the tape recorder (HDTR) is a prime source for bit errors. Each of these errors can degrade the image quality with the primary effect impacting the contrast ratio. Bit errors in the video stream prior to pulse compression are not nearly as serious as bit errors in the auxiliary data stream, especially when the aux data is used in the processor (SAPPHIRE) for determining specific signal processing coefficients. Figure 3-3 presents the input and output signal-to-noise ratio which can be obtained for a given number of quantization levels. In this figure, the ordinate shows the output clutter-to-noise ratio for a given number of quantization bits and an input signal-to-noise ratio. According to Figure 3-1, the input clutter-to-noise ratio to the A/D could be  $> 30$  dB. For such large clutter-to-noise ratios, Figure 3-3 implies that the resulting clutter-to-noise ratio at the A/D output is at most 25 dB for a 5 bit A/D converter.

### 3.1.3 Test Requirements

The image chain up to the SAPPHIRE processor is composed of phase history data which does not lend itself to easy testing. Historically, certain tests can be performed on the data stream, but the image quality parameters are associated with the final image (i.e., the output from the

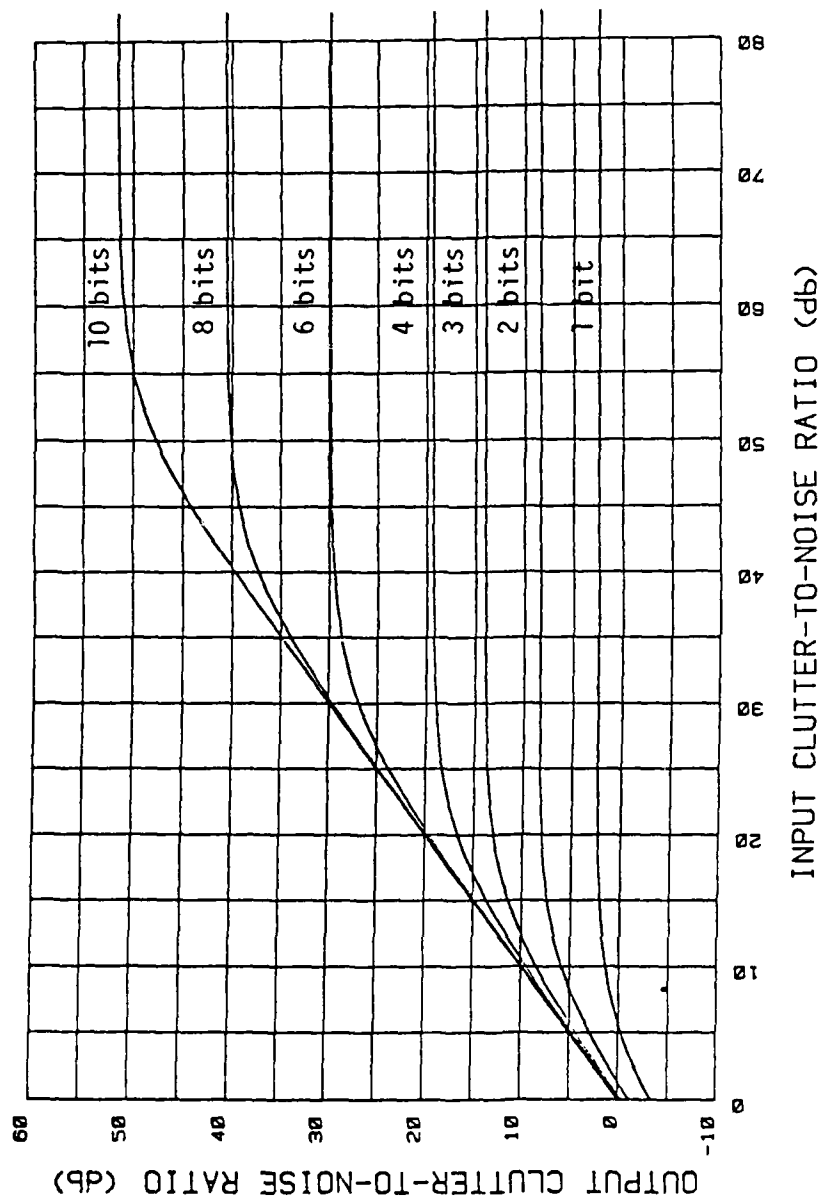


Figure 3-3. Analog-To-Digital Conversion Loss As a Function of Quantization Bits.

optical or digital processor). For the ABLE image chain we recommend that testing be addressed at the processor output.

#### 3.1.4 Sampling, Quantization and Compression

The UPD-4 radar system, as diagrammed in Figure 3-2, has little control over sampling or data compression, since these values are set by the Nyquist rate for sampling, and dynamic range compression is difficult for the dispersed phase history signals. The effect of under sampling the data is to cause aliasing of the signal and hence much unwanted noise or spurious signals. For the UPD-4 image chain we would not anticipate modifications of either sampling or dynamic range compression.

The quantization levels are set by the A/D convertor which was described in an earlier section, and the effects are illustrated in Figure 3-3.



## 3.2 SAPPHIRE PROCESSOR

### 3.2.1 General Comments

The SAPPHIRE processor receives dispersed phase and amplitude signals from the radar system through the data link, then compresses and detects this data, and outputs an 11 bit amplitude data stream (i.e., the data stream is the radar image). The output data stream is sampled image data with 11 bits of amplitude per sample. This data stream (dual ported -  $A_1/B_2$  and  $D_4/A_1$ ) then flows to the ACD for change detection and for pass-through to the ES. Within the processor there are range and azimuth compression, autofocusing, and motion compensation taking place, so that the highest quality image is established at the SAPPHIRE output plane. The processor also includes displays so that the output imagery can be viewed in real-time, and so that certain manual focus routines can be supported.

### 3.2.2 Image Quality

The image quality out of the SAPPHIRE is dependent on the quality of the data stream from the radar system and on the internal workings of the processor. Since the UPD-4 radar output is given for the ABLE program, and the SAPPHIRE processor is not to be significantly modified for this program, all we can address is the variance in image quality and its monitoring, and the display of SAPPHIRE data.

The major cause of variance in the output data is from the input radar signal variance, although there can be a great variance of output due to autofocus or incomplete focus. The lack of perfect autofocus can affect almost all the image quality parameters. The SAPPHIRE monitor could

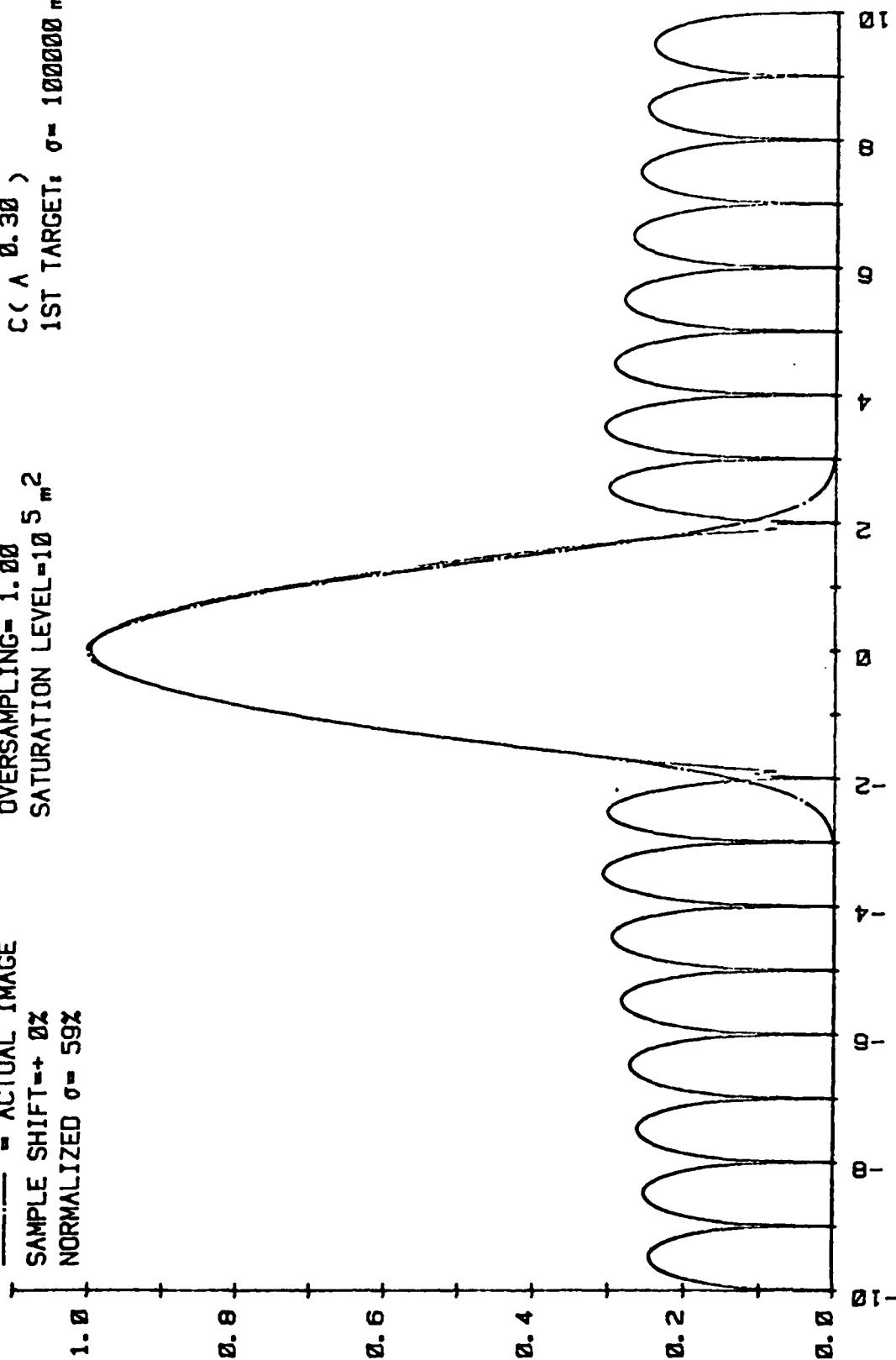
be used to monitor the output quality by selecting the appropriate section of the digital data stream and convolving the digital samples with a defined interpolation function (i.e., Gaussian), then plotting the resultant impulse response function. The fine resolution mode of UPD-4 can yield digital data which has the potential for a -35 dB Taylor weighted impulse response with -3 dB widths of 12-ft in range and 15-ft in cross range. These UPD-4 data usually have sample spacing of 10 ft in each dimension. If the UPD-4 data are error-free, SAPPHERE processing and Gaussian interpolation should yield impulse responses similar to those shown in Figures 3-4 through 3-6 (dashed curves). These curves represent the range dimension which has an ideal IPR width of 12 ft. These curves show the effects of different sample shifts with respect to the ideal mainlobe peak. A sample shift of 0% implies that the mainlobe peak of the impulse response has been sampled by the UPD-4 data. On the other hand, a sample shift of 50% corresponds to having the digital samples shifted by one-half the sampling interval. Also shown in Figures 3-4 through 3-6 is the error free impulse response of an analog processor (solid lines). These plots use an 11 bit input signal which has been compressed to 8 bits using a 0.3 power-law compression scheme (see Section 3.4). For these plots the -3 dB points are at a normalized output level of .9, and hence we see an excellent matching of the -3 dB to/with the IPR widths. At a level of -15 dB (i.e., .6 the normalized output scale), we see a small spreading up to 5% for the sampled image.

If we look at the two target cases where the targets are separated by 2 IPR widths, we see (in Figure 3-7) that there will be no dip between the two peaks. Figure 3-8 shows that these same two targets

are separated by 3 units, and, this time, we see a significant dip for the SAPPHIRE sampled image--but this is still much less than the analog equivalent. For the two-target case, we note that the apparent output image resolution can be greatly affected by the sampling, interpolation and grey scale remapping.

# GAUSSIAN INTERPOLATED IMAGE OF ONE POINT TARGET APPROXIMATE -35dB TAYLOR WEIGHTING

--- IDEAL IMAGE  
 --- ACTUAL IMAGE  
 SAMPLE SHIFT=+ 0%  
 NORMALIZED  $\sigma = 59\%$   
 K= 11 M= 8 N= 8  
 OVERSAMPLING= 1.00  
 SATURATION LEVEL=10<sup>5</sup> m<sup>2</sup>  
 C log( 2047A+1)  
 C( A 0.30 )  
 1ST TARGET:  $\sigma = 100000 \text{ m}^2$

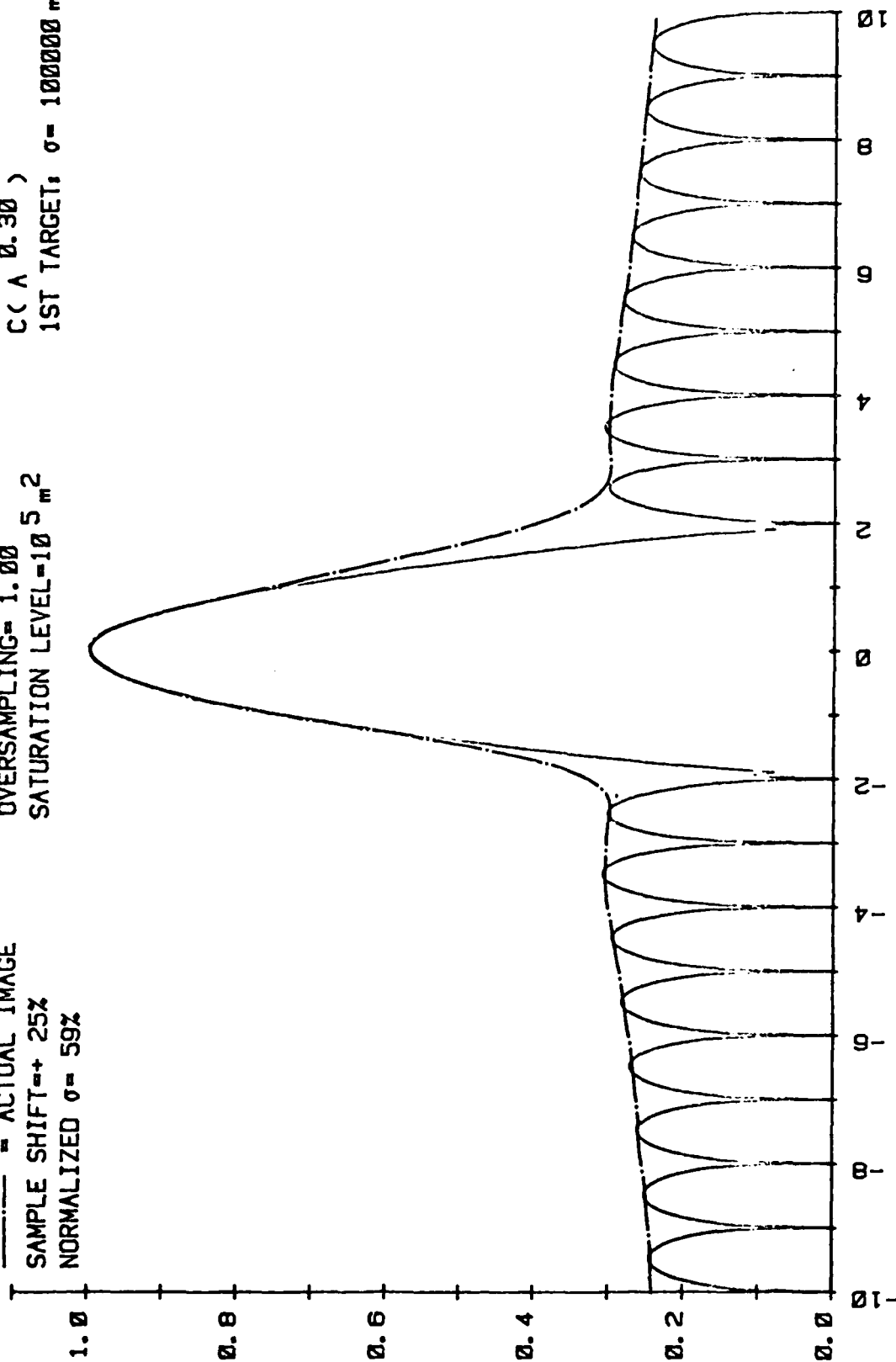


NORMALIZED DISTANCE

Figure 3-4. Simulated Output Zero Phase Shift

# GAUSSIAN INTERPOLATED IMAGE OF ONE POINT TARGET APPROXIMATE -35dB TAYLOR WEIGHTING

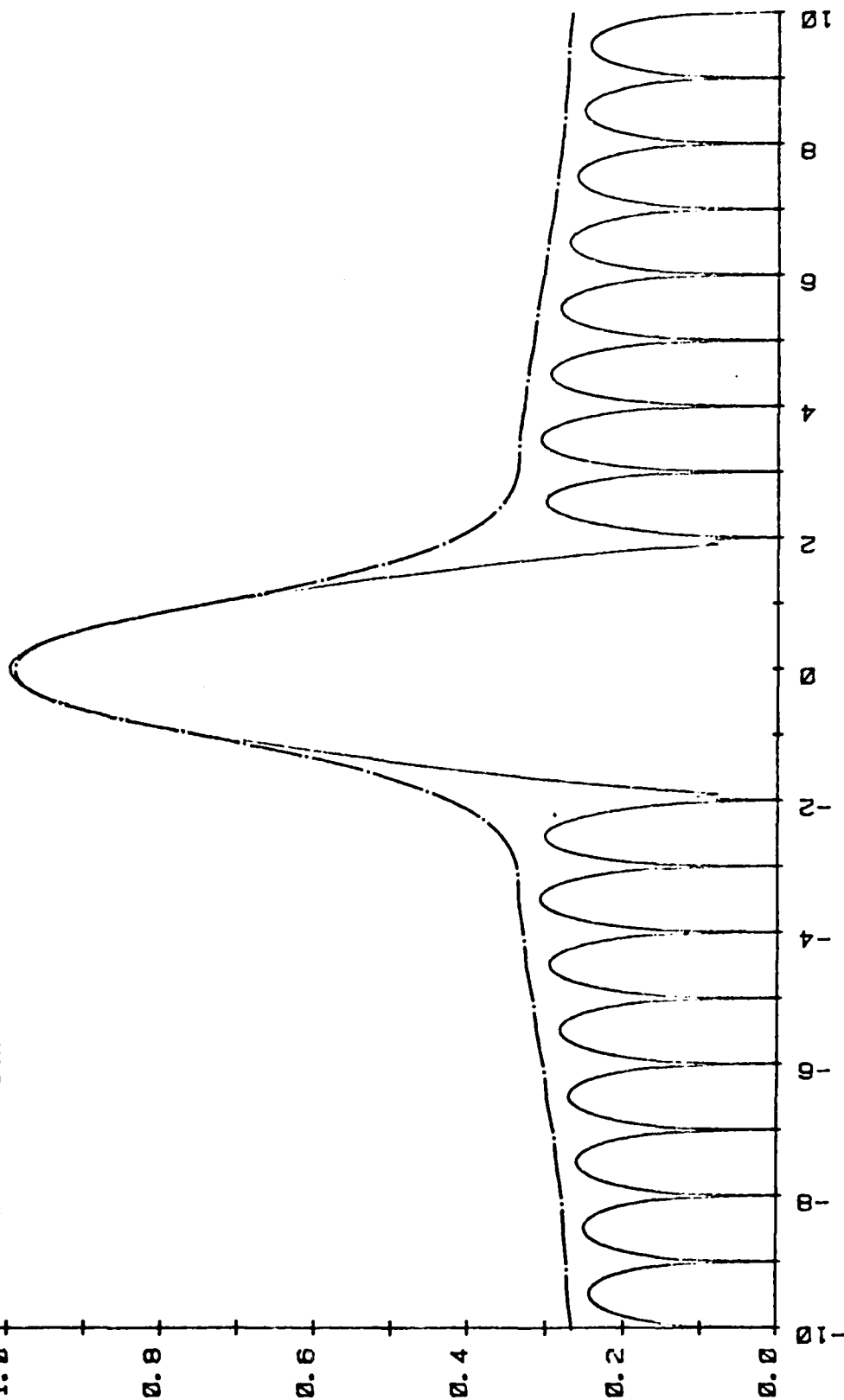
— = IDEAL IMAGE      K= 11      M= 8      N= 8      C log( 2047A+1)  
 - - - = ACTUAL IMAGE      OVERSAMPLING= 1.00      C( A 0.30 )  
 SAMPLE SHIFT=+ 25%      SATURATION LEVEL=10<sup>5</sup> m<sup>2</sup>  
 NORMALIZED  $\sigma$  = 59%      1ST TARGET:  $\sigma$  = 100000 m<sup>2</sup>



NORMALIZED DISTANCE  
 Figure 3-5. Simulated SAPPHIRE Output 25% Phase Shift

# GAUSSIAN INTERPOLATED IMAGE OF ONE POINT TARGET APPROXIMATE -35dB TAYLOR WEIGHTING

— = IDEAL IMAGE      K= 11      M= 8      N= 8      C log( 2047A+1)  
 - - - = ACTUAL IMAGE      OVERSAMPLING= 1.00      C( A 0.30 )  
 SAMPLE SHIFT=+ 50%      SATURATION LEVEL=10<sup>5</sup> m<sup>2</sup>  
 NORMALIZED σ= 59%      1ST TARGET: σ= 100000 m<sup>2</sup>



NORMALIZED DISTANCE  
 Figure 3-6. Simulated SAPPHIRE Output 50% Phase Shift

GAUSSIAN INTERPOLATED IMAGE OF TWO POINT TARGETS  
APPROXIMATE -35dB TAYLOR WEIGHTING

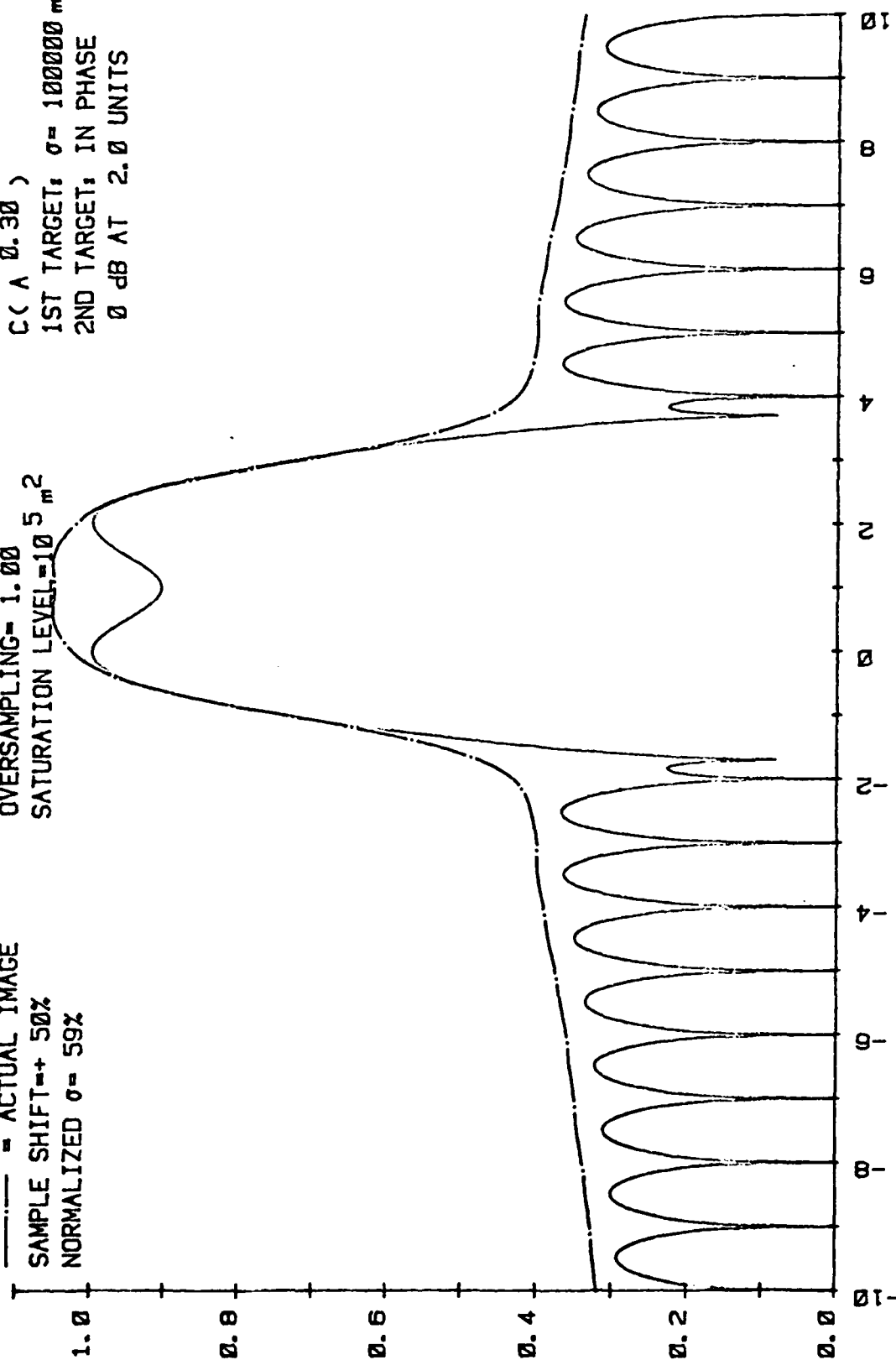
——— = IDEAL IMAGE  
 ——— = ACTUAL IMAGE  
 SAMPLE SHIFT = + 50%  
 NORMALIZED  $\sigma$  = 59%

```

11      M= 8      N= 8
OVERSAMPLING= 1.00
SATURATION LEVEL=10 5 2

```

C log( 2047A+1)  
C( A 0.30 )  
1ST TARGET:  $\sigma = 10000 m^2$   
2ND TARGET: IN PHASE  
0 dB AT 2.0 UNITS

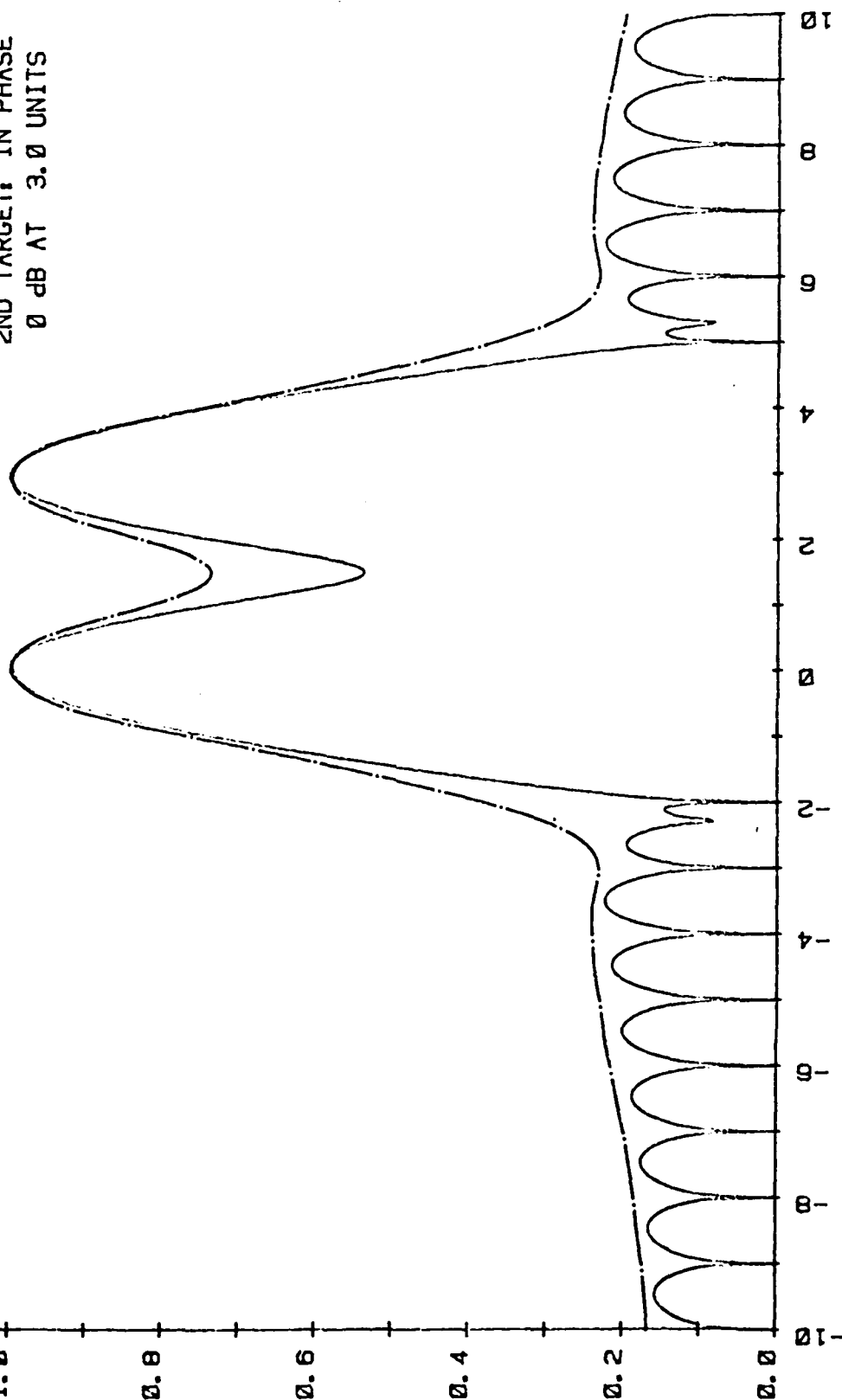


## NORMALIZED DISTANCE

Figure 3-7. Simulated SAPHIRE Output Two Targets Separated by Two IPR's

# GAUSSIAN INTERPOLATED IMAGE OF TWO POINT TARGETS APPROXIMATE -35dB TAYLOR WEIGHTING

— = IDEAL IMAGE       $K=11$        $M=8$        $N=8$        $C \log(2047A+1)$   
 - - - = ACTUAL IMAGE      OVERSAMPLING = 1.00       $C(A \ 0.30)$   
 SAMPLE SHIFT = + 50%      SATURATION LEVEL =  $10^5 m^2$   
 NORMALIZED  $\sigma = 59\%$   
 1ST TARGET:  $\sigma = 100000 m^2$   
 2ND TARGET: IN PHASE  
 0 dB AT 3.0 UNITS



NORMALIZED DISTANCE

Figure 3-8. Simulated SAPPHIRE Outputs Two Targets Separated by Three IPR's



### 3.3 AUTOMATIC CHANGE DETECTOR (ACD)

The ACDS is in the image path between the SAPPHIRE processor and the ES when ABLE is operating in the full-up mode. The transformations within the ACD will therefore directly impact image quality and its subsequent interpretability.

Figure 3-9 illustrates the 10 foot A channel image path through the ACDS while Figure 3-10 shows the 20 foot B channel path. The 20 foot image will not normally be furnished to the ES as a mission image therefore, this discussion will be concerned only with the A image path which will be used for interpretation.

Two processes affecting the A image quality are the bit errors associated with the mission storage and then MAPS compression/decompression processing.

Mission storage is on a high density (80 m byte) disks using the usual error protection and controls. BER in this case should be better than  $10^{-9}$ , which equates to a one pixel error every 150 ES frames. This is an insignificant amount.

The MAPS compression algorithm is an adaptive scheme with variable compression ratios which may be set for a desired level of image quality. The MAPS algorithm operates by selecting blocks containing  $2^n$  pixels ( $n = 1, 2, 3$ , or  $4$ ), and attempting to represent the block by a single mean value. The difference between the mean and each pixel intensity determines the level of compression ( $n$ ). The algorithm for selecting blocks is chosen to minimize blockiness and make the image more pleasing. One advantage of the MAPS algorithm is that it distributes bit errors over parts of the image rather than concentrating them in a line.

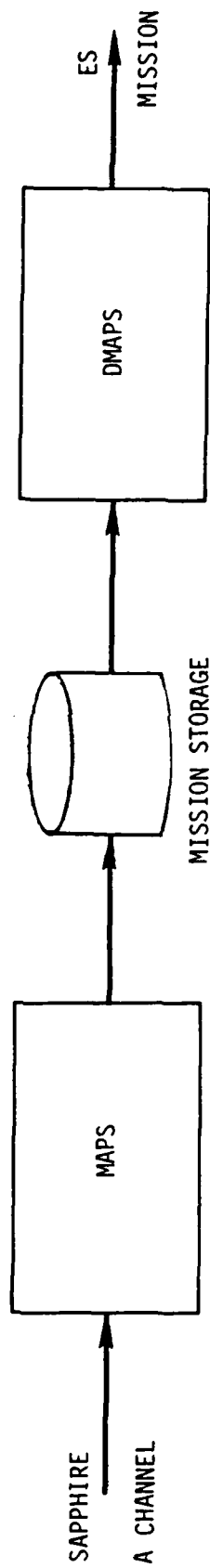


FIGURE 3-9. ACDS MISSION IMAGE PATH (10 FOOT).

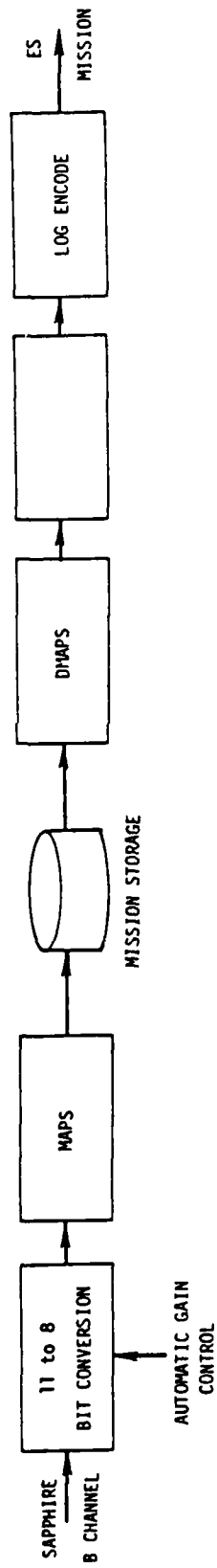


FIGURE 3-10. ACDS MISSION IMAGE PATH (20 FOOT)

The complexity of MAPS is not amenable to the straightforward IPR analysis employed elsewhere in this report, therefore no comparable quantification of MAPS impact on image quality is possible. Instead, we can only state the subjective observation that MAPS will degrade image quality in some way which will be significant at high compression ratios and of no consequence at low levels.

### 3.4 EXPLOITATION SUBSYSTEM (ES)

#### 3.4.1 General Description

The exploitation subsystem is that collection of subsystems that receives image data in digital form from the automatic change detector and presents this information on soft copy displays for interpretation. Figure 3-11 shows a block diagram of these functions. The primary functions involving the dual data stream are as follows:

- buffer,
- compression,
- gamma correction,
- displays/control (ACD), and
- resampling

The exploitation subsystem has the responsibility for the display of the imagery, and it is here that the image quality parameters discussed earlier are both displayed and measurable. In the digital data stream there is little affect on image quality parameters except for bit errors. The bit errors can cause spurious responses and can affect the measurement of the image quality parameters, but, for the most part, they do not impact most image quality parameters. These parameters are affected by compression, sampling and remapping at the displays. In the following sections we will discuss these effects.

#### 3.4.2 Interface Requirements

The exploitation subsystem interfaces with the ACD and the interpreter. From the ACD, the ES receives 8 bit log encoded data which has a 10 ft

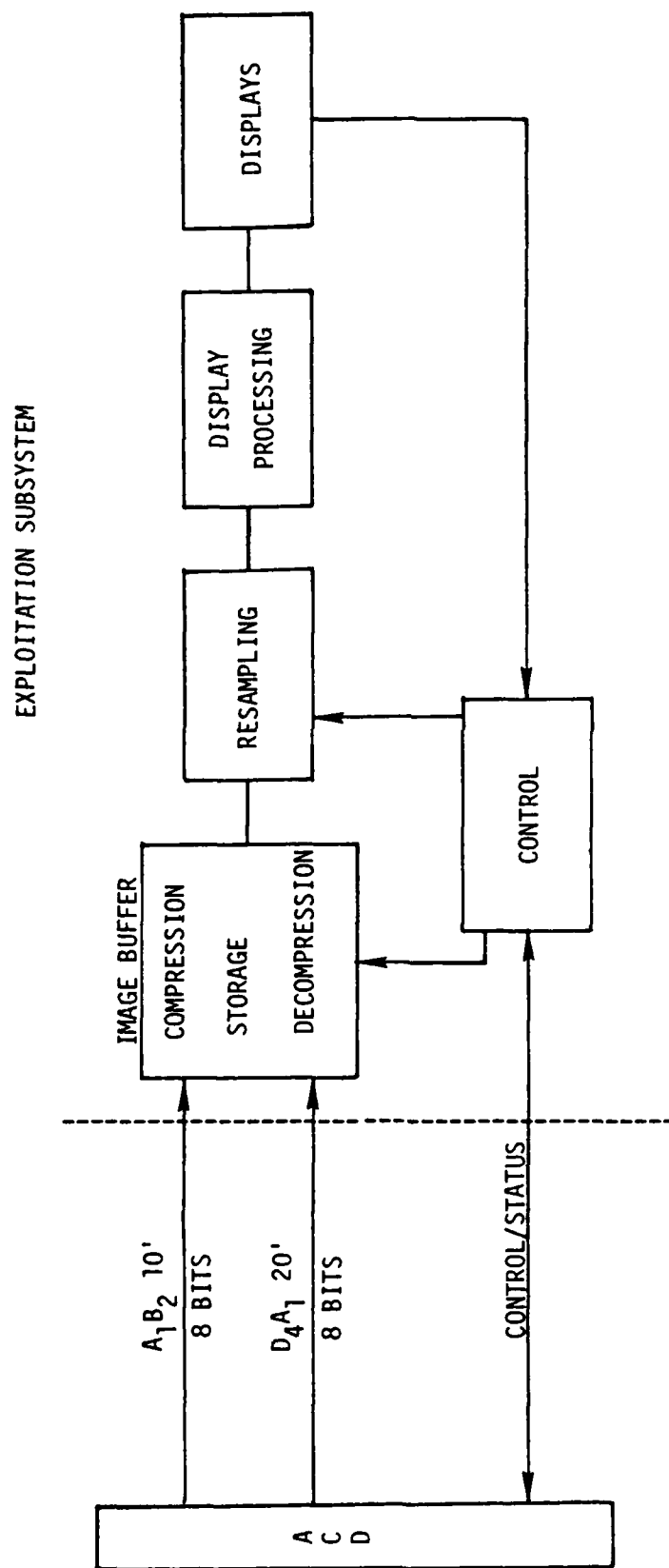


Figure 3-11. Exploitation Subsystem

sample spacing on one input line, and the second input line is 20 ft sample spacing at 8 bits. Also on this line are the changes which were detected by the ACD. One of the primary input data concerns is that the quality of the data, which has been compressed by SAPPHIRE from 11 bits to 8 bits and passed through ACD to ES, has been maintained. Figures 3-12 through 3-17 show the effects on signal amplitude fidelity of various logarithmic and power-law encoding schemes. In these figures we see 11 bit linear amplitude data compressed to 8 and 5 bits using log compression and then antilogged for comparison to the original data levels.

Figure 3-12 is a macroscopic view of this encoding process. In this figure we see the three curves:

1. linear amplitude data quantized to 8 bits ;
2. the logarithm of one above quantized to 8 bits;
3. the antilog of two above quantized to 8 bits .

The third curve has been artificially displaced upwards by one unit so that it can be distinguished from the first one. Note on curve 3 the wiggles are caused by quantization effects and not by artifacts from a poor plotter. Figure 3-13 is a plot of the per cent error as a function of the input level and final quantization level. Specifically, the 11 bit linear amplitude data was compressed logarithmically and quantized to 8 bits. The data was next antilogged, keeping only the number of discrete levels offered by 8 bits, and plotted to represent the error between the original input value and the resulting value after compression and decompression. For example, consider any original input value level and its final output value. For an eleven to

# EFFECTS OF LOG ENCODING

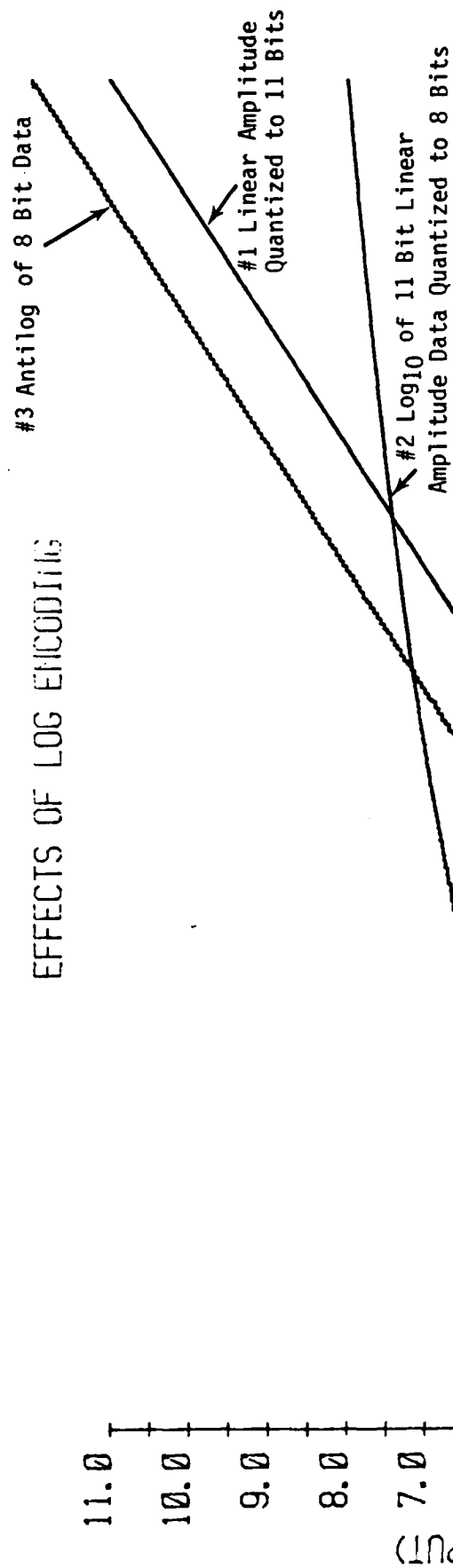


Figure 3-12. 11 Bit to 8 Bit Log Encoding



# EFFECT OF LOG ENCODING

11 BIT DATA TO 8 BITS

$$Y = C \log(bA + 1) \quad b = 1.00$$

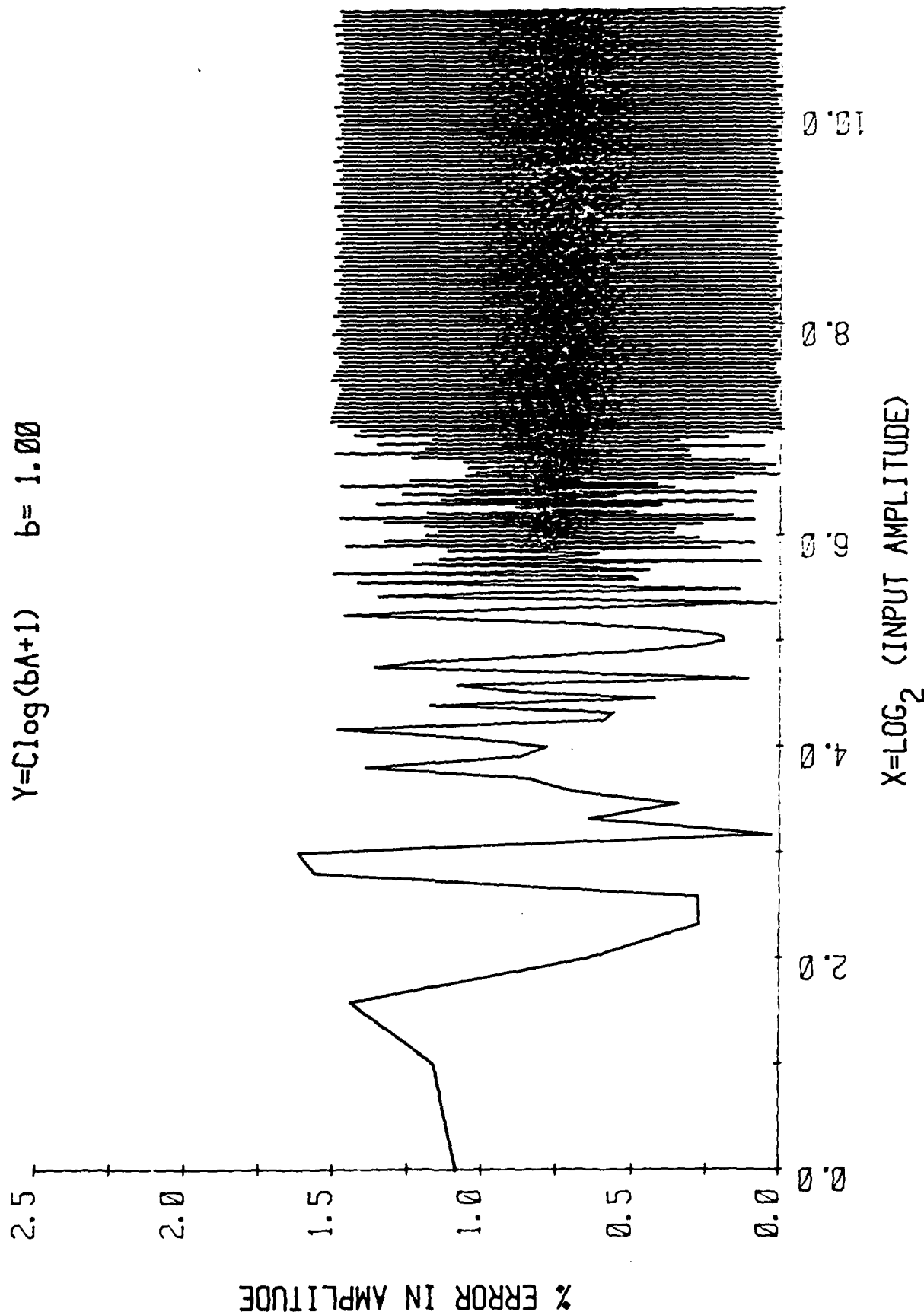


Figure 3-13. Percent Error for 11 Bit to 8 Bit Log Encoding

# EFFECTS OF LOG ENCODING

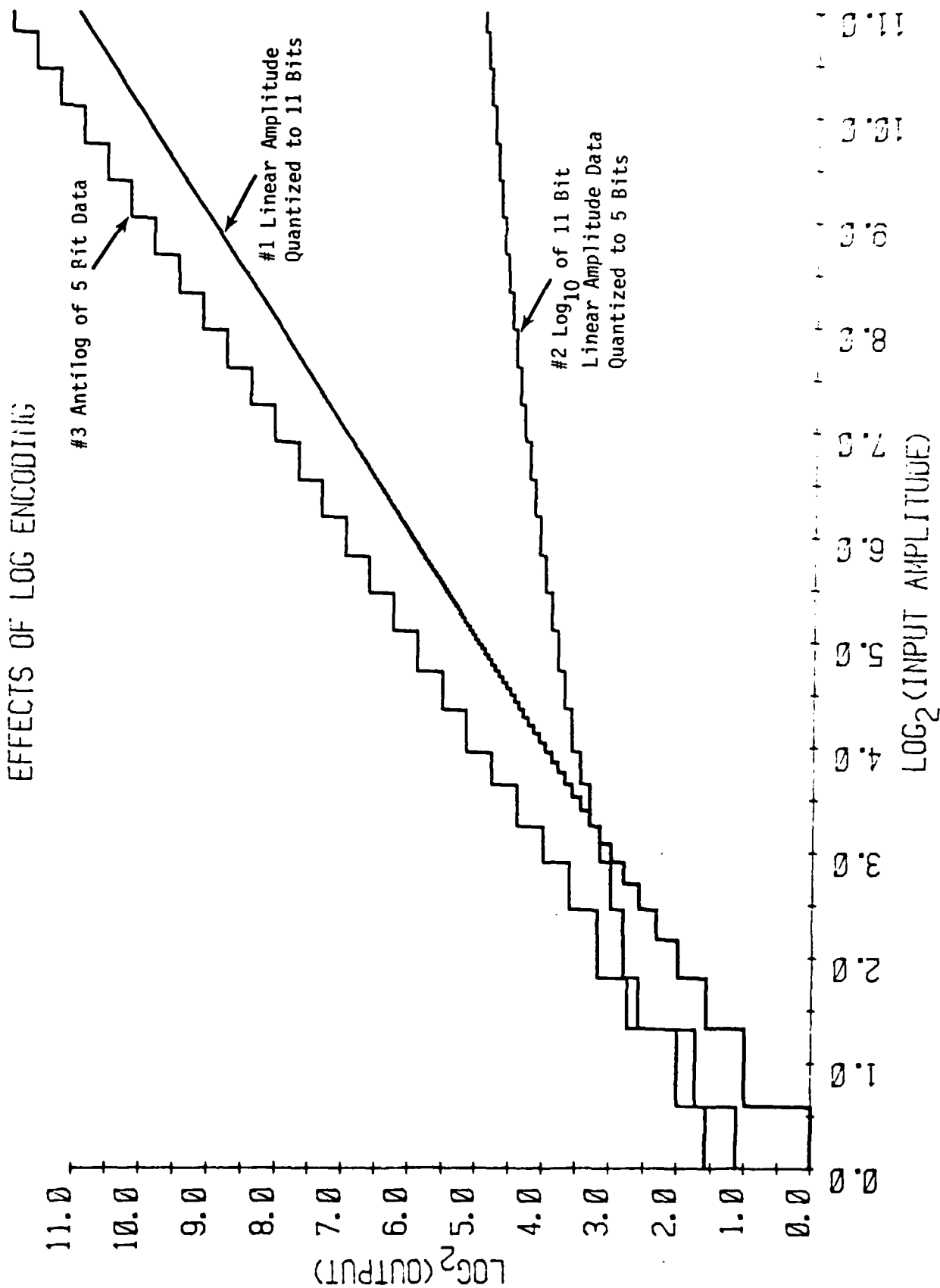


Figure 3-14. 11 Bit to 5 Bit Log Encoding

# EFFECT OF LOG ENCODING

11 BIT DATA TO 5 BITS

$$Y = C \log(bA+1) \quad b = 1.00$$

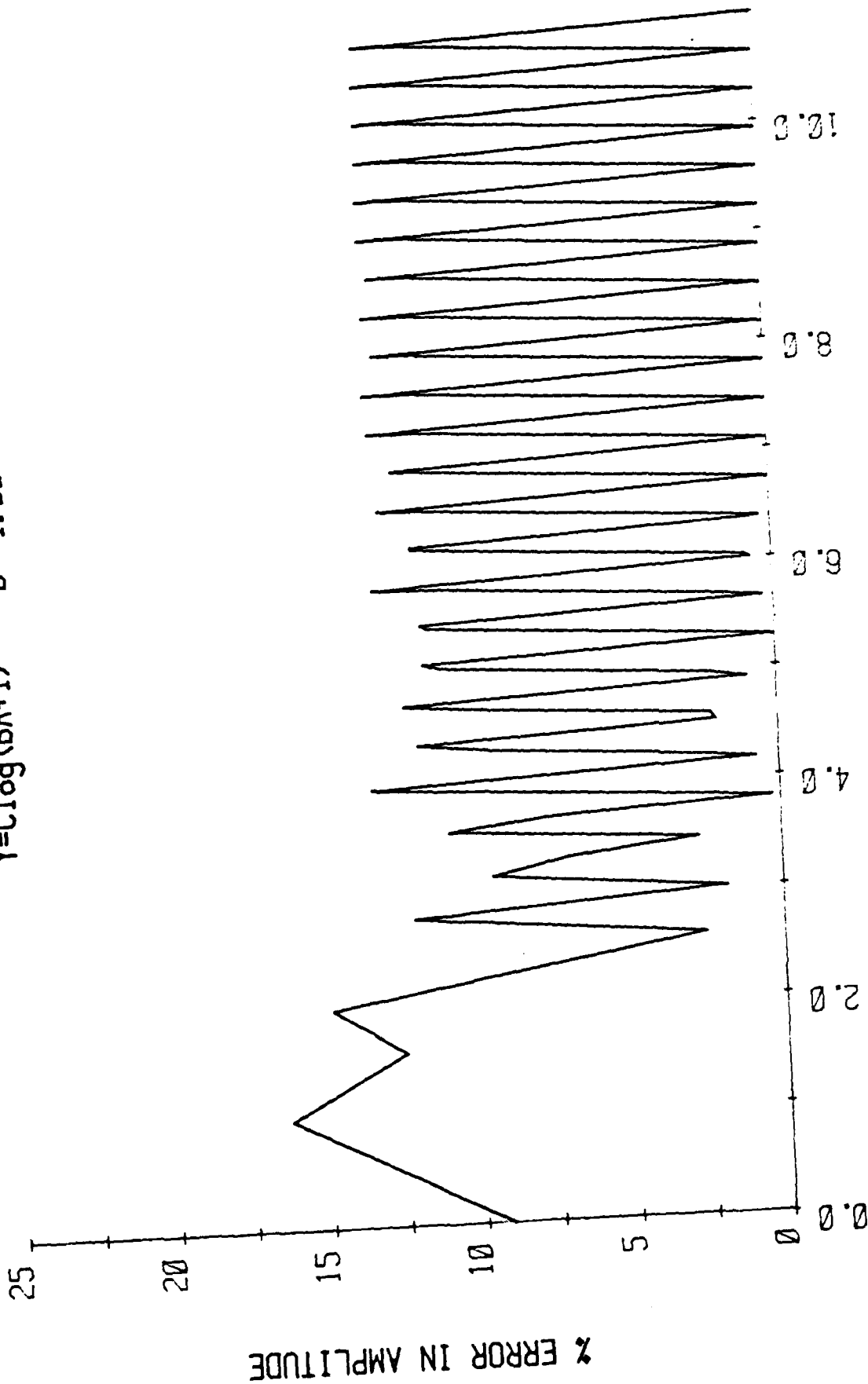


Figure 3-15. Percent Error for 11 Bit to 5 Bit Log Encoding

# EFFECTS OF POWER-LAW ENCODING

11 BIT DATA TO 8 BITS

$$Y=C(A^b) \quad b=0.50$$

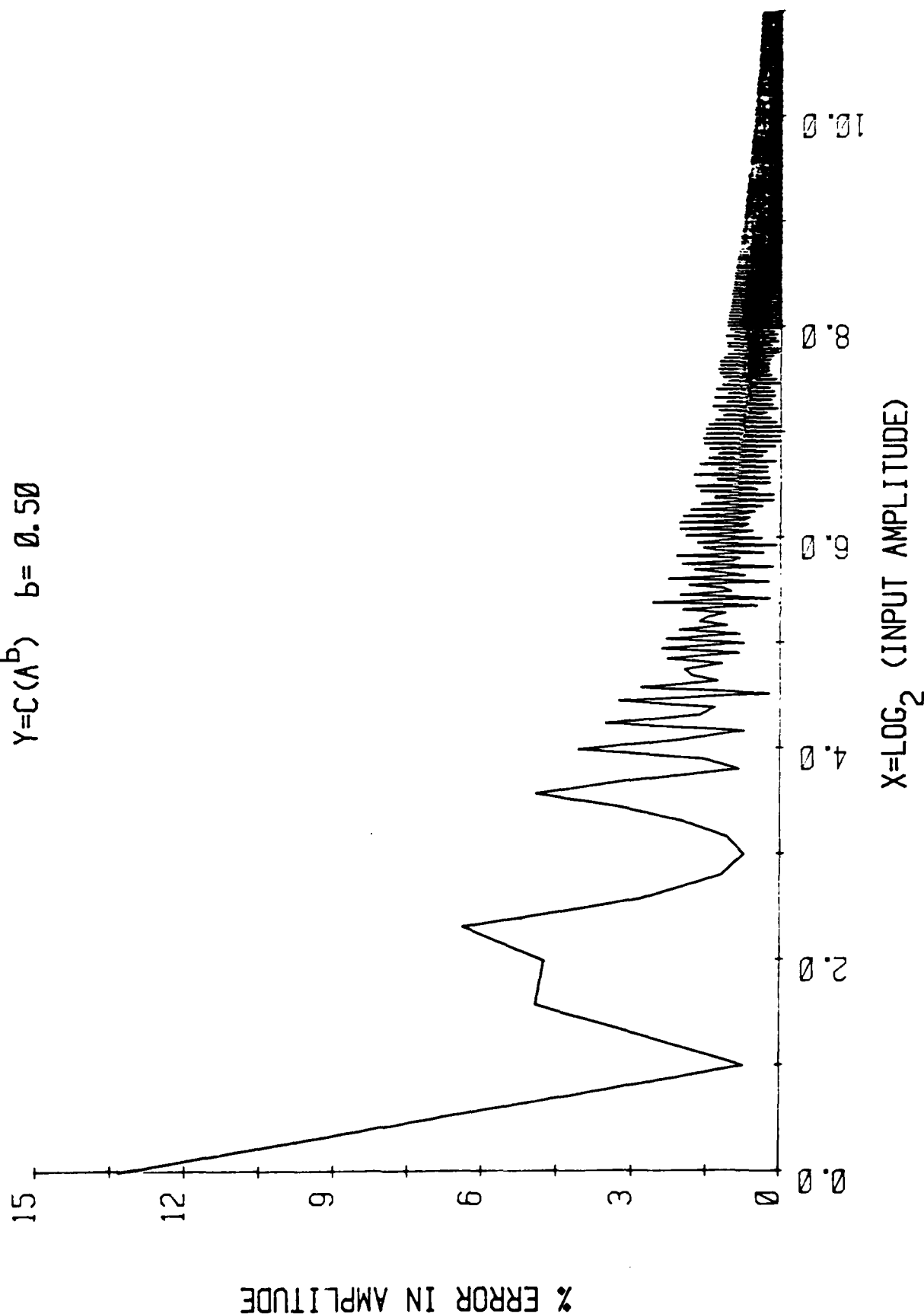


Figure 3-16. 11 Bit to 8 Bit Power-Law Encoding

# EFFECTS OF POWER-LAW ENCODING

11 BIT DATA TO 5 BITS

$$Y=C(A^b) \quad b=0.50$$

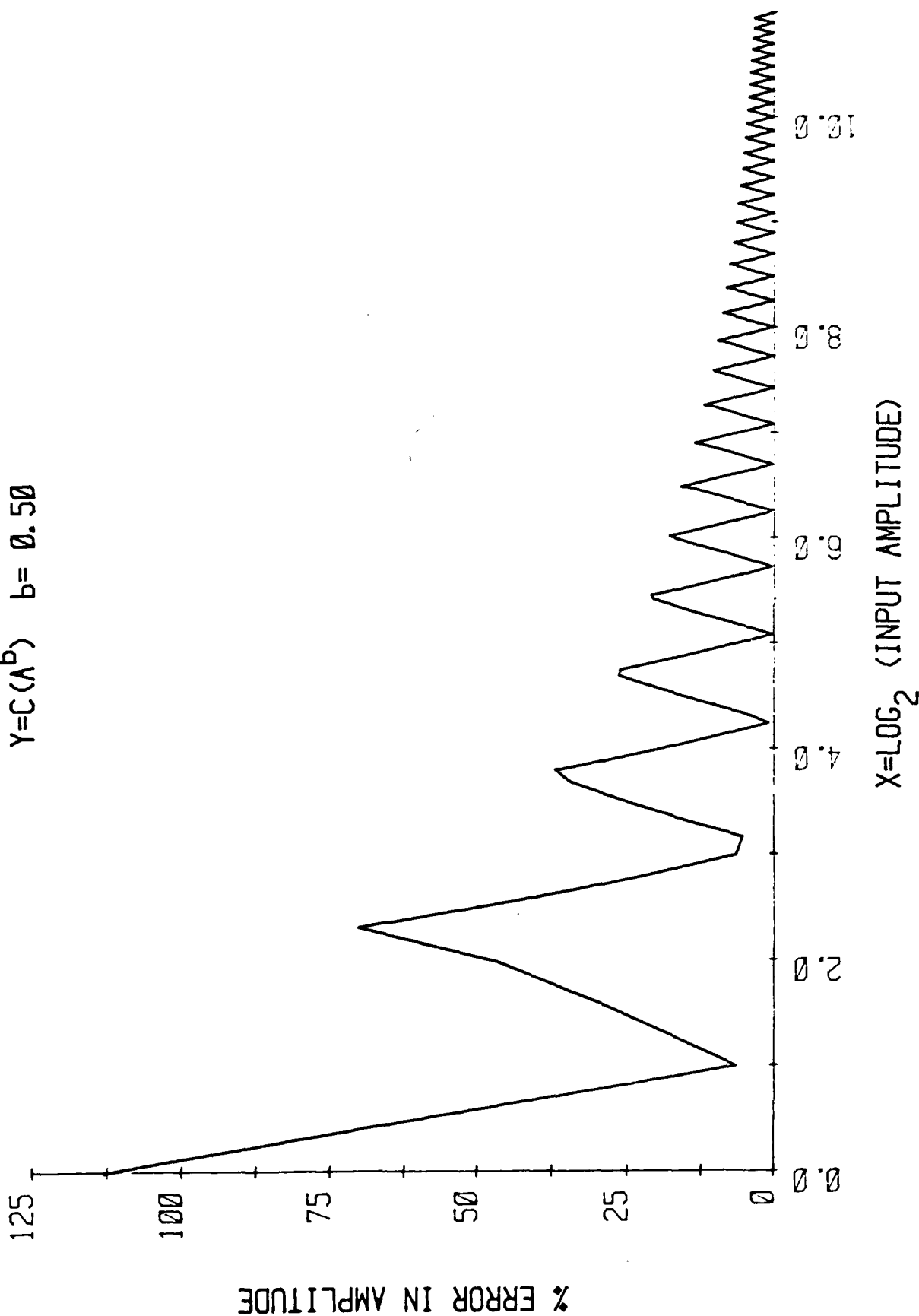


Figure 3-17. 11 Bit to 5 Bit Power-Law Encoding

eight bit system, there will be a maximum error of less than 2% in amplitude from the target's original value. Figures 3-14 and 3-15 show the macroscopic and microscopic errors plotted as a function of input level for 5 bit quantization with 11 bit input data and logarithmic compression. Figures 3-16 and 3-17 show the effects of using a power-law (i.e.,  $CA^b$ ) compression scheme for 8 bit and 5 bit output data. In this approach, the errors are small for high intensity targets and large for the small targets.

The output of the ES is soft copy display to the interpreter. At this output, the CRT's can add significant errors and modifications to all the image quality parameters.<sup>1</sup> Figure 3-18 shows that CRT output luminance is not necessarily linearly related to the command level. This artifact would effect the image intensity fidelity parameter. Likewise, the CRT spot size and shape can effect the impulse response size and shape, as well as contrast ratio, etc. The following sections on sampling and compression will illustrate these effects.

#### 3.4.3 Compression

In Figure 3-4 the block diagram for the ES, we depict a data compression function within the Image Buffer. The purpose of the compression function is to reduce the number of image bits from 8 bits to 4 bits average.

---

<sup>1</sup>Briggs, Dr. J., "Procedures for Determining Digital CRT Displays Best Gammon Function".

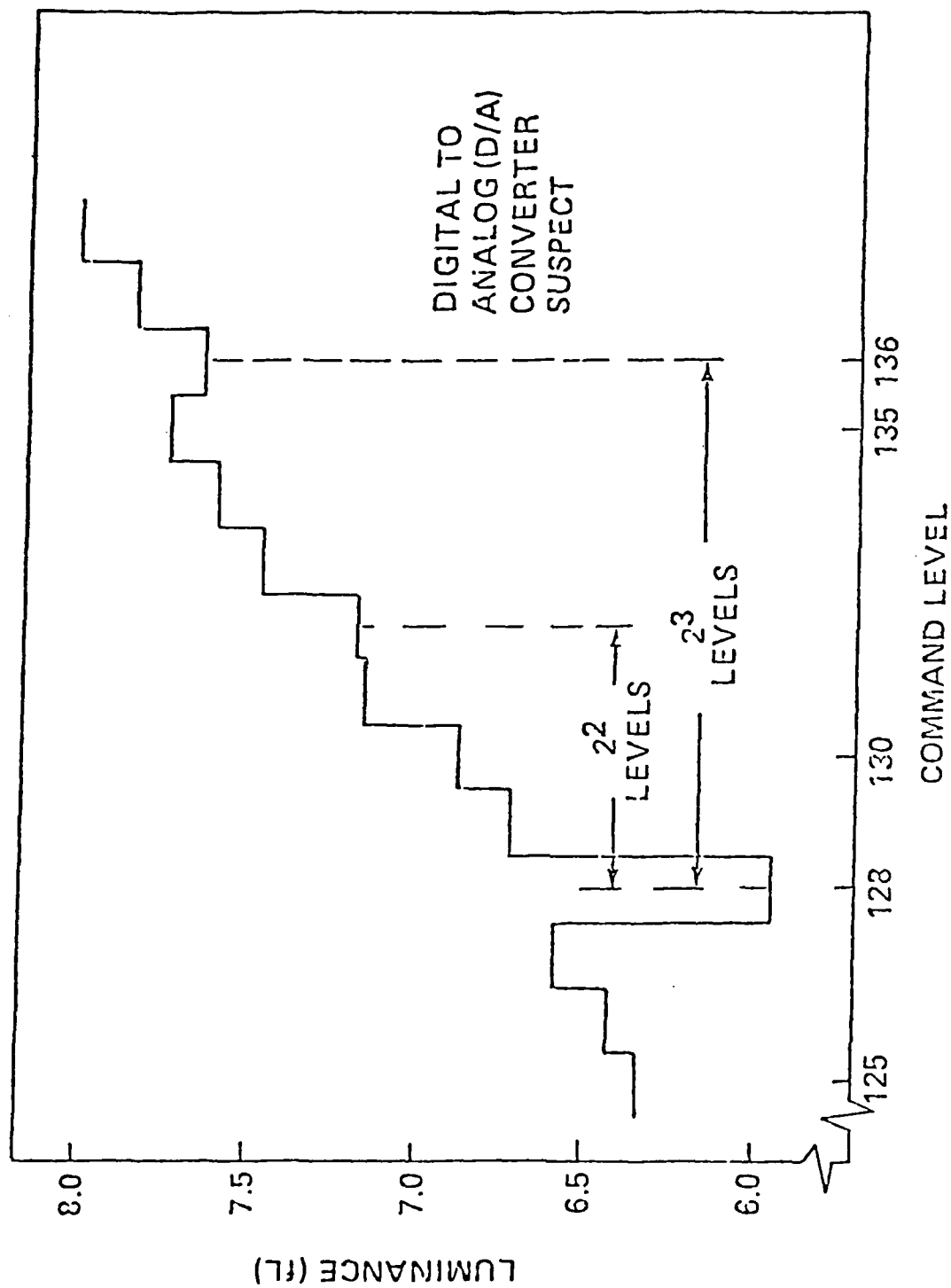


Figure 3-18. Example of Irregularities in Digital CRT Display's Gamma Function (Real Data)  
(From Briggs - Ref. 1)

Some of the data compression approaches to be considered are:

- 2-D cosine transform,
- DPCM,
- Huffman code, and
- Power-law/logarithmic.

The 2-D cosine transform is used to disperse image data not too dissimilar from the original dispersed phase history data, and it reduces the number of bits stored in the transform plane. Differential pulse code modulation, DPCM, operates on the premise that neighboring pixels are highly correlated. The radar data with its coherent source and specular output scenes offers an interesting challenge to this type of encoder. Huffman encoding utilizes the scene statistics to encode those image intensity values which occur with high frequency and with short word lengths (i.e., fewer bits per pixel). Given the radar scene histogram with the large percentage of pixels in the lower level bits, a Huffman code should offer some data compression without any image quality impacts.

The last compression code (i.e., logarithmic/power-law compression) also offers an interesting approach. Figure 3-19 is a plot of four point targets of different amplitudes quantized to 11 bits. In this plot, the data was cosine weighted and quantized to 11 bits, similar to the output from the SAPPHIRE processor. The sampling rate is infinite (i.e., analog), and the target sizes range from  $10^6 \text{ ft}^2$  to  $1 \text{ ft}^2$ . In Figure 3-20, we selected the  $10^6 \text{ ft}^2$  target at 11 bits and compressed it to 8 bits using a logarithmic compression scheme and a power-law compression scheme.



# PROCESSOR AMPLITUDE RESPONSE (COSINE WEIGHTING) K= 11

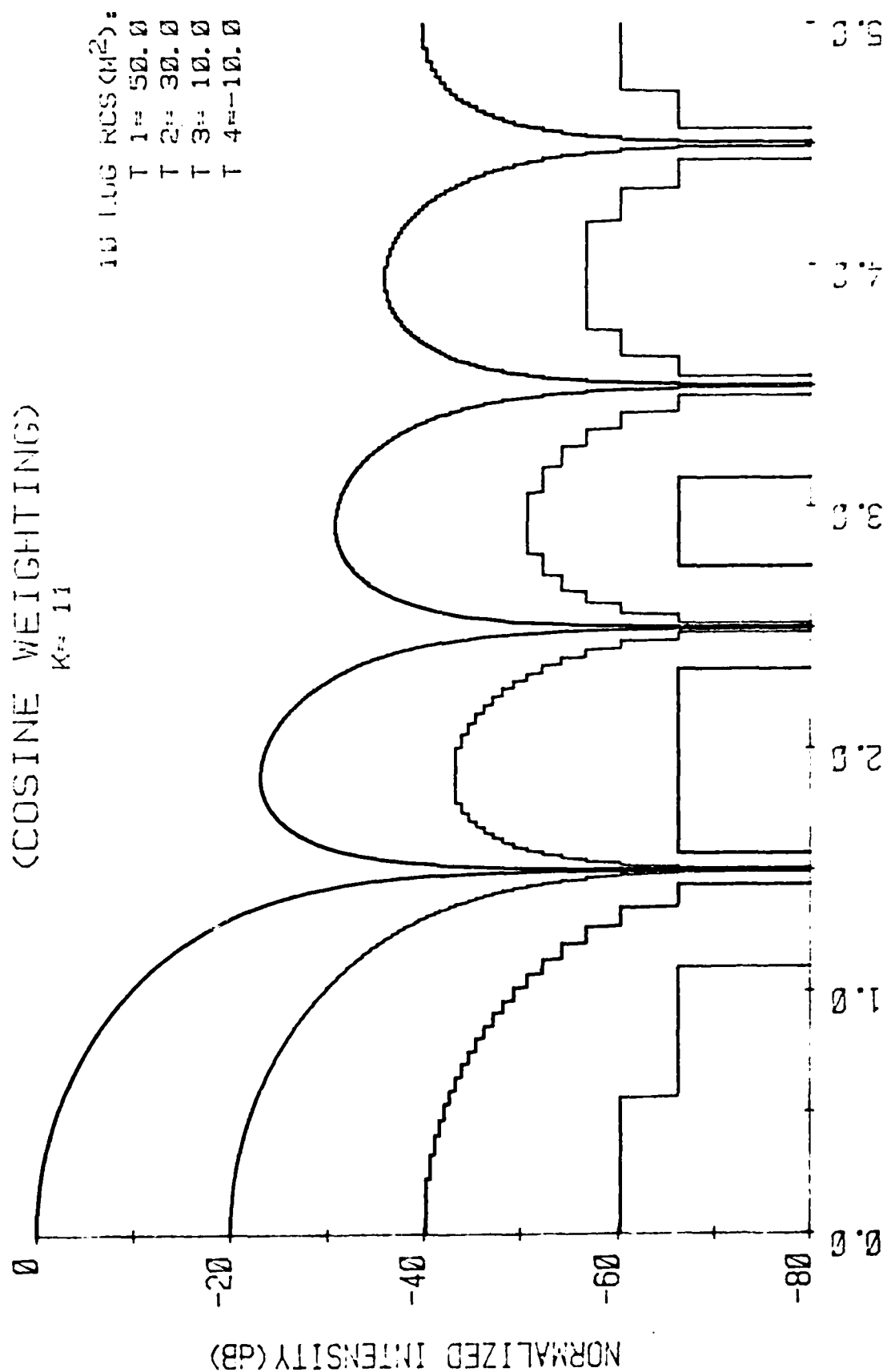


Figure 3-19. Four Point Targets Quantized to 11 Bits

# PROCESSOR OUTPUT RESPONSE (COSINE WEIGHTING)

$K=11$   $M=8$

$C \lambda^b$   $b=0.553$

$C \log(L\lambda+1)$   $b=20.47$

$10 \log RCS(M^2)$   
 $T = 50.0$

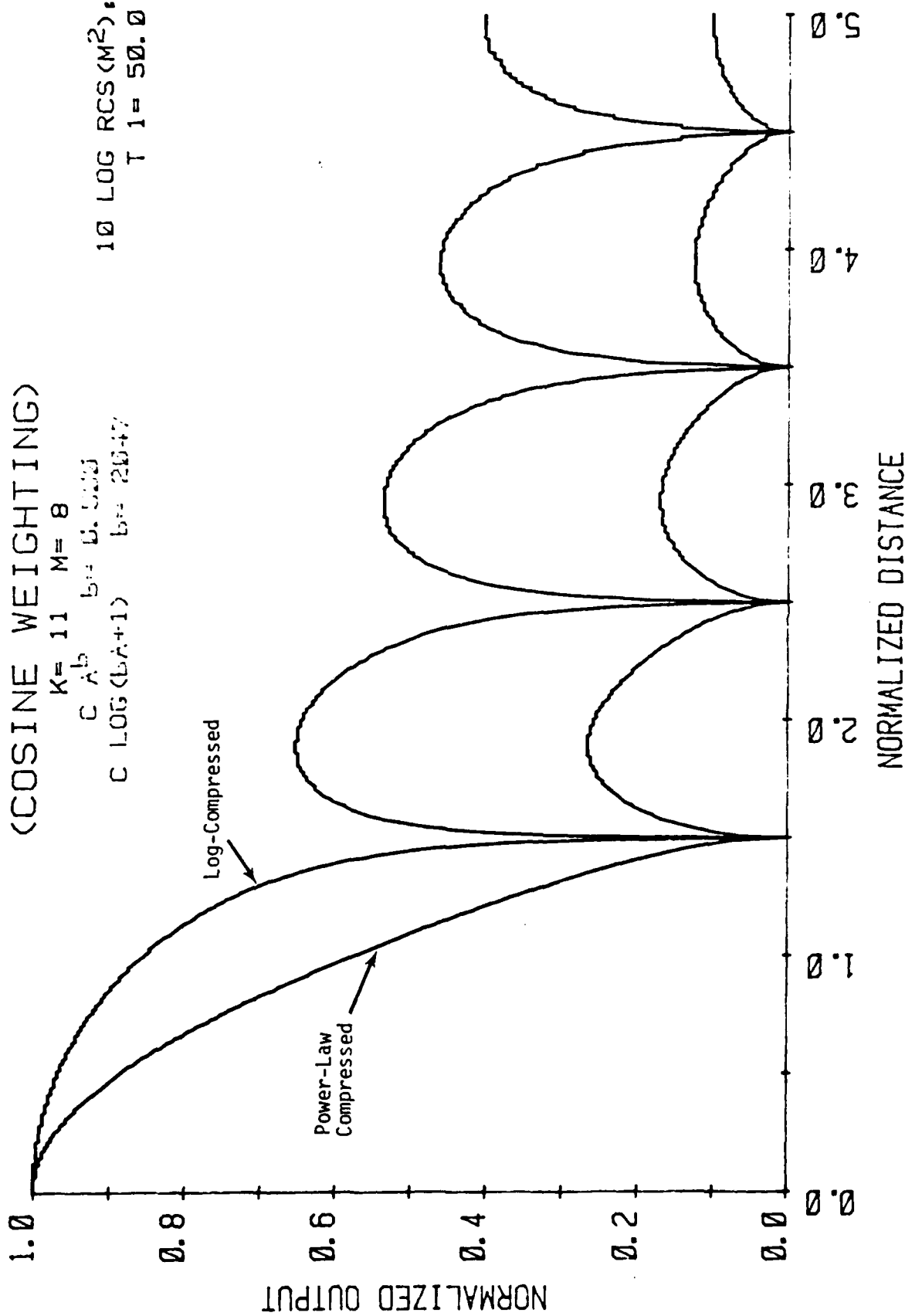


Figure 3-20. Comparison of Power-Law & Logarithmic Compression Schemes

We note that the side-lobe- to main-lobe- ratio is better for power-law compression. It is worthy to note that radar interpreters have empirically selected the power-law compression approach over the logarithmic compression.

In Figure 3-21 we have plotted four IPR's that range in size from  $10^6 \text{ft}^2$  to  $1 \text{ft}^2$ , and each of these IPR's has been power-law compressed and quantized to 8 bits. In this figure, we log compressed the original 11 bit data to 8 bits, then took the antilog at 8 bits, and power-law compressed this result with 8 bits quantization. An overlay of this figure with a direct 11 bit to 8 bit power-law compression (Figure 3-22) reveals an almost imperceptible difference in the IPR shapes. Figures 3-23 and 3-24 show the effects of this same compression scheme if 5 bits are used for log encoding and power law compression. When these results are interpolated with the CRT writing beam (i.e., Gaussian), the impulse response function will be considerably smoother.

These examples indicate that some image quality will be lost due to compression. In an attempt to quantify this degradation, a simulation model was developed to generate simulated impulse responses using different compression algorithms. The model is diagrammed as Figure 3-25.

Three types of compressions were investigated with the model. They are log encoding (Figure 3-26), and two types of DPCM. The first type of DPCM assigns bits according to Table 3-1, which was supplied by Goodyear Aerospace Company as the algorithm used in the ABLE system (Figure 3-27). The second type of DPCM assigns bits in a linear fashion (Figure 3-28). A 9 bit storage register

TABLE 3-1. ABLE DPCM CODE.

DPCM CODE TABLE			
DIFFERENCE $\Delta$	QUANTIZER OUTPUT	CODER OUTPUT	DECODER OUTPUT
-255 $\rightarrow$ -107	-125	0	Same as Quantizer Output
-106 $\rightarrow$ -45	-65	1	
-44 $\rightarrow$ -19	-28	2	
-18 $\rightarrow$ -10	-13	3	
-9 $\rightarrow$ -5	-6	4	
-4 $\rightarrow$ -3	-3	5	
-2	-2	6	
-1	-1	7	
0 $\rightarrow$ 1	1	8	
2	2	9	
3 $\rightarrow$ 4	3	10	
5 $\rightarrow$ 9	6	11	
10 $\rightarrow$ 18	13	12	
19 $\rightarrow$ 44	28	13	
45 $\rightarrow$ 106	65	14	
107 $\rightarrow$ 255	125	15	

# DATA COMPRESSION OUTPUT (COSINE WEIGHTING)

K= 11 M= 8 N= 8  
C LOG(bA+1) b= 20.77.000  
C A<sup>d</sup> d= 0.500

10 LOG RCS (m<sup>2</sup>):  
T 1= 50.0  
T 2= 30.0  
T 3= 10.0  
T 4= 15.0

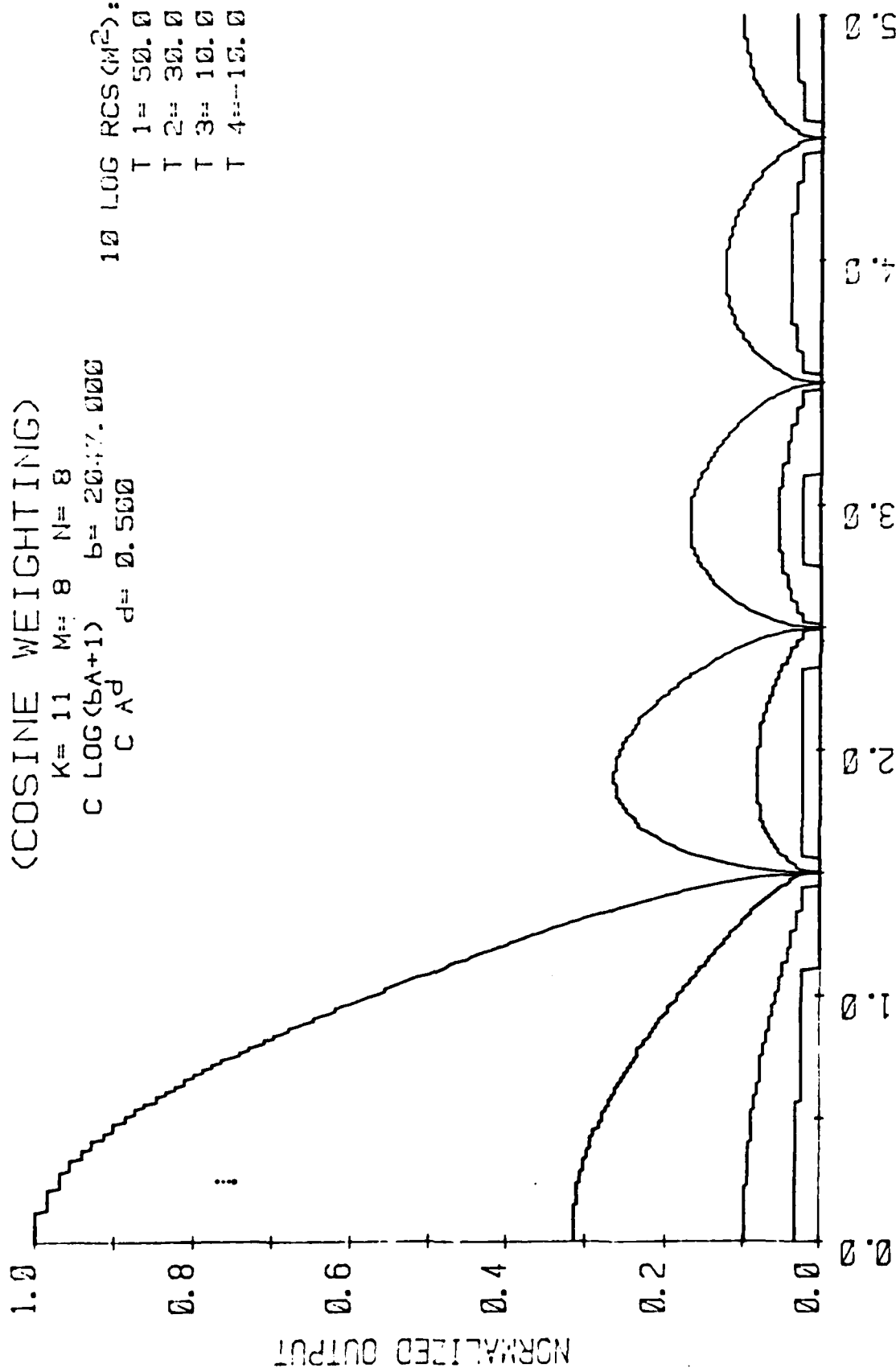


Figure 3-21. Log Encoded/Power-Law Compressed to 8 Bits

# DATA COMPRESSION OUTPUT (COSINE WEIGHTING)

K= 11 M= 8 N= 8  
C A<sup>b</sup> b= 0.500  
C A<sup>d</sup> d= 0.500

10 1.00 RCS (M<sup>2</sup>):  
T 1= 50.0  
T 2= 30.0  
T 3= 10.0  
T 4= -10.0

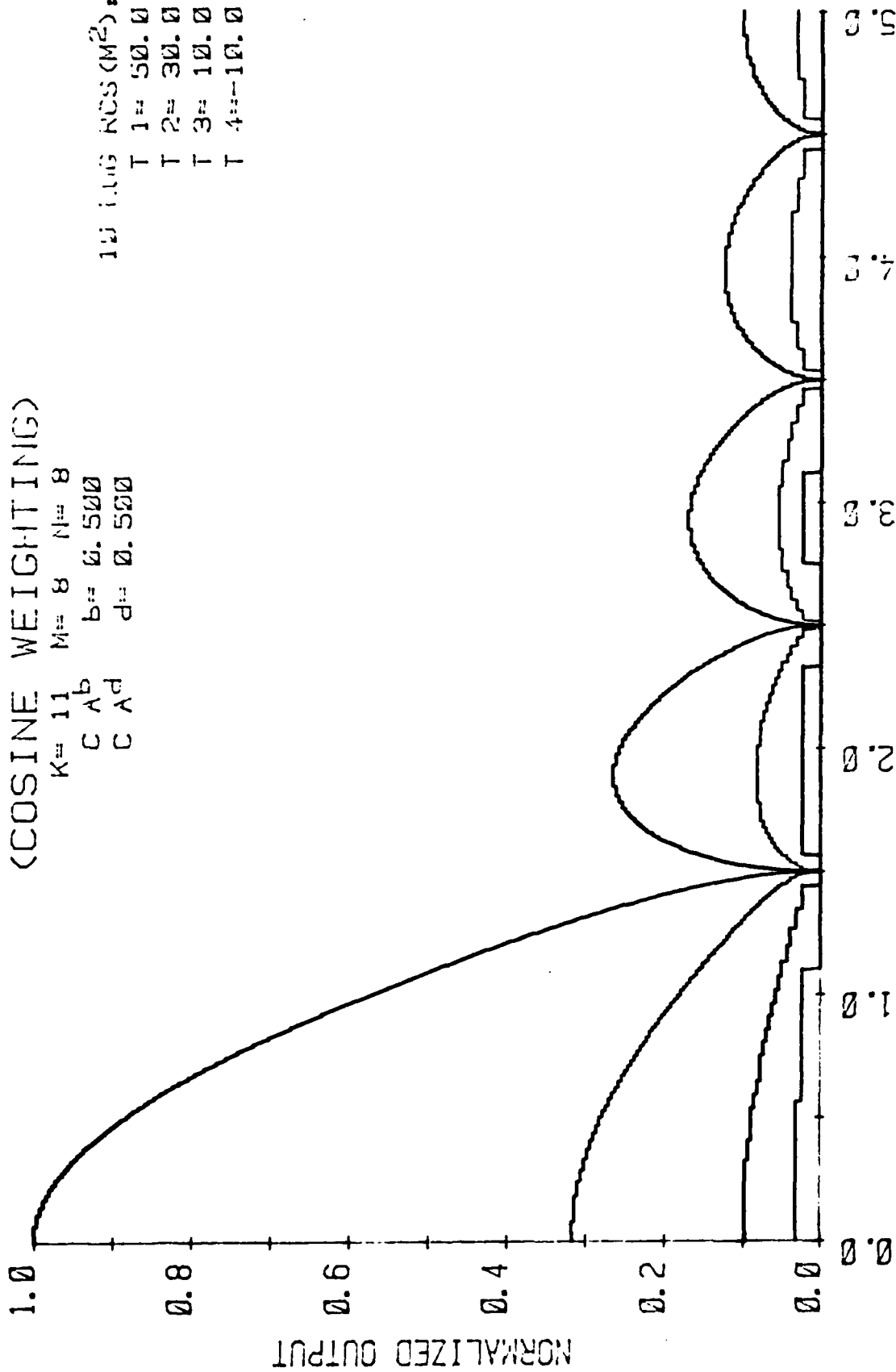


Figure 3-22. Direct Power-Law Compression to 8 Bits

# PROCESSOR OUTPUT RESPONSE (COSINE WEIGHTING)

$K=11$   $M=5$

$C \lambda^b$   $b=0.503$

$C \text{ LOG}(bA+1)$   $b=20.17$

$10 \text{ LOG RCS}(M^2)$   
 $T 1=50.0$

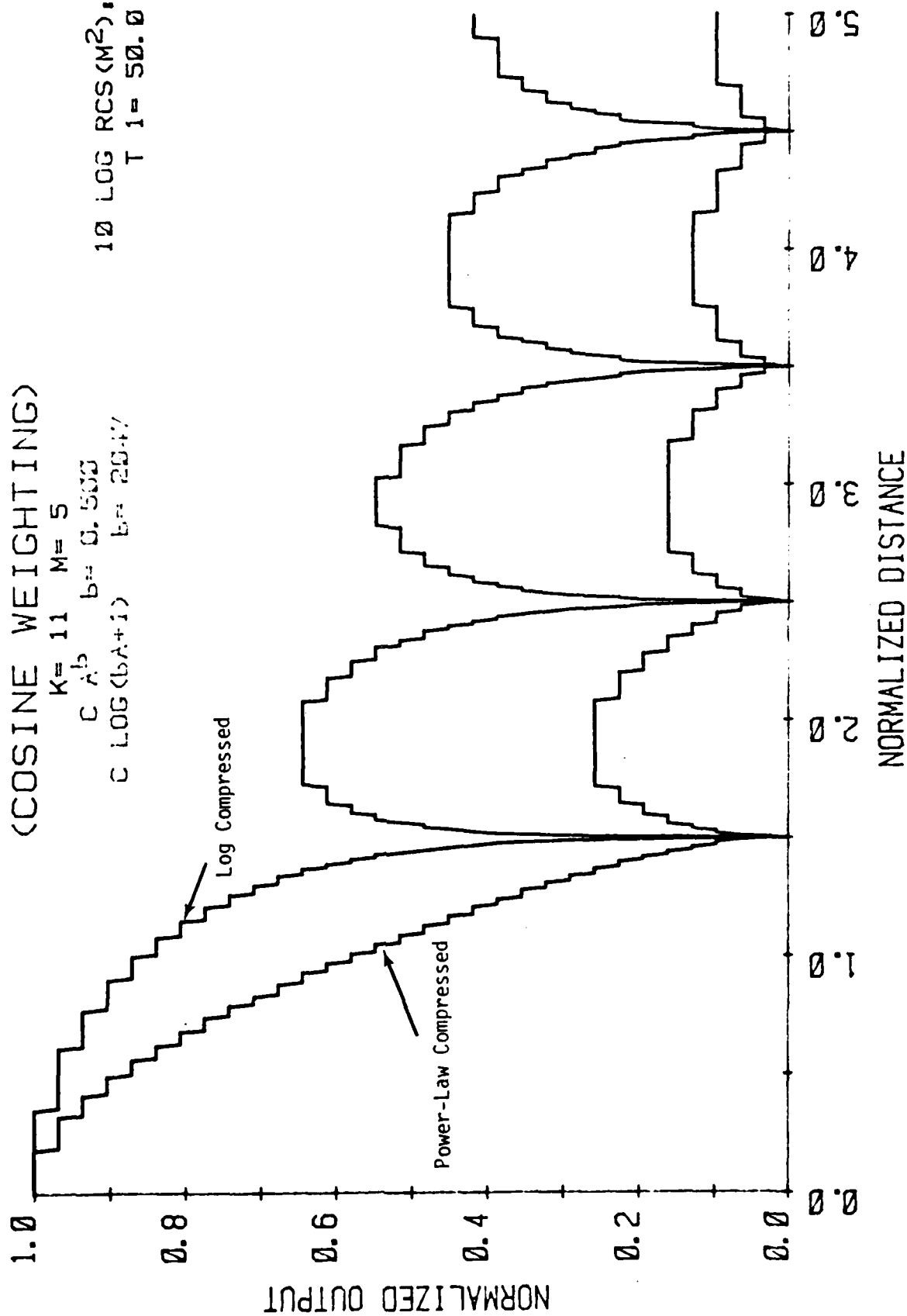
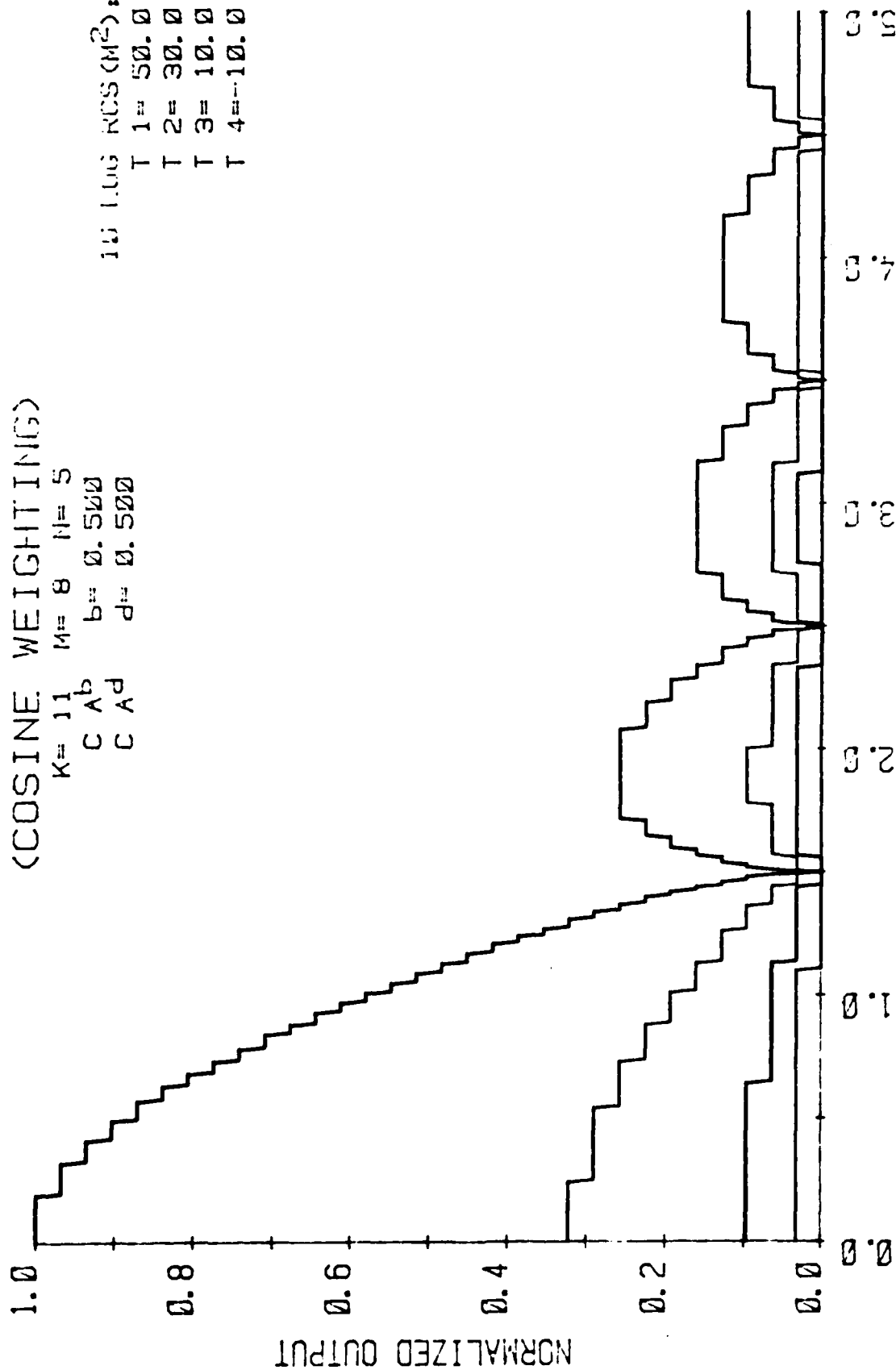


Figure 3-23. Log Encoded/Power-Law Compressed to 5 Bits

# DATA COMPRESSION OUTPUT (COSINE WEIGHTING)

K= 11 M= 8 N= 5  
C A<sup>b</sup> b= 0.500  
C A<sup>d</sup> d= 0.500

10 LOG RCS (M<sup>2</sup>):  
T 1= 50.0  
T 2= 30.0  
T 3= 10.0  
T 4= -10.0



NORMALIZED DISTANCE

Figure 3-24. Direct Power-Law Compression to 5 Bits



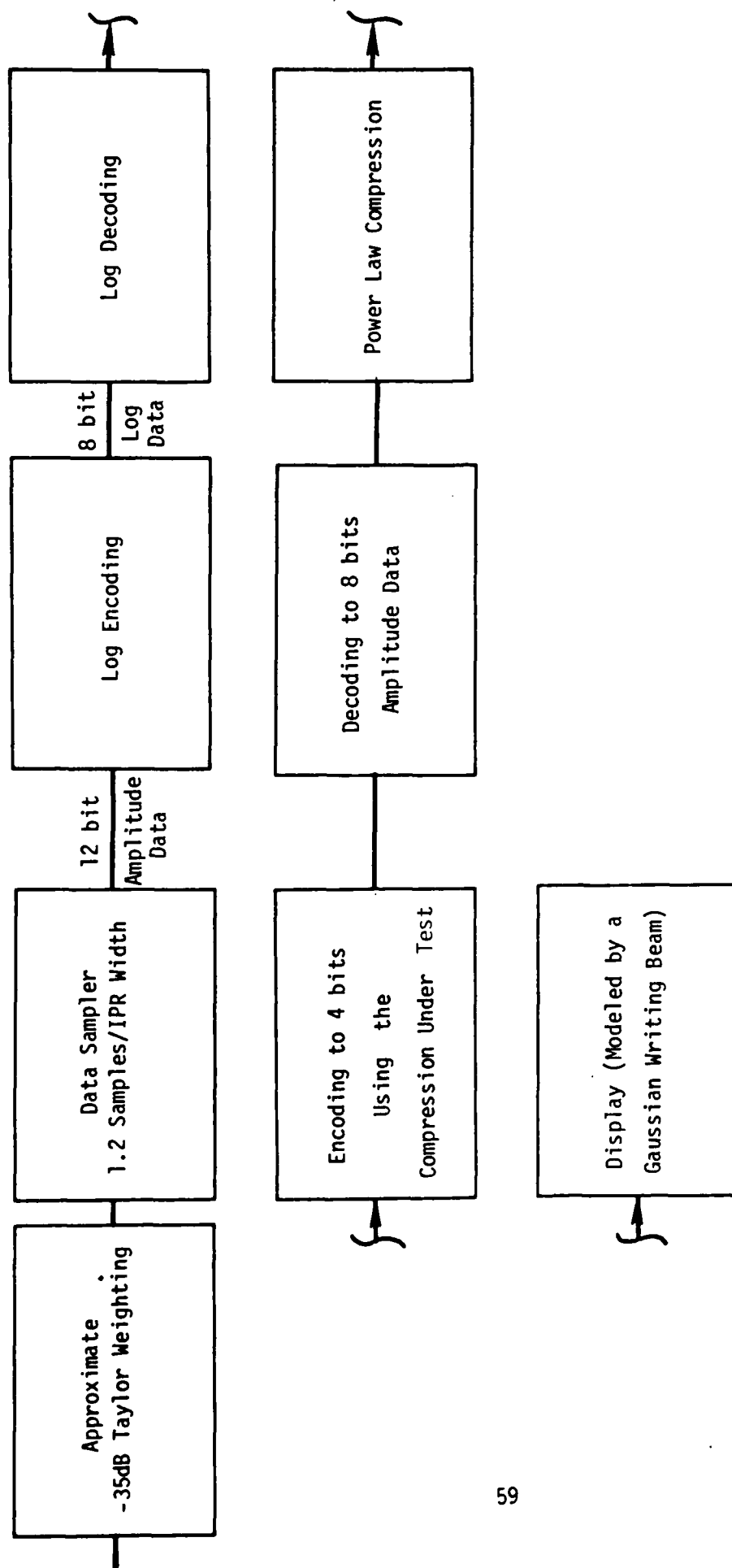


FIGURE 3-25.

ABLE 1 IMPULSE RESPONSE USING 4-BIT LOG STORAGE  
(APPROXIMATE -35dB TAYLOR WEIGHTING) N= 8  
K= 12 M= 4  
C  $\log(\max(A, 1))$   
IDEAL IMAGE  
ACTUAL IMAGE  
SHIFT=+ 50%  
ING RATE= 1.00\*NYQUIST C/A 0.50  
ZE= 50%

\_\_\_\_\_ = IDEAL IMAGE  
 \_\_\_\_\_ = ACTUAL IMAGE  
 \_\_\_\_\_ = ACTUAL IMAGE

SAMPLE SHIFT = + 50%  
= ACTUAL IMAGE

SAMPLING RATE

SAMPLING RATE= 1.00

SPOT SIZE = 59%

C' (A 0.50)

SATURATION LEVEL-106 m<sup>2</sup>

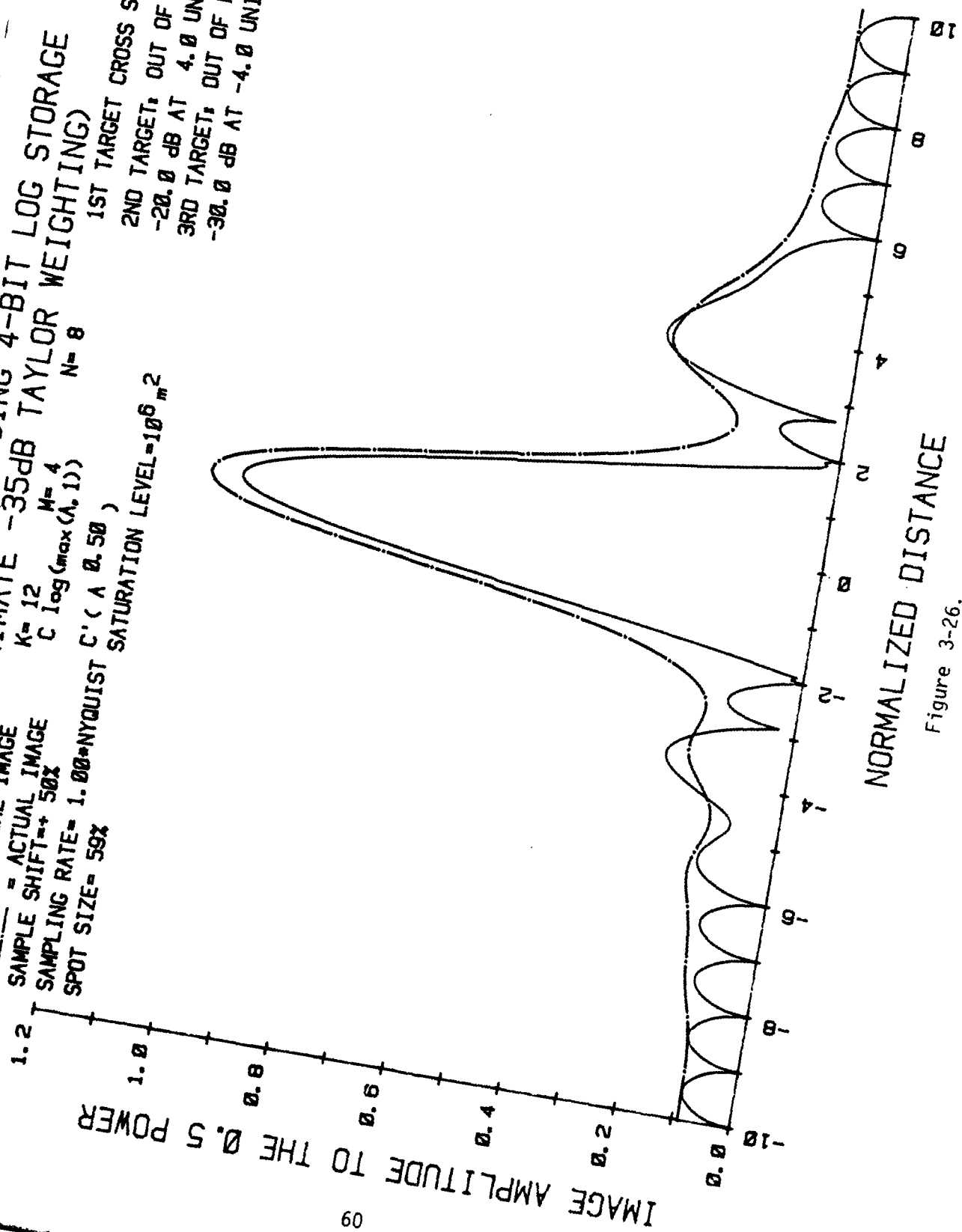
1ST TARGET CROSS SECTION  $\sigma = 105 \text{ m}^2$   
2ND TARGET: OUT OF RANGE  
-20 g

END TARGET: OUT OF PHASE  
-20.0 dB AT 4.0

4.0 DB AT 4.0 UNITS  
BRD TARGET, OUT

30.0 dB AT -4.0

SLING Ø 4.0 UNITS



# ABLE 1 IMPULSE RESPONSE USING GAC-DPCM STORAGE (APPROXIMATE -35dB TAYLOR WEIGHTING)

--- = IDEAL IMAGE       $K=12$        $M=8$        $N=8$       RADAR CROSS SECTION  $\sigma=10^5 m^2$   
 --- = ACTUAL IMAGE       $C \log(\max(A, 1))$   
 SAMPLE SHIFT = 50%  
 SAMPLING RATE = 1.00\*NYQUIST      SATURATION LEVEL =  $10^5 m^2$   
 SPOT SIZE = 59%

2ND TARGET: OUT OF PHASE  
 -20.0 dB AT 4.0 UNITS  
 3RD TARGET: OUT OF PHASE  
 -30.0 dB AT -4.0 UNITS

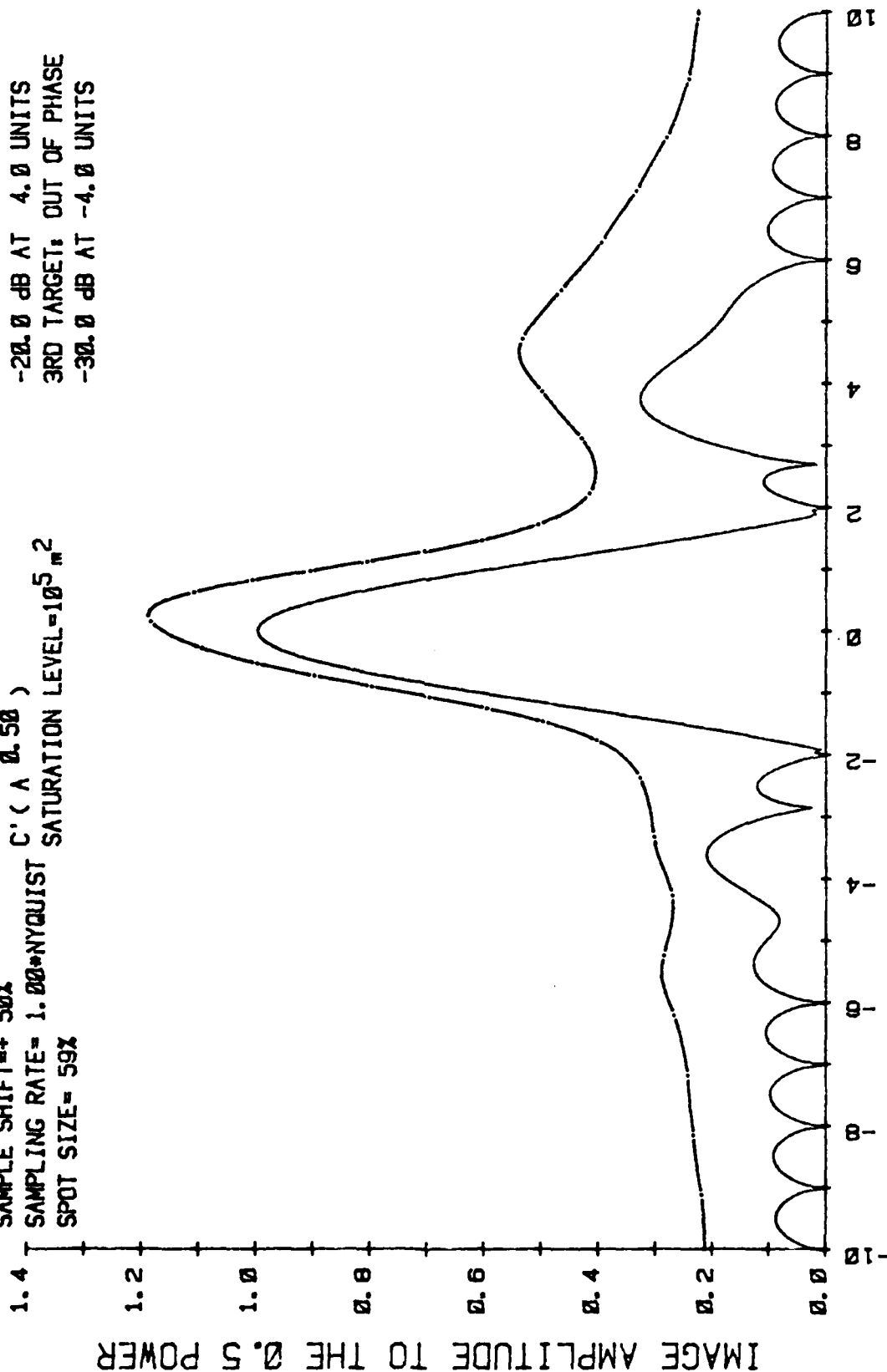


Figure 3-27.

# ABLE 1 IMPULSE RESPONSE USING BUFFERED LINEAR DPCM STORAGE (APPROXIMATE -35dB TAYLOR WEIGHTING)

— = IDEAL IMAGE     $K=12$      $M=8$      $N=8$     RADAR CROSS SECTION  $\sigma=10^5 \text{ m}^2$   
 - - - = ACTUAL IMAGE     $C \log(\max(A, 1))$   
 SAMPLE SHIFT = + 50%  
 SAMPLING RATE = 1.00\*NYQUIST    SATURATION LEVEL =  $10^5 \text{ m}^2$   
 SPOT SIZE = 59%

2ND TARGET: OUT OF PHASE  
 -20.0 dB AT 4.0 UNITS  
 3RD TARGET: OUT OF PHASE  
 -30.0 dB AT -4.0 UNITS

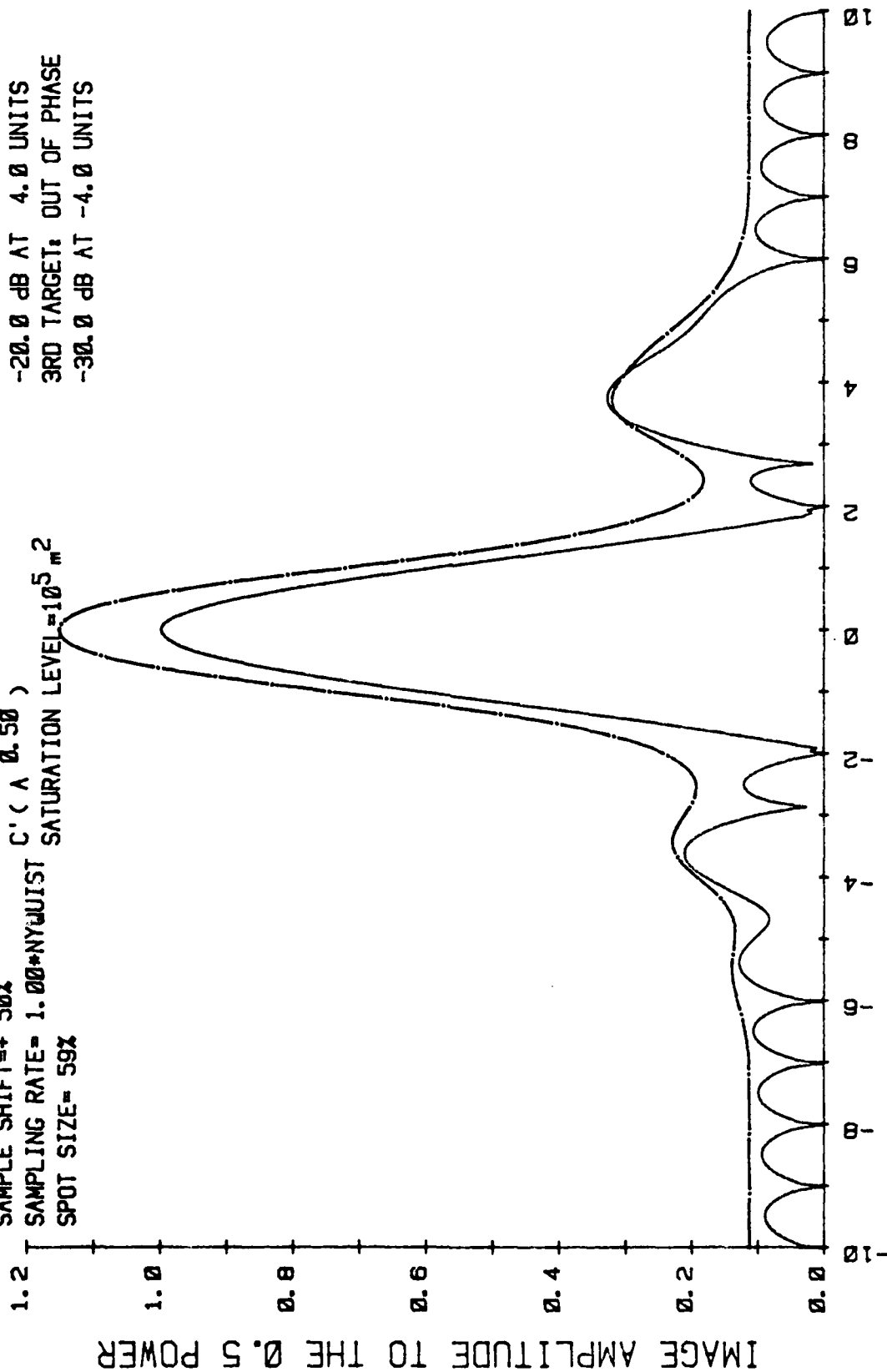


Figure 3-28.

was included in the linear DPCM to handle overflows. If an overflow occurred the succeeding sample was calculated and the value of the storage registered, added to the sample. If the sum exceeded the maximum value representable by the sample, the difference was stored and then added to the next sample until the register was empty. The addition of this register minimized the effect of slew rate limitations inherent in DPCM and also prevented the propagation of slew rate induced errors down the remainder of the range line.

Examination of Figures 3-26 through 3-28 reveals that for identical systems, log encoding introduced the least amount of image degradation.

The DPCM algorithm supplied by Goodyear displays slew rate limitations resulting in a shift in the output response with respect to the input, poor amplitude fidelity, and a loss in modulation between closely spaced targets.

The buffered linear DPCM response is comparable with the log compressed response with the exception of poorer amplitude fidelity.

2-D cosine transform compression was not modeled due to the large increase in hardware required to implement it in the ABLE system.

Huffman coding also was not modeled since an accurate evaluation would require modeling an entire image rather than a single impulse response to determine the reduction in stored bits and the effect on the output image quality. An examination of available image amplitude histograms, however, suggests that the Huffman code would be operating on non-optimal data unless a new code was implemented for each image, yielding less than the expected image compression.

#### 3.4.4 Sampling

The quality of the CRT displayed imagery will depend on a number of factors, including the sampling rate and the relative CRT spot size and shape with respect to the pixel spacings. For the ABLE system the sampling rate is set by SAPPHIRE and resampled in the ES. Given a sampling rate and a signal weighting function (i.e., for SAPPHIRE -30dB Taylor weighting), the CRT's can be selected and data rates adjusted to provide a high quality image on the CRT that will allow maximum image utility. At the CRT display, all the image quality parameters, which we believe are equatable to utility, are displayed and are measurable. The spot size and shape and hence affect the following:

- IPR (resolution),
- peak sidelobes,
- contrast ratio, and
- intensity fidelity.

The CRT receives digital samples from the resampling filters and interpolates the sample with the electron beam (which acts as an interpolator) and produces shaped samples on the CRT screen. Since the CRT inherently has a Gaussian shape spot electron beam, it is reasonable to evaluate the impact of such a spot shape on the output displayed image (Figures 3-29 through 3-33). These curves show the ideal analog (infinitely sampled) impulse response in solid lines, and the resultant impulse response after sampling and interpolation as dotted lines. These figures show cosine weighted IPR's interpolated with one-sigma spot sizes from 20% to 100% of the pixel spacing under ideal sampling

GAUSSIAN INTERPOLATION OF A SAMPLED IMPULSE RESPONSE  
 SIGMA OF GAUSSIAN SPOT= 20% OF SAMPLING INTERVAL SAMPLING SHIFT OF 0%  
 COSINE WT.:  $A^b$ ;  $b^b$ ;  $b^b$  0.30  
 SAMPLING RATE= 1.25\*NYQUIST

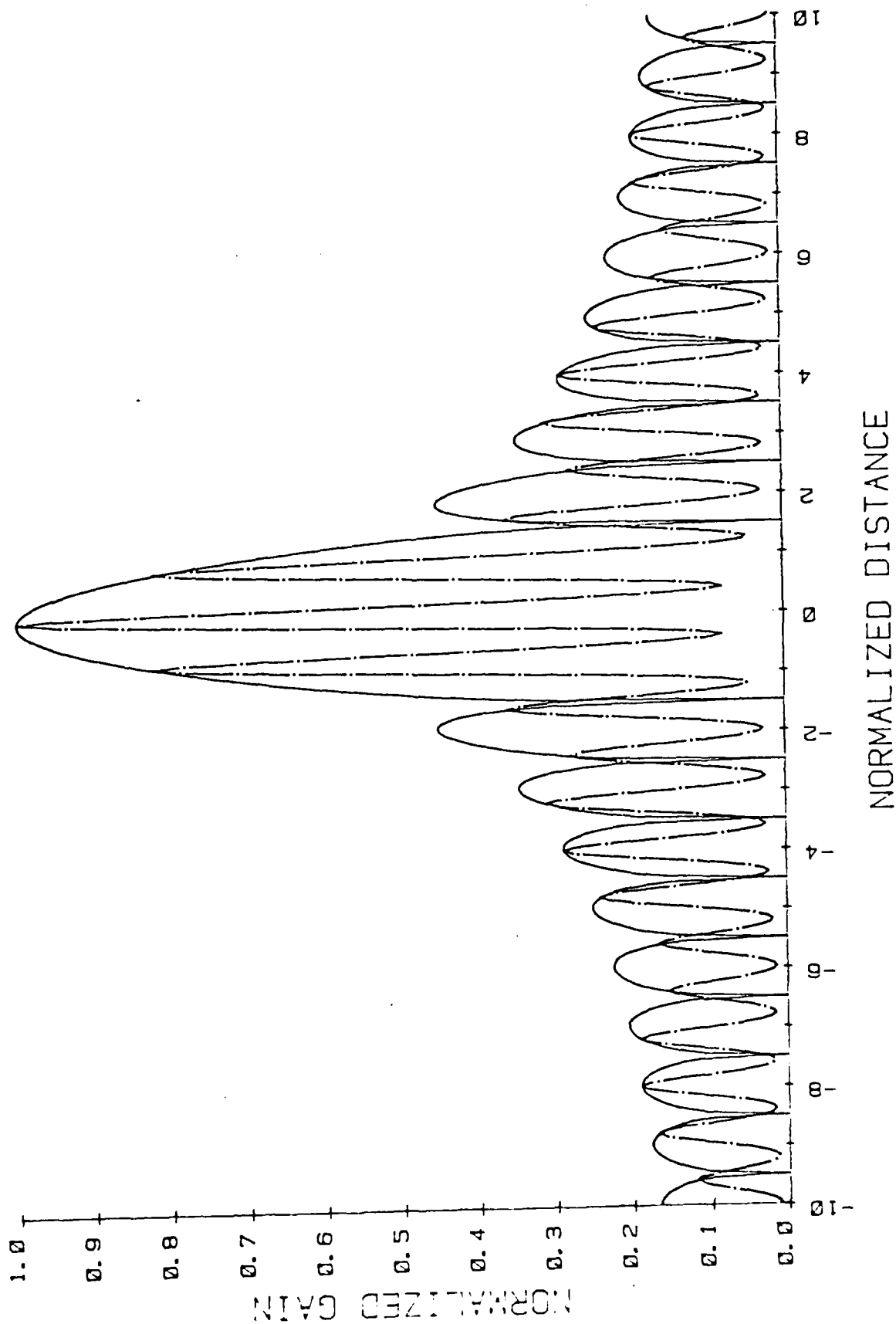


Figure 3-29. Gaussian Spot  $\sigma$  20% of Sample Distance

# GAUSSIAN INTERPOLATION OF A SAMPLED IMPULSE RESPONSE

SIGMA OF GAUSSIAN SPOT= 40% OF SAMPLING INTERVAL SAMPLING SHIFT OF 0%

COSINE WT.:  $A^b$  ;  $b = 0.30$

SAMPLING RATE= 1.25\*NYQUIST

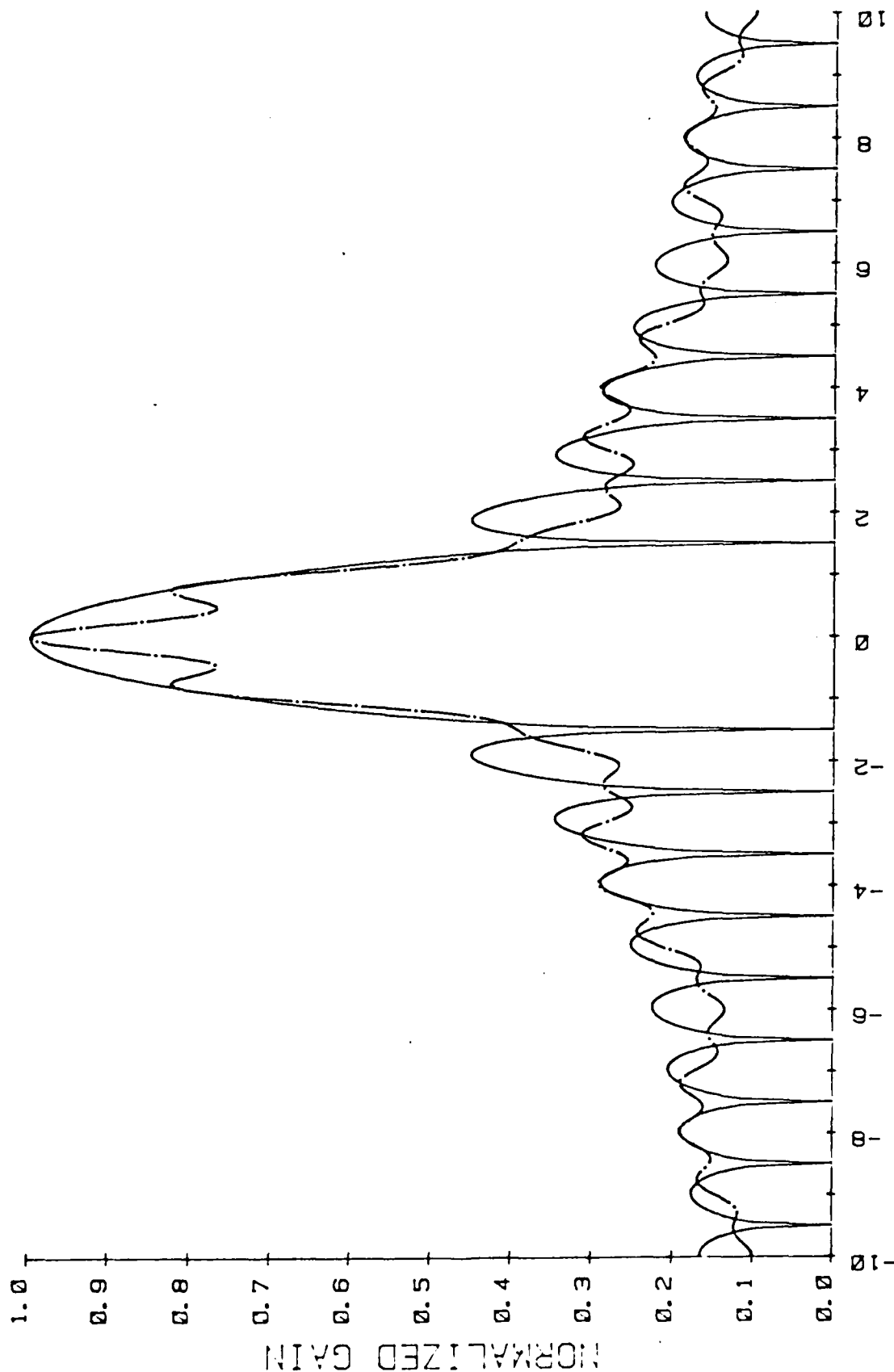


Figure 3-30. Gaussian Spot  $\sigma$  40% of Sampled Distance



# GAUSSIAN INTERPOLATION OF A SAMPLED IMPULSE RESPONSE

SIGMA OF GAUSSIAN SPOT= 60% OF SAMPLING INTERVAL SAMPLING SHIFT OF 0%

COSINE WT.:  $A^b$  ;  $b=0.30$

SAMPLING RATE= 1.25\*NYQUIST

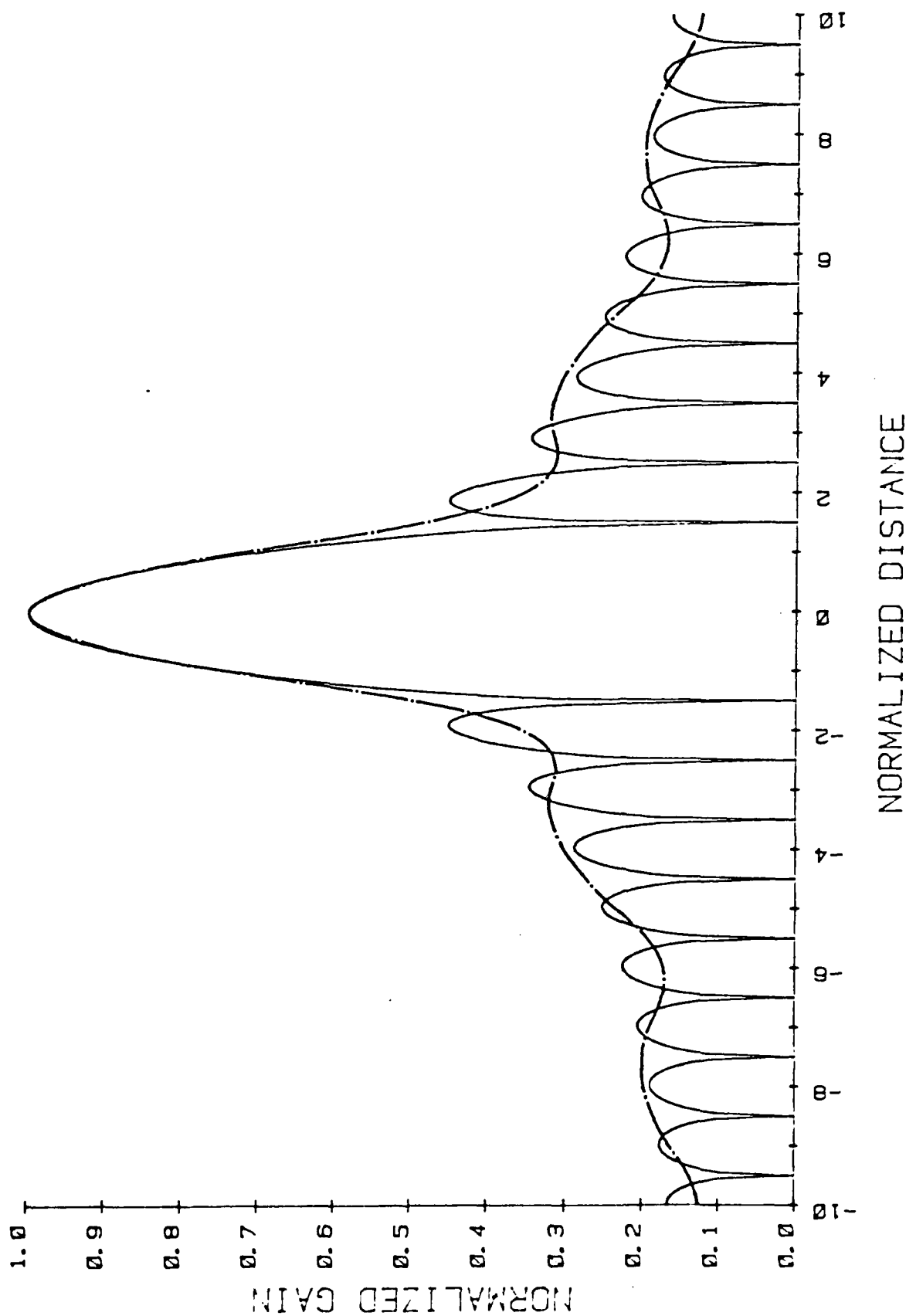


Figure 3-31. Gaussian Spot  $\sigma$  60% of Sampled Distance

# GAUSSIAN INTERPOLATION OF A SAMPLED IMPULSE RESPONSE

SIGMA OF GAUSSIAN SPOT= 80% OF SAMPLING INTERVAL      SAMPLING SHIFT OF 0%

COSINE WT.:  $\lambda^b$  ;  $b' = 0.30$

SAMPLING RATE= 1.25\*NYQUIST

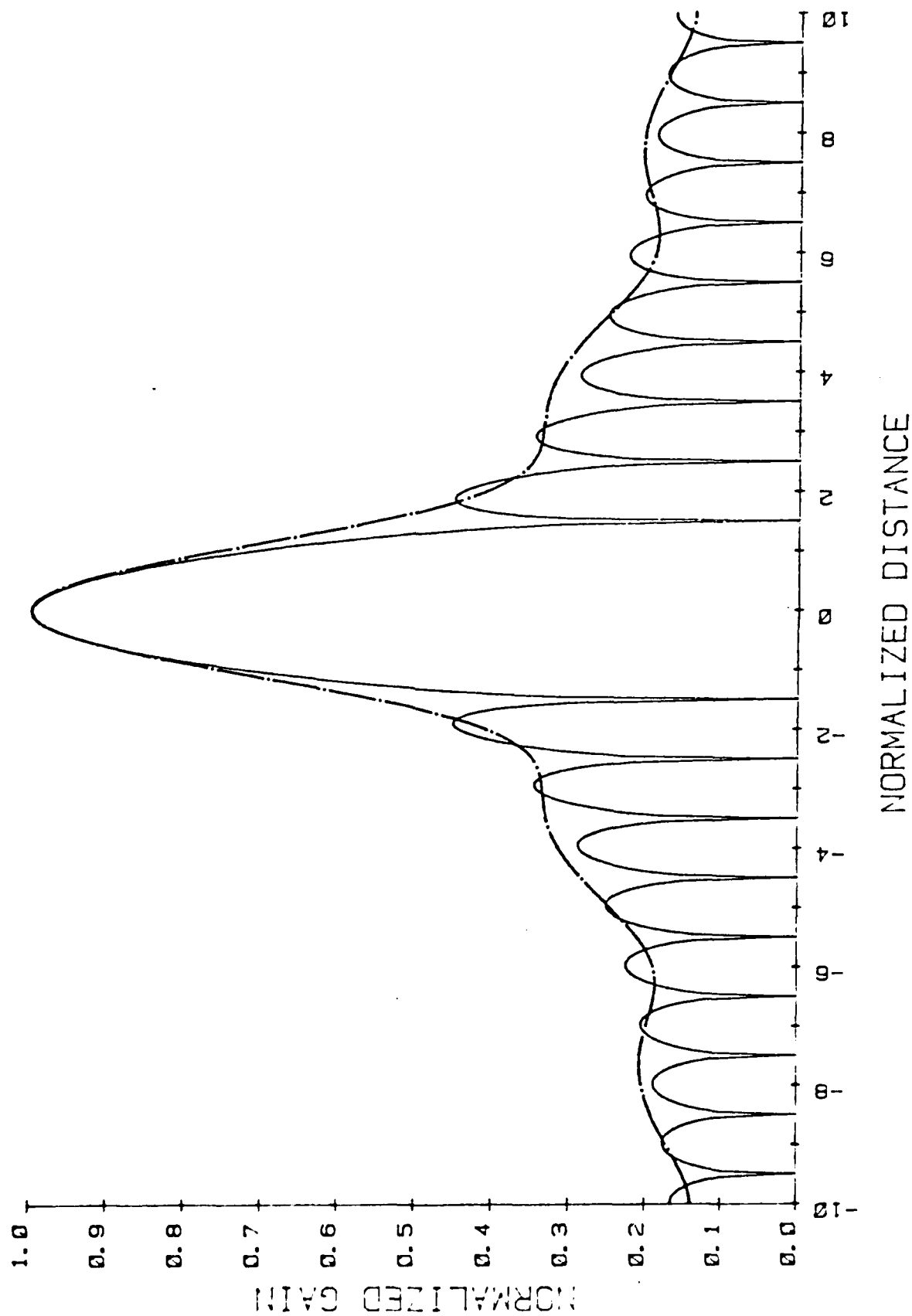


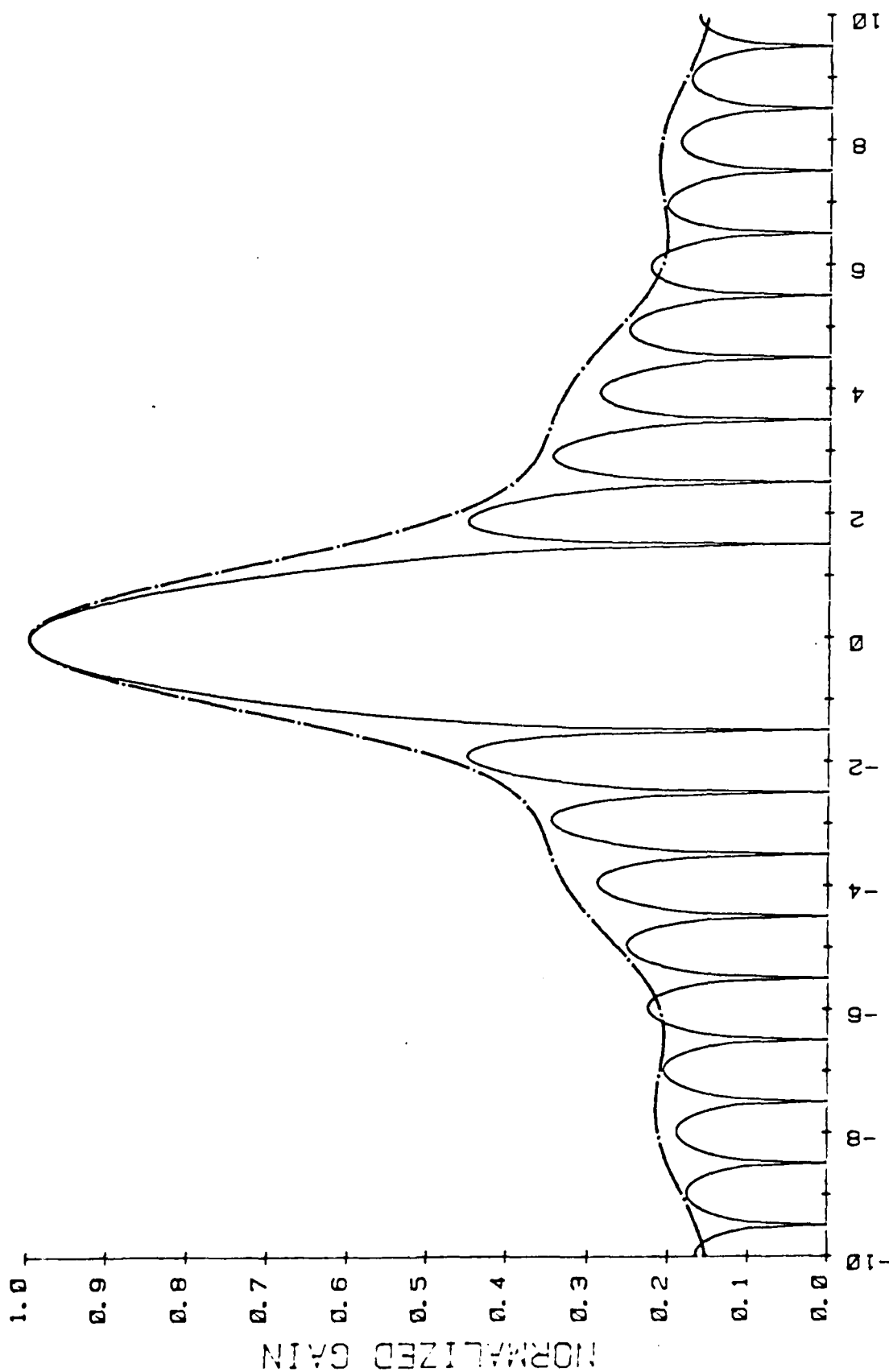
Figure 3-32. Gaussian Spot  $\sigma$  80% of Sampled Distance

# GAUSSIAN INTERPOLATION OF A SAMPLED IMPULSE RESPONSE

SIGMA OF GAUSSIAN SPOT= 100% OF SAMPLING INTERVAL SAMPLING SHIFT OF 0%

COSINE WT.:  $\lambda^b$ ;  $b = 0.30$

SAMPLING RATE= 1.25\*NYQUIST



NORMALIZED DISTANCE

Figure 3-33. Gaussian Spot  $\sigma$  100% of Sampled Distance

shift conditions; that is, 0% shift. For interpolated spot sizes less than 60%, the main lobe is poorly reconstructed at the peak, although the resolution is retained (i.e., single points have multiple peaks). For spot sizes greater than 60%, widening of the main lobe becomes apparent with no significant improvement in the reconstruction of the main lobe peak. Note that the main lobe definition is loosely dependent on the spot size from 50% to 80%. In fact, spot sizes up to 100% only introduce minimal broadening of the main lobe while maintaining the desired side lobe levels.

The sampling rate of 1.25 times Nyquist, noted on Figures 3-29 to 3-33 is the sampling rate at I and Q prior to signal detection. For a -30 dB Taylor weighting and 1.25 sampling rate, we would find about 1.5 samples per 3 dB IPR width. From this we might expect the 10 ft ABLE sample spacing to yield 15 ft 3 dB IPR width, if we wanted the same sampled-to-analog curve fit. Earlier we showed an under-sampled case where the -3 dB curve fit was good but the -15 dB fit was poor. Note that the CRT Gaussian spot size is given at one-sigma value and related to the sampling spacing.

In order to show the effect of increased sampling rate for a given spot size (i.e.,  $\sigma = 59\%$  of sample spacing), we show Figures 3-34 through 3-38. In these figures, the sampling rate is varied from Nyquist to two times Nyquist. From these figures, it appears that 1.25 times Nyquist is an adequate sampling ratio to fit the main lobe down to -15 dB and to represent the side lobe envelope.

A more complex question is: what would happen if two targets were in close proximity--could they be resolved for these conditions? Figure 3-39 shows two targets which are separated by two units (i.e., the peak of one target is located over the first null of the second target) and which are assumed to be in phase so that the energy of each adds constructively. For this

# GAUSSIAN INTERPOLATED IMAGE OF ONE POINT TARGET

## COSINE WEIGHTING

— IDEAL IMAGE  
 - - - ACTUAL IMAGE  
 SAMPLE SHIFT  $\rightarrow 0^\circ$   
 NORMALIZED  $\sigma = 59\%$   
 K=15 M=8 N=8  
 1.00\*NYQUIST  
 SATURATION LEVEL=10<sup>5</sup> m<sup>2</sup>  
 C log( 32767A+1)  
 C( A 0.30 )  
 1ST TARGET:  $\sigma = 100000 \text{ m}^2$

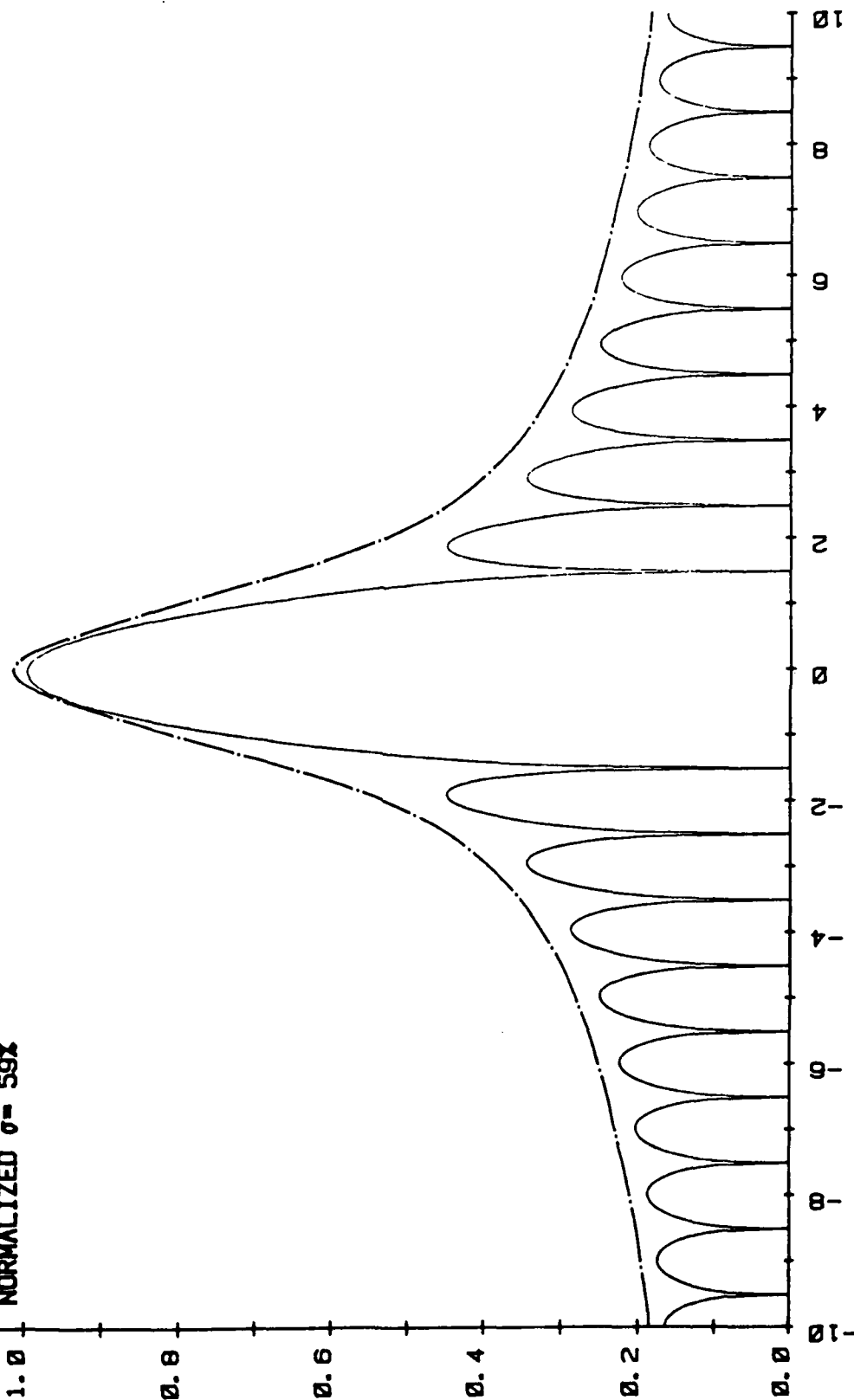


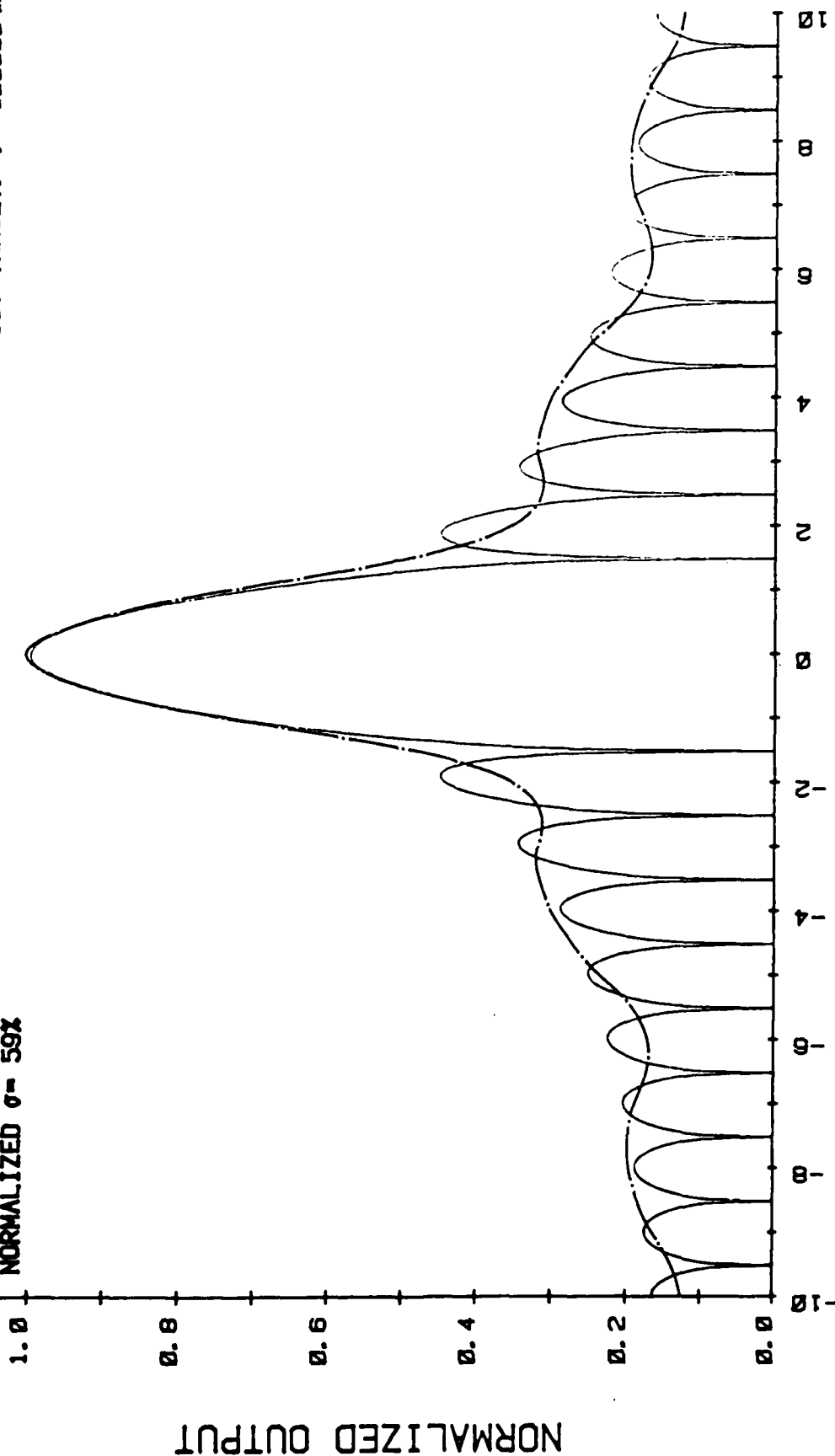
Figure 3-34. Sampling Rate 1 x Nyquist

# GAUSSIAN INTERPOLATED IMAGE OF ONE POINT TARGET COSINE WEIGHTING

$C \log(32767A+1)$   
 $C(A \ 0.30)$   
 1ST TARGET,  $\sigma = 100000 \text{ m}^2$

$K=15$     $M=8$     $N=8$   
 $1.25 \times \text{NYQUIST}$   
 $\text{SATURATION LEVEL} = 10^{-5} \text{ m}^2$

$\text{---}$  - IDEAL IMAGE  
 $\text{---}$  - ACTUAL IMAGE  
 $\text{---}$  - SAMPLE SHIFT  $\rightarrow 0X$   
 $\text{---}$  - NORMALIZED  $\sigma = 59\%$



NORMALIZED DISTANCE

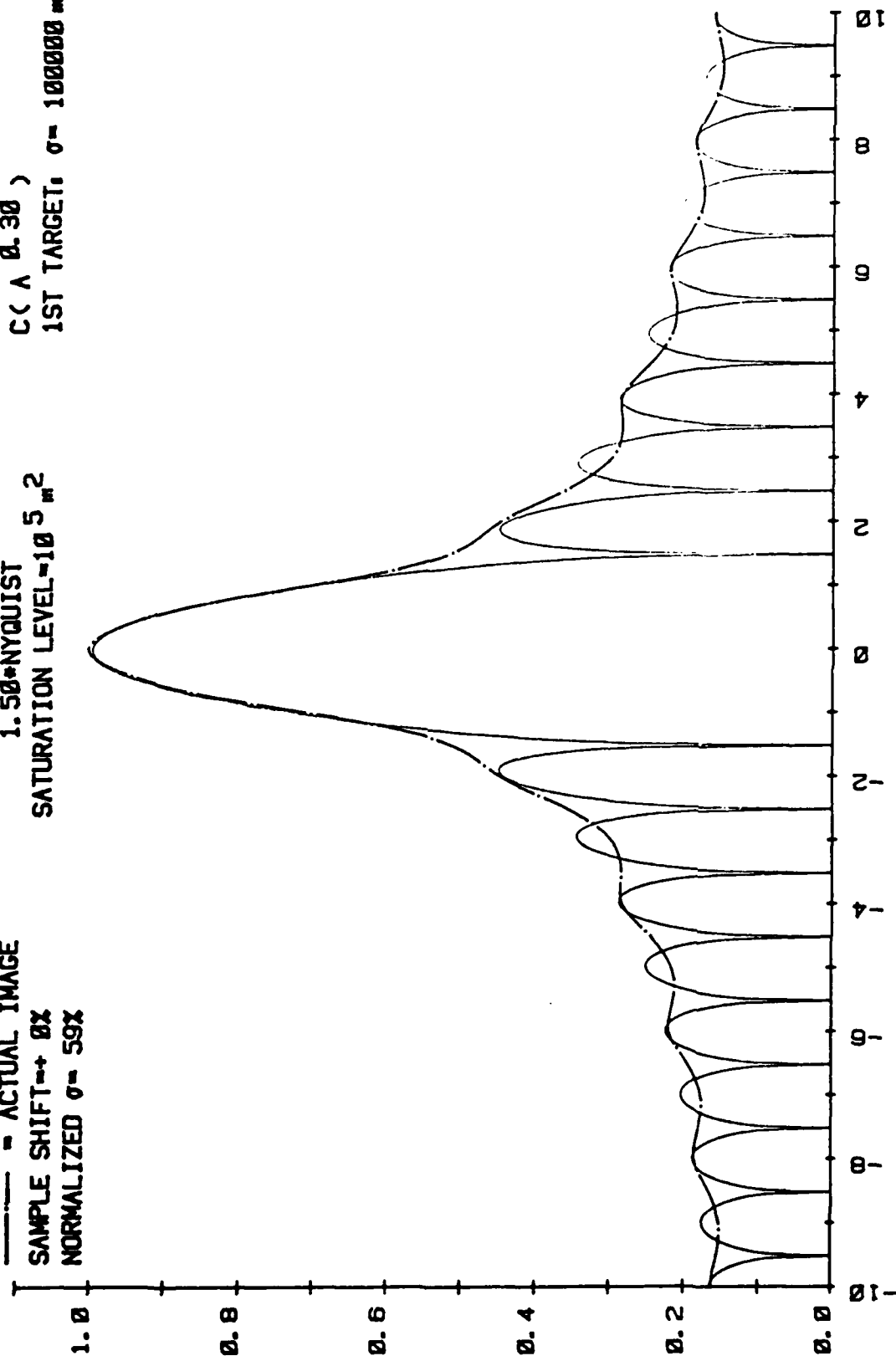
Figure 3-35. Sampling Rate  $1.25 \times \text{Nyquist}$

# GAUSSIAN INTERPOLATED IMAGE OF ONE POINT TARGET COSINE WEIGHTING

— IDEAL IMAGE  
 - - - ACTUAL IMAGE  
 SAMPLE SHIFT  $\rightarrow$  0X  
 NORMALIZED  $\sigma = 59\%$

$K = 15$      $M = 8$      $N = 8$   
 $1.58 \times \text{NYQUIST}$   
 SATURATION LEVEL  $\sim 10^5 \text{ m}^2$

$C \log(32767A+1)$   
 $C(A \ 0.30)$   
 1ST TARGET:  $\sigma = 100000 \text{ m}^2$



NORMALIZED DISTANCE

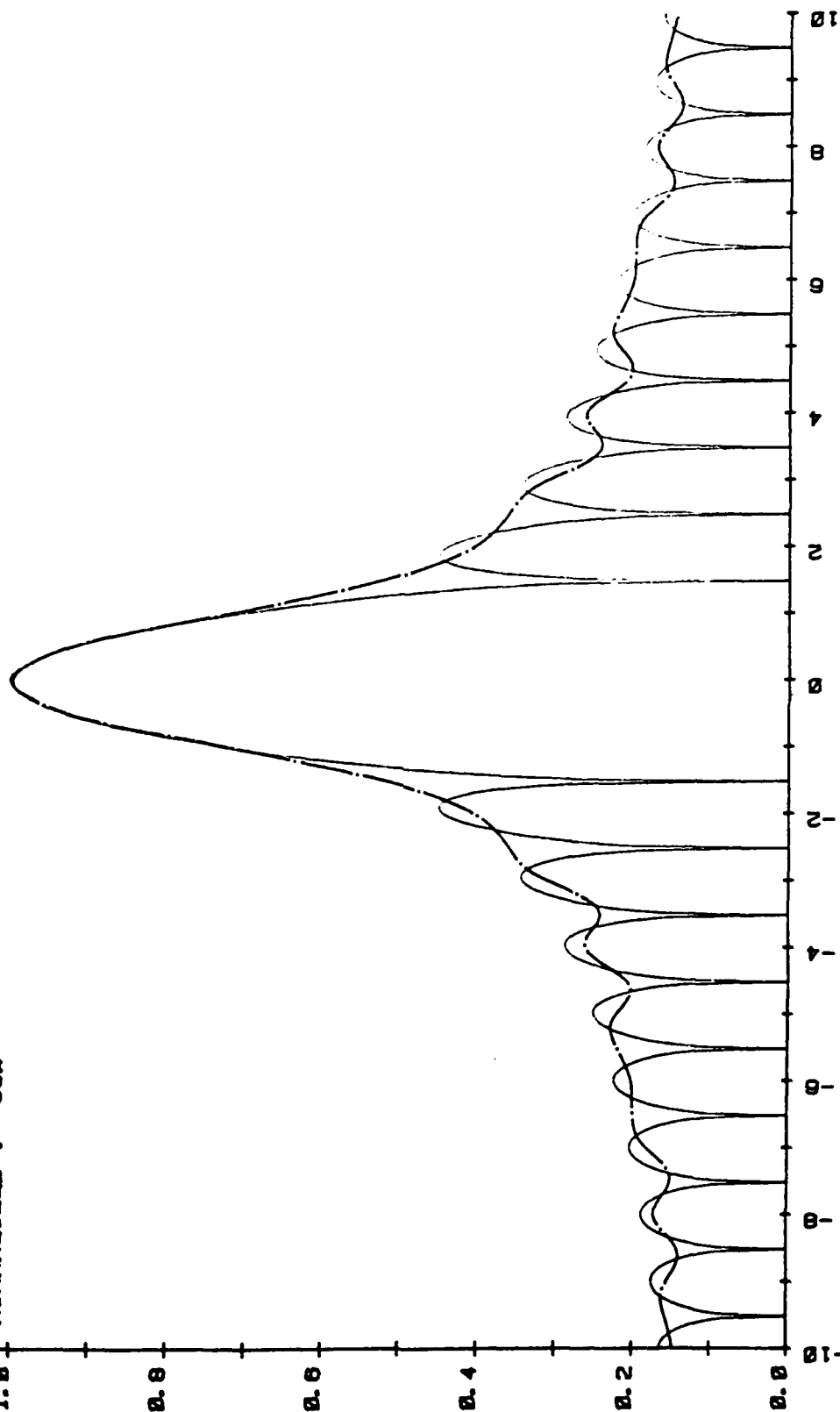
Figure 3-36. Sampling Rate  $1.5 \times \text{Nyquist}$

# GAUSSIAN INTERPOLATED IMAGE OF ONE POINT TARGET COSINE WEIGHTING

$C \log(32767A+1)$   
 $C(A \ 0.30)$   
 1ST TARGET:  $\sigma = 100000 \text{ m}^2$

$K=15$      $M=8$      $N=8$   
 $1.75 \times \text{NYQUIST}$   
 SATURATION LEVEL  $= 10^5 \text{ m}^2$

— IDEAL IMAGE  
 - - - ACTUAL IMAGE  
 SAMPLE SHIFT  $\rightarrow 0X$   
 NORMALIZED  $\sigma = 59X$



NORMALIZED DISTANCE

Figure 3-37. Sampling Rate  $1.75 \times \text{Nyquist}$



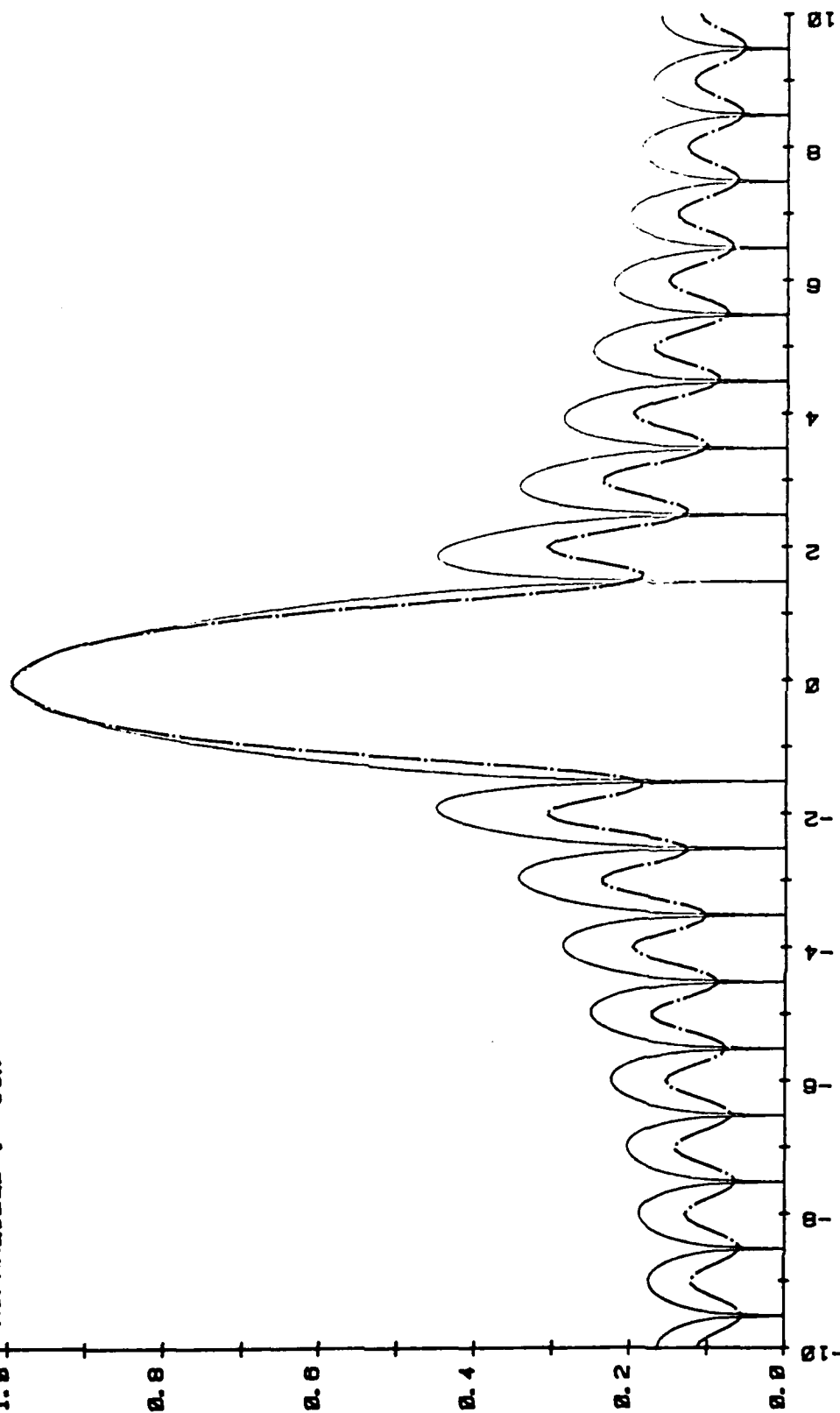
# GAUSSIAN INTERPOLATED IMAGE OF ONE POINT TARGET

## COSINE WEIGHTING

$C \log(32767A+1)$   
 $C(A \ 0.30)$   
 1ST TARGET:  $\sigma = 100000 \text{ m}^2$

$K=15$     $M=8$     $N=8$   
 $2.00 \times \text{NYQUIST}$   
 SATURATION LEVEL  $= 10^5 \text{ m}^2$

— IDEAL IMAGE  
 - - - ACTUAL IMAGE  
 SAMPLE SHIFT  $\rightarrow 0X$   
 NORMALIZED  $\sigma = 59X$



NORMALIZED DISTANCE

Figure 3-38. Sampling Rate  $2 \times \text{Nyquist}$

# DISPLAYED IMAGE OF TWO POINT TARGETS

(IN PHASE)

WEIGHTING: APP. -35dB TAYLOR

TARGET SEPARATION: 2.00

RELATIVE TARGET SIZE: 0.00 dB

POWER LAW: 0.50

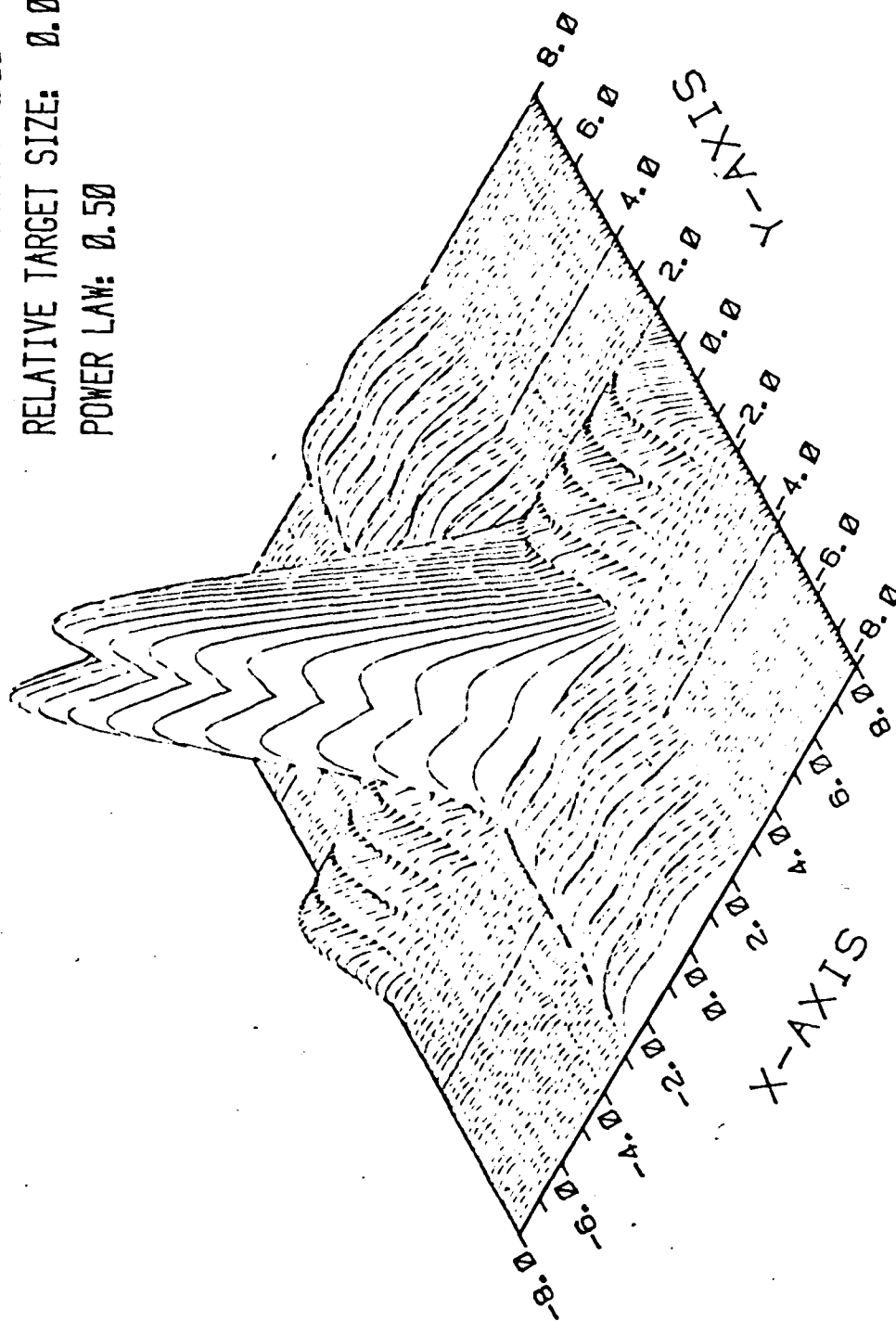


Figure 3-39.

figure we also assume infinite sampling or analog signals. When sampling is finite the modulation between the two peaks is reduced, since that is a point of higher frequency information than that of the main lobe. Figures 3-40 through 3-43 show the effects of increasing the Nyquist sampling rate from one times Nyquist to two times Nyquist. Note that at the higher sampling frequencies we approach the theoretical dip (modulation) level for the two targets. Figure 3-44 is a plot of the modulation depth as a function of Nyquist sampling frequency for various exponents and power-law compression. The primary cases we are considering are  $P = .3$  and  $P = .5$ . For the SAPPHIRE/ABLE system, we should expect about 0.05 to 0.1 modulation depth for the 15-ft IPR case, Taylor weighting, and a power-law compression scheme with an exponent between .3 and .5.

#### 3.4.5 Testing

The testing of the output of the CRT is relatively straightforward, since the image quality parameters are presented in the same form as they are specified. The discussion in Section 2.2.1 (Radar Image Quality Considerations and Verification) reviews how the CRT output could be verified without having to independently scan each point target. We recommend this approach for the ES outputs.

# GAUSSIAN INTERPOLATED IMAGE OF TWO POINT TARGETS APPROXIMATE TAYLOR WEIGHTING

IDEAL IMAGE       $K=15$        $H=0$        $1.03 \times \text{NYQUIST}$   
 ACTUAL IMAGE       $K=15$        $H=0$        $1.03 \times \text{NYQUIST}$   
 SAMPLE SHIFT  $\pm 0.2$   
 NORMALIZED SIGMA  $= 59\%$

0.10 (0.007A+1)  
 CCA (A. 53)  
 2ND TARGET: III PHASE  
 0 dB AT -2.0 UNITS

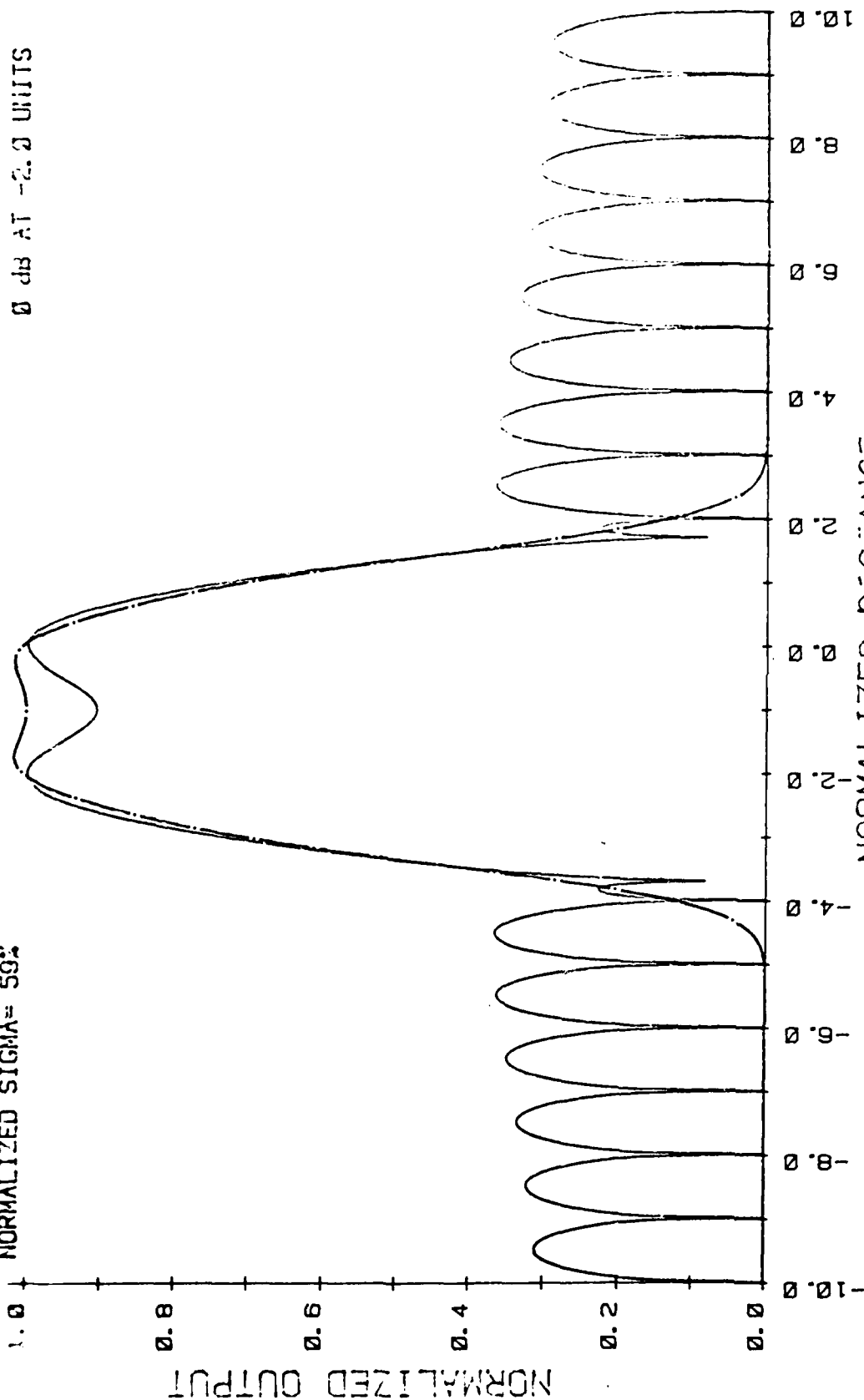


Figure 3-40. Effects of Sampling ( $1 \times \text{Nyquist}$ ) on Two Point Targets

# GAUSSIAN INTERPOLATED IMAGE OF TWO POINT TARGETS APPROXIMATE TAYLOR WEIGHTING

$C \log(32.07A+1)$   
 $C(A \cdot 2.33)$   
 240 TAPSET IN POLAR  
 0 dB AT -2.0 UNITS

$K=15$   $M=8$   
 $1.25 \times \text{NYQUIST}$

--- = IDEAL IMAGE  
 --- = ACTUAL IMAGE  
 SAMPLE SHIFT = 0.25  
 NORMALIZED SIGMA = 50%

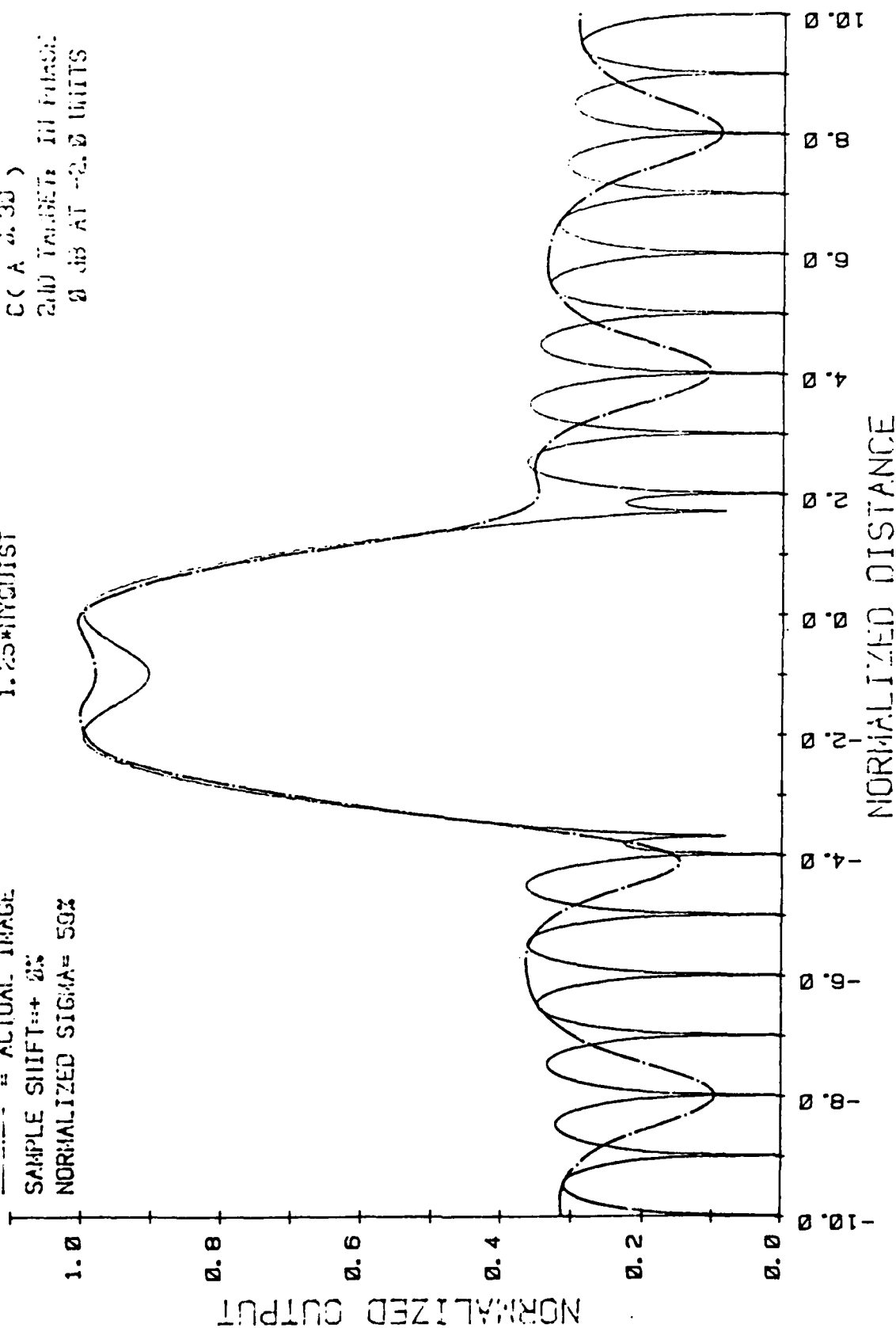


Figure 3-41. Effects of Sampling ( $1.25 \times \text{Nyquist}$ ) on Two Point Targets

# GAUSSIAN INTERPOLATED IMAGE OF TWO POINT TARGETS APPROXIMATE TAYLOR WEIGHTING

$C \log(0.0007A+1)$   
 $C(A \cdot 0.93)$   
 TWO TARGETS IN PHASE  
 8 db AT -4.0 DBTS

$K=15$   $N=8$   
 $1.55 \times \text{NYQUIST}$

--- " IDEAL IMAGE  
 - - - " ACTUAL IMAGE  
 SAMPLE SHIFT = 0.5  
 NORMALIZED SIGMA = 0.93

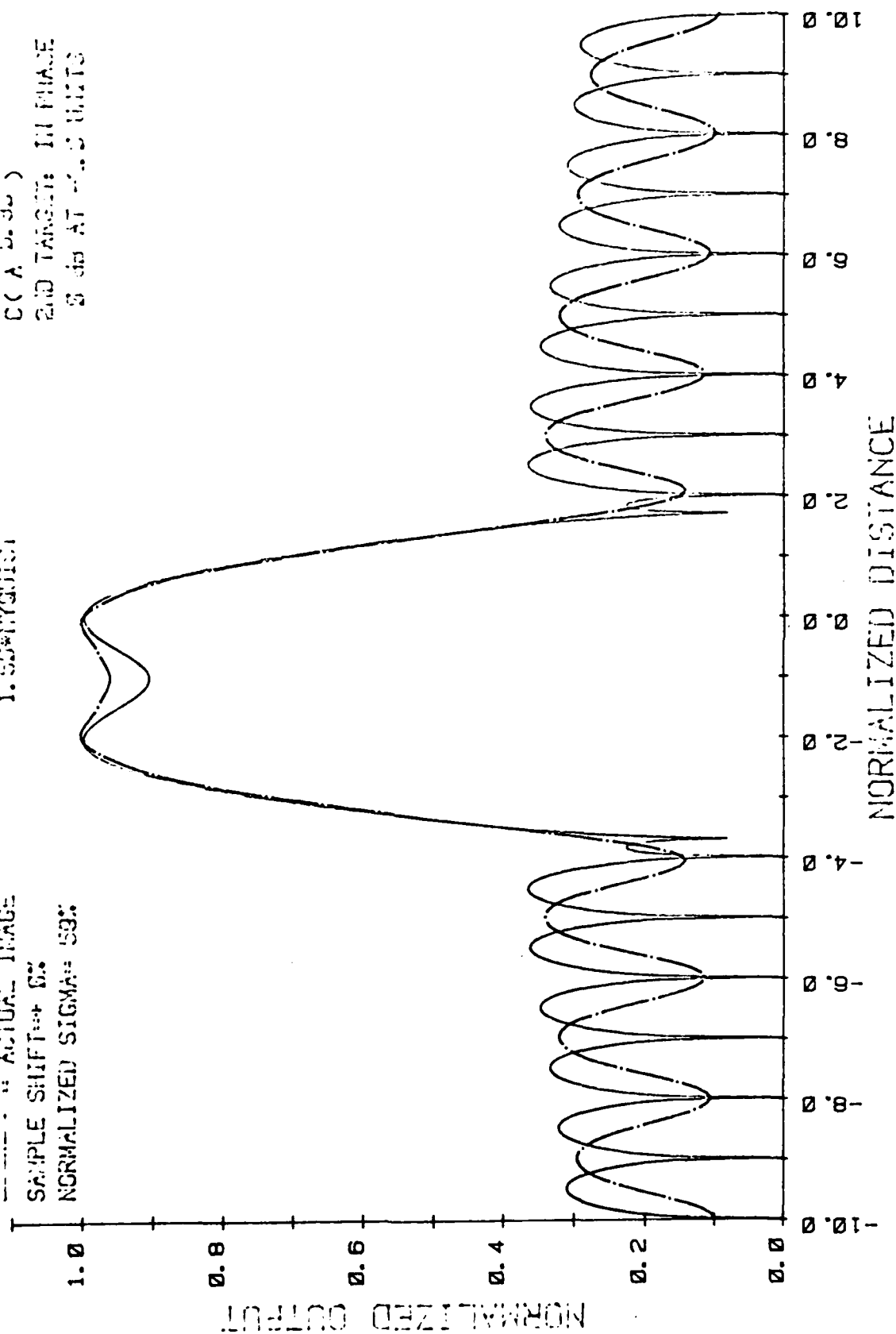


Figure 3-42. Effects of Sampling ( $1.5 \times \text{Nyquist}$ ) on Two Point Targets

# GAUSSIAN INTERPOLATED IMAGE OF TWO POINT TARGETS APPROXIMATE TAYLOR WEIGHTING

$C \log(3226/A+1)$   
 $C(A \cdot 33)$   
 2ND TARGET IN PHASE  
 3 dB AT -2.0 UNITS

$K=15$   $N=8$   
 $2.52 \times \text{NYQUIST}$

--- IDEAL IMAGE  
 --- ACTUAL IMAGE  
 SAMPLE SHIFT = 0%  
 NORMALIZED SIGMA = 59%

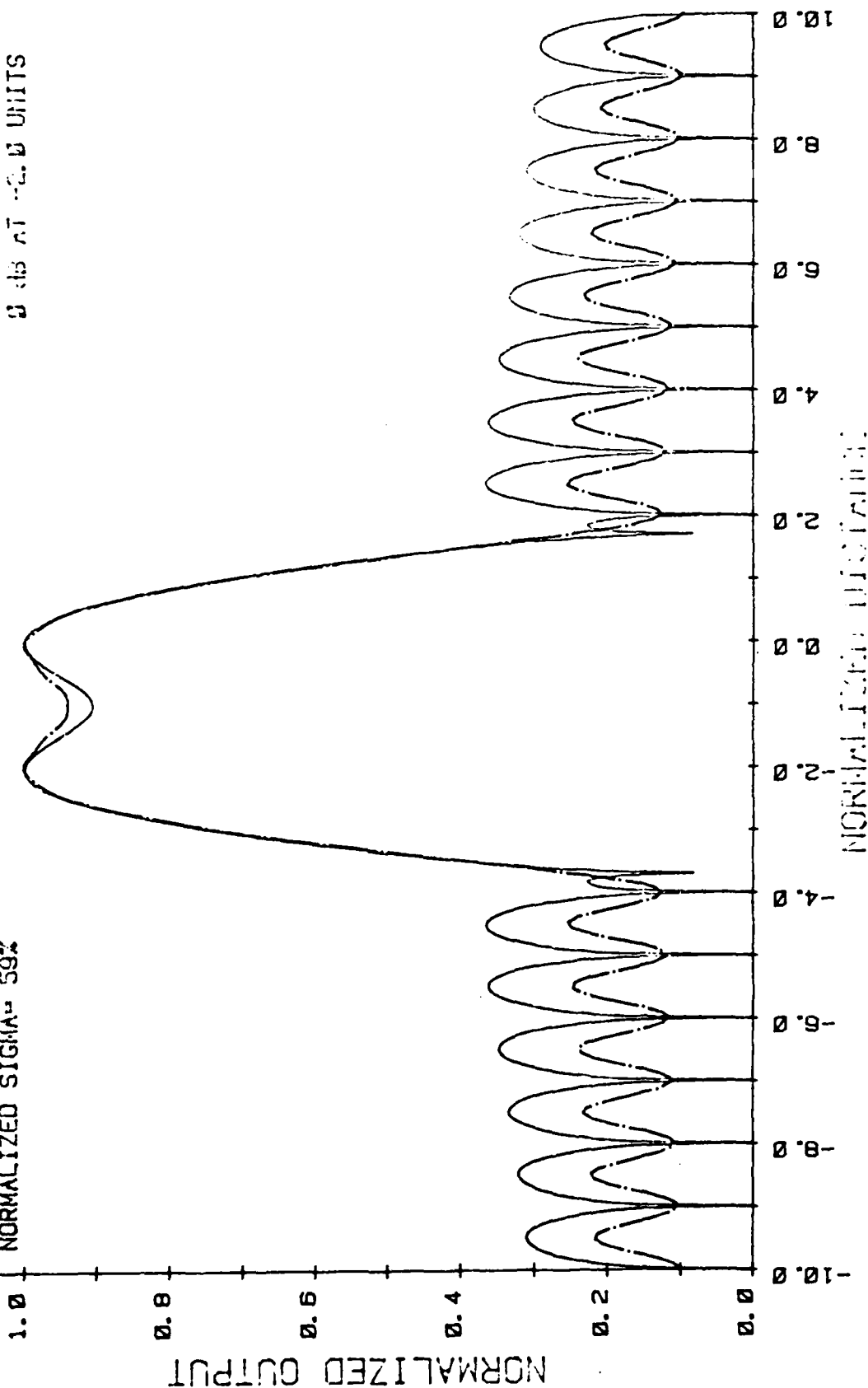


Figure 3-43. Effects of Sampling ( $2 \times \text{Nyquist}$ ) on Two Point Targets

OPTIMIZED MODULATION DEPTH FOR GAUSSIAN INTERPOLATION  
 OF TWO POINT TARGETS WITH POWER LAW COMPRESSION AS A PARAMETER  
 APPROXIMATE TAYLOR WEIGHTING (-35dB)  
 TARGET SEPARATION= 2.0\*3dB WIDTH

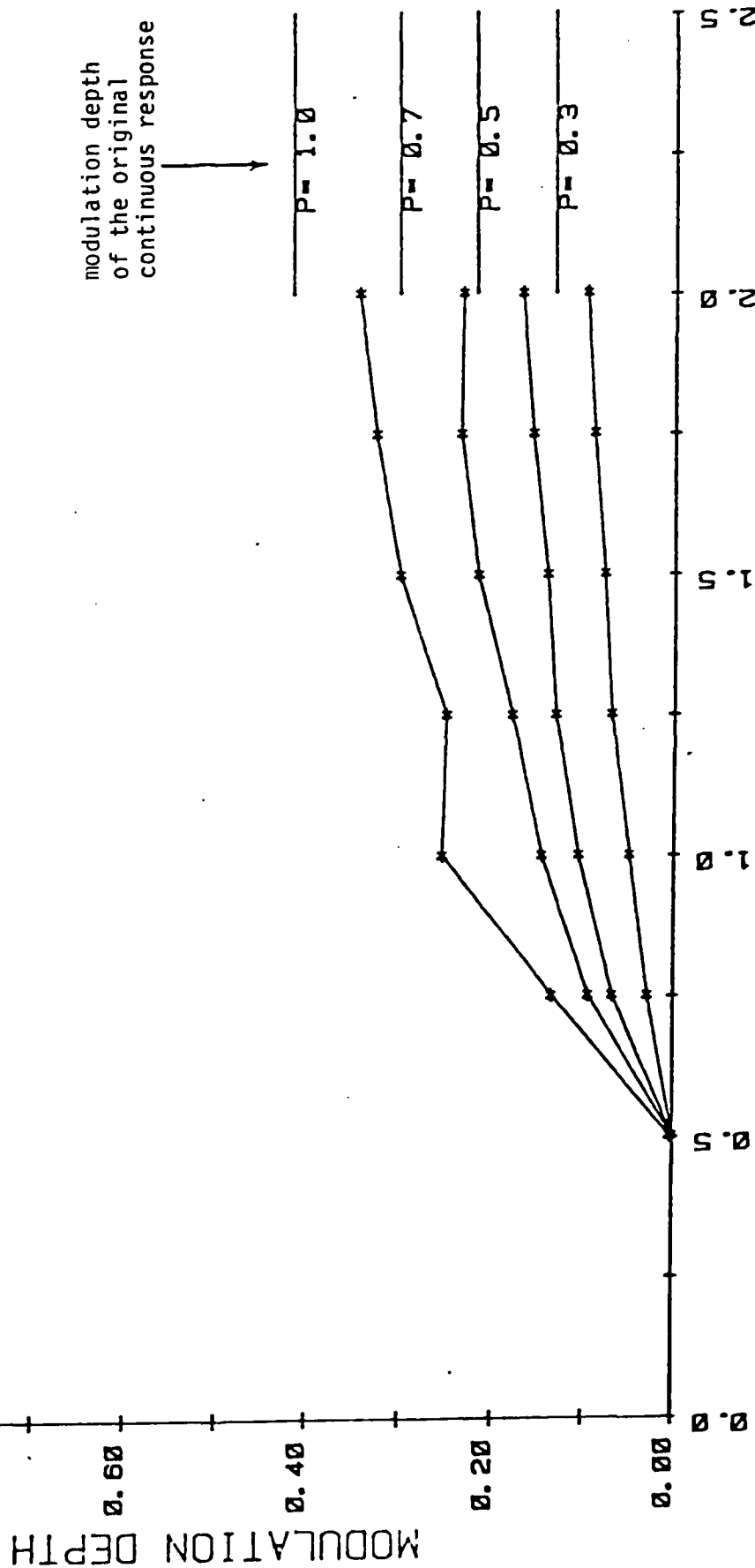


Figure 3-44. Modulation Depth vs. Sampling Frequency



#### 4.0 CONCLUSIONS AND RECOMMENDATIONS

Using the computer models and analyses presented in Section 3, it should be possible to conduct a comprehensive image chain model of the entire ABLE system. The final image chain results should be used to guide interface requirements, testing, operational image quality checks and maintenance procedures.

The following key subsystem image chain elements will require additional contractor support in order to complete the ABLE system image chain analysis. These areas include:

##### SAPPHIRE Subsystem:

- Impulse response (UPD-4 and UPD-6 modes 5 and 6 and modes 7 and 8 for both  $A_1/B_2$  and  $D_4/A_1$  outputs)
- Peak sidelobes (ISLR and CR)
- Image focus characteristics (manual/auto)
- System noise (spurious and arithmetic)
- Motion compensation
- Dynamic range
- Compression effects
- BER and effects for image and auxiliary data
- Sampling

##### ACD Subsystem

- Compression Effects (MAPS)
- Bit level (quantization per pixel)
- BER
- Control interfaces SAP/ACD, ES/ACD, and EMC/ACD
- Sampling rate
- Change data

### Exploitation Subsystem

- BER
- Compression (DPCM, etc.)
- Resampling
- Adjacent cell averaging (interpolation)
- Display factors
  - interpolation/spotsize
  - brightness
  - display/human visual level matching
  - special functions
  - human factors
  - gamma correction
- Situation display features format (EMC)
- Collateral data base interface (EMC)
- Control/data retrieval interface to ACD and EMC

The items presented above represent the initial top level areas of concern. It is our contention that after program offices and associate contractors review the various subsystem designs, areas will be highlighted, resulting in more complete ABLE image analysis; consequently, this will help to ensure the best possible radar image quality and data utility.

14 SAI-TR-04-165-1-A

SECURITY CLASSIFICATION OF THIS PAGE (When Data Entered)

REPORT DOCUMENTATION PAGE		READ INSTRUCTIONS BEFORE COMPLETING FORM
1. REPORT NUMBER	2. GOVT ACCESSION NO.	3. RECIPIENT'S CATALOG NUMBER
	AD-A088853	
4. TITLE (and Subtitle)	5. TYPE OF REPORT & PERIOD COVERED	
ABLE IMAGE CHAIN ANALYSIS	FINAL rept.	
6. AUTHOR(s)	7. PERFORMING ORG. REPORT NUMBER	8. CONTRACT OR GRANT NUMBER(s)
Jerry/Zelenka	TR-04-165-1	F33657-79-C-0178
9. PERFORMING ORGANIZATION NAME AND ADDRESS	10. PROGRAM ELEMENT, PROJECT, TASK AREA & WORK UNIT NUMBERS	
Science Applications, Inc. 5055 E. Broadway, Suite A-214 Tucson, AZ 85711		
11. CONTROLLING OFFICE NAME AND ADDRESS	12. REPORT DATE	13. NUMBER OF PAGES
Aeronautical Systems Division UPD-X Program Office (AERW) WPAFB, Ohio	27 August 1980	
14. MONITORING AGENCY NAME & ADDRESS (if different from Controlling Office)	15. SECURITY CLASS. (of this report)	
	Unclassified	
16. DISTRIBUTION STATEMENT (of this Report)		
Approved for public release, distribution unlimited. Copies of this document may be obtained from the Defense Documentation Center, Cameron Station, Alexandria, VA 22304		
17. DISTRIBUTION STATEMENT (of the abstract entered in Block 20, if different from Report)		
18. SUPPLEMENTARY NOTES		
19. KEY WORDS (Continue on reverse side if necessary and identify by block number)		
Radar Performance                      Mapping Radar Radar System Performance              Radar Exploitation Synthetic Aperture Radar (SAR)        Image Quality Side Looking Radar		
20. ABSTRACT (Continue on reverse side if necessary and identify by block number)		
This report seeks to help in establishing Advanced Building Block for Large Area Exploitation system image chain elements, the ABLE data flow, and ABLE interface and test requirements. The document also reviews critical ABLE image chain problem areas, including image sampling requirements, radar image quantization, radar image compression techniques (DPCM, MAPS, etc.), and radar image data display requirements for both hard and soft copy devices.		

DD FORM 1 JAN 73 1473 EDITION OF 1 NOV 65 IS OBSOLETE

SECURITY CLASSIFICATION OF THIS PAGE (When Data Entered)

411268

AW

DATE  
FILMED  
- 8